

NPS ARCHIVE  
1967  
HERRELL, O.

Civil Engineer

THE EFFECTS OF GLYCOLIC ACID  
AND DOW LATEX 464 (SARAN) ON  
THE STRENGTH AND MICROSTRUC-  
TURE OF NEAT CEMENT PASTE

by

ORVAL GLENN HERRELL

and

ALAN EDWARD SMITH

Course I

June 1967

THE  
UNIVERSITY OF CHICAGO  
PRESS

THE EFFECTS OF GLYCOLIC ACID AND DOW  
LATEX 464 (SARAN) ON THE STRENGTH AND  
MICROSTRUCTURE OF NEAT CEMENT PASTE

by

ORVAL GLENN HERRELL  
BS, United States Naval Academy  
(1964)

and

ALAN EDWARD SMITH  
BS, United States Naval Academy  
(1961)

Submitted in partial fulfillment  
of the requirements for the degree of

Civil Engineer

at the  
Massachusetts Institute of Technology

(1967)

Signature of Author. . . . .

Department of Civil Engineering, 19 May 1967

Signature of Co-author . . . . .

Department of Civil Engineering, 19 May 1967

Certified by . . . . .

Thesis Supervisor

Accepted by. . . . .

Chairman, Departmental Committee on Graduate Students

5 ARCHIVE

~~thesis~~ ~~11/11~~

07

BRELL, O.



ABSTRACT

THE EFFECTS OF GLYCOLIC ACID AND DOW  
LATEX 464 (SARAN) ON THE STRENGTH AND  
MICROSTRUCTURE OF NEAT CEMENT PASTE

by

ORVAL GLENN HERRELL

and

ALAN EDWARD SMITH

Submitted to the Department of Civil Engineering on 19 May 1967,  
in partial fulfillment of the requirements for the degree of  
Civil Engineer.

The primary objective of this thesis was to identify certain microscopic strength mechanisms which are operative in portland cement and its component phases in the presence of glycolic acid and latex, two additives which are known to enhance the physical properties of portland cement concrete.

To accomplish this objective, electron microscope specimens were made from bottle hydrated preparations of portland cement and its component phases, alone and with each of the additives. In addition, compressive and flexural strength tests were conducted on macroscopic specimens in order to establish a degree of correlation between the microscopic studies and certain physical properties observed in neat cement paste.

It was found that glycolic acid causes significant changes in the morphology of the microstructure of portland cement and all of its component phases. These changes are responsible for a significant increase in the compressive strength of neat cement paste and a slight increase in its flexural strength. The retardation of the hydration of tricalcium aluminate and tetracalcium aluminoferrite, together with the acceleration of the hydration of dicalcium silicate and tricalcium silicate is believed to be responsible for the strength increases achieved.



It was found that latex is responsible for a change in the morphology of the initial hydration products of tricalcium aluminate due to a chemical reaction rather than a physical one. However, the change in morphology can not be related to any macroscopic result. It is believed that a continuous latex network is responsible for a significant increase in early flexural strength of macroscopic test specimens. Since no significant increases in compressive strength were observed in these specimens, it is believed that latex increases the bond strength between matrix and aggregate to achieve significant strength increases in mortars.

Thesis Supervisor:

Fred Moavenzadeh

Title:

Professor of Civil Engineering



## ACKNOWLEDGEMENTS

The authors wish to convey their gratitude to Professors Fred Moavenzadeh and R. Brady Williamson for their advice and suggestions during the preparation of this thesis.

For their cooperation and assistance during the experimental work of this thesis the authors are very thankful to Mr. Harry Greenlaw and Joe Nemec.

The authors are also thankful to Miss Caroline G. Whitney for her typing of this thesis.

To our wives for their patience and encouragement throughout the course of this thesis we are forever grateful.





## TABLE OF CONTENTS

<u>CHAPTER</u>	<u>PAGE</u>
1. Introduction	1
2. Background	4
2.1 Electron Microscopy	4
2.2 Hydration of Portland Cement	5
2.3 Identification of Gel Phases	6
2.4 Strength Theories	10
2.5 Specimen Preparation	12
2.6 Admixtures	14
2.7 Effects of Admixtures on Microstructure	16
3. Experimental Procedure	19
3.1 Development of Test Program	19
3.2 Materials and Equipment	24
3.3 Specimen Preparation	25
3.4 Specimen Identification	27
3.5 Macroscopic Testing of Specimens	29
3.6 Microscopic Studies of Specimens	30
4. Macroscopic Results	34
4.1 Compressive Strength	34
4.2 Flexural Strength	39
4.3 Modulus of Elasticity	44
5. Microscopic Results	47
5.1 Presentation of Results	47
5.2 Discussion of Results	48



## TABLE OF CONTENTS (Continued)

<u>CHAPTER</u>	<u>PAGE</u>
5.2.1. Glycolic Acid - Bottle Hydrated Preparations	48
a. Hydration of $C_3S$ - Tricalcium Silicate	48
b. Hydration of $C_2S$ - Dicalcium Silicate	51
c. Hydration of $C_4AF$ - Tetra-calcium Aluminoferrite	55
d. Hydration of $C_3A$ - Tricalcium Aluminate	59
e. Hydration of $C_3A$ - Tricalcium Aluminate and $CaSO_4$ - Gypsum	62
f. Hydration of Portland Cement	66
g. Summary of Results	70
5.2.2. Dow Latex - Bottle Hydrated Preparations	73
a. Hydration of $C_3S$ - Tricalcium Silicate	73
b. Hydration of $C_2S$ - Dicalcium Silicate	73
c. Hydration of $C_4AF$ - Tetra-calcium Aluminoferrite	75
d. Hydration of $C_3A$ - Tricalcium Aluminate	77
e. Hydration of Portland Cement	79
f. Summary of Results	80





## TABLE OF CONTENTS (Continued)

<u>CHAPTER</u>	<u>PAGE</u>
5.2.3. Hardened Cement Paste Preparations	81
a. Powdered Paste Dispersed in Alcohol	82
b. Powdered Paste Dispersed in Water	82
5.3 Relation of Microscopic Results to Strength Characteristics	83
5.3.1. Effects of Glycolic Acid	84
5.3.2. Effects of Dow Latex 464	87
6. Summary of Results and Conclusions	90
6.1 Summary of Results	90
6.2 Conclusions	92
7. Recommendations	95
Bibliography	97
Appendix I - Electron Micrographs	
Appendix II - List of Figures	
Appendix III - List of Tables	



## CHAPTER 1 - INTRODUCTION

Since the days of the Romans, admixtures have been used to a certain extent in the manufacture of concrete. In the United States, the use of admixtures became commonplace in the 1930's, with various forms of calcium chloride being used most frequently (1). At the present time a wide range of admixtures are available under various classifications including accelerators, retarders, waterproofers, workability aids, surface active agents, air entraining agents and pozzolanas (2). The future holds forth promise for new and improved admixtures which will further enhance the physical properties of hardened concrete.

The most important of the physical properties of concrete is strength, which is the most desired property and the most thoroughly investigated property due to ease of measurement (3). The development of admixtures which provide increased strength in concrete can lead to a more economical mix. While strength is the primary consideration, it is not the only one. Admixtures which increase the strength of concrete must do so without adversely affecting its other physical properties.



Of paramount interest in the study of cement is the mechanism through which strength is achieved. The use of admixtures provides simply another variable in the determination of strength mechanisms. The best method available at the present time to study the development of strength in the microstructure of cement is by means of the electron microscope which is capable of developing magnifications on the order of 200,000X.

Two of the newest and most publicized admixtures available commercially are glycolic acid marketed under the trade name, Hydroxyacetic Acid (4), and Latex 464 (Saran) (5), both of which have achieved impressive strength increases in concrete and mortars, respectively. The purpose of this thesis is to investigate in detail the effects of these two admixtures on the strength and the microstructure of neat cement paste.

To determine the strength of the neat cement paste, both with and without the admixtures, physical tests of cylinders in compression and beams in flexure were conducted. To study the effects of the admixtures on the microstructure of cement, specimens were prepared for viewing and analyzing on the electron microscope. Specimens were made from portland





cement and each of its major constituents and from the powdered paste of the ruptured cylinders.

The intention of this thesis is to analyze the physical characteristics of the internal structure. The intention is not necessarily to analyze the chemical composition of the phases observed nor to investigate chemical reactions resulting from the use of admixtures, except as characterized by their physical appearance. For this reason use was not made of diffraction patterns or x-ray diffraction to determine the composition of the phases observed.

In summary, then, it is the intention of this thesis to study the effects of glycolic acid and latex upon the microstructure of portland cement by means of the electron microscope, and to relate the physical structure of the neat cement paste to its strength as determined in compression and flexural tests.



## CHAPTER 2 - BACKGROUND

Before undertaking a study of this nature, it is necessary to review the literature and determine to what extent the microstructure of cement, with and without additives, has been investigated and identified by earlier researchers.

### 2.1 ELECTRON MICROSCOPY

The use of electron microscopy to study the microstructure of cement dates back about twenty-five years (6). One of the earliest studies was conducted by Sliepceвич, Gildart and Katz (7) at the University of Michigan, using water suspension of portland cement and its primary components. It is interesting to note at this early date the concern over specimen contamination due to atmospheric carbon dioxide. However the true identification of the contaminants was not made until several years later (8). Probably the most recent and most complete publication of micrographs of portland cement and its constituents is the work of Grudemo (6).

In the words of Grudemo:

It is for systems of particles within the colloidal and microcrystalline range of sizes...that the electron microscope has found its chief application. In cement





research EM methods can be used: 1) to study the morphology of particles, texture of particle aggregates, crystal habits and crystal growth phenomena, 2) to characterize different phases by means of their appearance in pure or comparison preparations, and to identify from these observations similar phases when they appear in cement paste mixtures, and 3) to observe changes in the morphology or crystallization properties of these phases caused by variation in composition, temperature, age of the sample, or preparation method applied.

The use of electron microscopy to relate physical properties of cement to its internal microstructure is further justified by Copeland and Schulz (9), who foresee increased efforts along these lines in the future. It is hoped that this thesis will provide a small step in that direction.

## 2.2 HYDRATION OF PORTLAND CEMENT

To understand and explain what one observes when studying the microstructure of cement, it is necessary to study the constituents of which cement is composed, as well as their hydration products (2, 10).

Basically, cement is produced as the result of the reaction of limestone and clay in a kiln. The product of the kiln reaction, or clinker, is ground into the fine powder we know as cement. Four components account for approximately 90-95% of the content of cement. These are tricalcium silicate ( $C_3S$ ), dicalcium silicate ( $C_2S$ ), tricalcium



aluminate ( $C_3A$ ), and tetracalcium aluminoferrite ( $C_4AF$ ). In addition, a small amount of gypsum is added to the clinker to retard the hydration of  $C_3A$  and protect against a "flash set".

In the hydration of portland cement  $C_3S$  and  $C_2S$  react with water to form calcium hydroxide and a phase commonly referred to as tobermorite gel. The  $C_3A$  and  $C_4AF$  react with water and calcium hydroxide to form calcium aluminoferrite hydrate and tetracalcium aluminate hydrate. Finally, the reaction of  $C_3A$  with gypsum and water produces calcium mono-sulfoaluminate (10).

### 2.3 IDENTIFICATION OF GEL PHASES

The portland cement gel is a non-homogeneous mixture of several phases. Grudemo has identified the three major gel phases (8, 6) observed in electron microscopy. The predominant gel phase is referred to as the C-S-H gel phase, which is produced by the hydration of  $C_3S$  and  $C_2S$  and is believed to be structurally related to the mineral tobermorite. The second gel phase is known as the C-H gel phase or hydrated lime, also produced as a result of the hydration of  $C_3S$  and  $C_2S$ . The third phase of importance is known as the C-A-H gel phase which is composed of the hydration products of  $C_3A$  and is rather complex in nature.



The C-H phase is identified by thin and transparent hexagonal plates. However, carbon dioxide contaminated C-H may appear as spheres or rounded platelets, aggregated in chains. In earlier studies such structures were mistakenly identified as the hydration products of  $C_3S$  and  $C_2S$  (7).

The C-A-H gel phase is similar in physical appearance to the C-H gel phase, that is, it consists primarily of thin, transparent hexagonal plates. These hexagonal plates are the first hydration products of  $C_3A$  and  $C_4AF$ . In the hydration of  $C_3A$ , after about one day, isometric hydrogarnet crystals begin to form, and after a time an equilibrium is reached in which the isometric forms and the hexagonal plates are present in nearly equal amounts. The appearance of the hydration products of  $C_3A$  changes dramatically when a small amount of gypsum is added prior to hydration. The initial hydration product then has the appearance of long rods with sharply cutoff ends. After the gypsum is exhausted the rods decompose, and hexagonal plates begin to form as the hydration of  $C_3A$  continues. However, with the addition of gypsum, the isometric hydrogarnet crystals do not appear in the hydration of  $C_3A$ .





The hydration of  $C_3S$  and  $C_2S$  yields the C-S-H phase and the C-H phase, which has already been discussed. The C-S-H phase is physically similar to the mineral tobermorite and is often referred to as the "tobermorite-like" phase (11). One variety of tobermorite, known as C-S-H [I], in the form of thin, flexible sheets or foils, sometimes giving the impression of a fine fibrous structure, has been observed in EM studies as a product in the C-S-H phase. C-S-H [I] particles have also assumed fibrous or needle-like appearances. The C-S-H [I] phase has been observed in the hydration products of  $C_3S$  and portland cement. Another variety of tobermorite, known as C-S-H [II], has been observed and consists of bundles of fibers with split or tapering ends. Some observations of C-S-H [II] have been made in the hydration of  $C_2S$ . Gard, Howison and Taylor (12) concluded that the C-S-H [I] and C-S-H [II] phases are probably intermediate stages in the formation of tobermorite. Observations of the C-S-H gel phase of hardened  $C_3S$  and  $C_2S$  pastes have revealed masses of small irregular particles and rather long, straight rod-like particles, sometimes resembling needles. In  $C_3S$  pastes the rods are more slender, while in  $C_2S$  pastes they are thicker and more compact. In general, this rod-like



phase is related to the C-S-H [II] phase previously discussed. Further observations of the hydration of  $C_2S$  and  $C_3S$  have revealed that water penetrates into  $C_2S$  particles, resulting in internal hydration and the splitting of the particles into columnar particles. However,  $C_3S$  particles become covered with foils or fibers during the early stages of hydration, while a process similar to that of  $C_2S$  takes place later during hydration.

As is now evident from the previous discussions of the gel phases, the individual elements of the microstructure, even within a single phase, can differ greatly in physical appearance as a result of many variables including age, curing conditions, water-cement ratio, etc (6). In fact, Brunauer (13) describes tobermorite as "a series of hydrates of continuously varying compositions." Furthermore, there may be a physical resemblance between unrelated constituents of different phases, such as the hexagonal plates of the C-H and C-A-H phases and the rod-like elements of the C-S-H and C-A-H phases. However, such constituents can be identified by means of electron diffraction.

Having determined the physical appearance of the microstructure of the various gel phases in the constituents of



portland cement, it remains to identify the various phases in portland cement itself. Grudemo (14) observed a mixture of elements of various types. He observed that gel particle elements seemed finer and more irregular than those observed in pure silicate pastes. However, in general, EM data in this area is incomplete. Interaction between ions and ionic groups of the different constituents will occur frequently during hydration, disturbing the formation of pure phase hydration products previously identified (8, 6). Therefore, the appearance of the final hydration products of portland cement can not be accurately predicted from observations of the hydration products of its individual constituents (15).

#### 2.4 STRENGTH THEORIES

The study of the microstructure of cement has given rise to numerous theories which account for the strength of cement in terms of its structure. According to Brunauer (13), tobermorite gel is the most important factor in the strength of cement. It is the major hydration product of  $C_3S$  and  $C_2S$ , both of which have been shown to be responsible for the ultimate strength of cement (2, 16).  $C_3A$  affects the early set and early strength of cement, but is nonetheless a relatively poor contributor to the ultimate strength of cement, as is  $C_4AF$ .



Copeland and Schulz (9) observed the formation of clusters of acicular particles at the time of initial set and concluded that the interlocking and growing together of these clusters caused final hardening. To explain the presence of laths and sheets and the absence of acicular particles in more hydrated pastes, they further concluded that growth of the particle must take place transverse to the axis of the needles formed initially.

Hansen (17) theorized that when the rodlike formations or clusters of needles come into contact, they form bonds by "superposition of the atomic structure in the contact areas". He further observed that these rods eventually fill all the space and bonds increase greatly in number. These bonds are "probably one of the sources of strength and rigidity of cement paste."

Grudemo (8) considered a similar theory advanced by Bernal, that the network of interlocking fibers is responsible for the ultimate strength. He also considered Bogue's theory, that the important structural elements are small gel globules coagulated into larger aggregates which form links with adjoining aggregates. Grudemo finally concluded





that there was some truth in both theories, but that they needed to be modified to agree with later observations.

## 2.5 SPECIMEN PREPARATION

In order to study effectively the microstructure of cement and to develop reasonable strength theories, much consideration has been given by investigators to the various methods of specimen preparation for the electron microscope. Grudemo (6) notes the desirability of leaving the original gel structure intact. However, it is necessary to grind the hardened paste into a fine powder in order to prepare specimens for the microscope. Some investigators have reported that grinding does not disturb the finer details of the paste structure. The powder can then be placed dry on an EM specimen film or dispersed in a fluid such as alcohol that will not attack the specimen. Ultrasonic vibration has been successfully used to achieve better dispersions in suspensions, and then a drop is placed on the specimen film. Water is generally considered an unsatisfactory medium in which to disperse powdered pastes since it causes rehydration of the paste and destroys the original microstructure. Copeland and Schulz (9) reported that with curing times in excess of two days it is difficult to disperse the pastes sufficiently



to observe any detail in the microstructure. While Grudemo (14) has achieved a certain measure of success in dispersing powdered pastes, he nevertheless concluded that "by far the largest part of the cement pastes examined consists of exceedingly ill-formed, colloidal products, in which it is sometimes difficult to discern any definite morphology." Copeland and Schulz reached the same conclusion.

Another method used by many investigators (7, 9) is the hydration of cement or its constituents in an excess amount of water. In this manner complete setting of the paste is prevented, since the excess water prevents the formation of bonds between all the particles in the paste. The water suspension is then easily dispersed to allow a thorough observation of the microstructure. This satisfies Bogue's (18) criteria for good micrographs, namely that crystals or fibers be exceedingly thin with little overlapping. The drawback to this method is that hydration of individual particles or groups of particles proceeds unimpaired by the effect of adjacent particles or groups of particles. Thus, the microstructure observed differs considerably from the microstructure of pastes where the close proximity of adjacent particles has a marked effect on the hydration and



growth of the particles. As a result, there exists at present no method of specimen preparation which will yield a completely accurate and detailed view of the microstructure of cement pastes.

Most investigators have found it desirable to prepare specimens in a carbon-dioxide free atmosphere in order to avoid the carbon contamination associated with the C-H phase as previously noted. At any rate, the morphology of contaminants has been identified and may be readily detected in specimens prepared with carbon dioxide in the atmosphere.

## 2.6 ADMIXTURES

Having reviewed much of the previous work done in the area of electron microscopy, it would now be well to investigate briefly the area of admixtures. Two important classes of admixtures are accelerators and retarders. Since strength is of primary concern, it is necessary to consider the effects of admixtures upon the strength of cement. By use of accelerators, such as calcium chloride, the twenty-eight day strength of cement can be achieved in about seven days. Ultimately, however, the strength of untreated cement will approach that of cement treated with calcium chloride,



indicating that the additive has simply speeded up the hydration process rather than accomplishing a physical change in the final appearance of the microstructure.

Retarders are used to delay the set of cement, but have been shown to accelerate the strength development at early ages (3), even though setting time is delayed. Retarders have achieved increases in strength by improving consistency and thus allowing a water reduction. However, strength increases haven't always been completely accounted for by the reduced w/c ratio alone (3, 19). Thus, some other mechanism is responsible for strength increases.

Remarkable strength increases have been achieved by means of glycolic acid, a retarder (4). Test results have shown compressive strength increases in concrete on the order of 30%. In addition, increases in flexural strength have been observed, although to a much lesser degree. Clearly some mechanism other than water reduction is taking place in order to account for these strength increases.

Remarkable strength increases have been achieved in cement mortars by means of latex additives (5). However, the quantity of latex required to achieve these strength





increases is so great as to prove uneconomical in concrete. No data has been published on the effects of latex in neat cement pastes.

## 2.7 EFFECTS OF ADMIXTURES ON MICROSTRUCTURE

Physical testing on the macroscopic level can easily be accomplished to substantiate the beneficial effects of admixtures which increase the strength of cement. However, we must turn to the electron microscope in order to observe any physical changes in the microstructure brought about by the use of admixtures.

Grudemo (6) reports that admixtures can cause interaction between ions and ionic groups during hydration, resulting in a disturbance in the regular formation of hydrates. Rosenberg (20) concluded that no chemical reaction took place between calcium chloride and  $C_3S$  or  $C_2S$ . He further concluded that calcium chloride acts as a catalyst to accelerate the strength increase of  $C_3S$ . Our previous work in this area (21) is generally in agreement with Rosenberg's findings. Kurczyk (8) concluded that the addition of small amounts of gypsum or calcium chloride decreased the size of the needle-like crystals of the tobermorite gel phase and increased the compressive



strength of cement paste. Wagner (22) concluded that the action of latex was primarily a physical one, but he acknowledged the possibility of a chemical reaction for certain varieties of latex. Beyond these findings little work has been done to investigate the effects of admixtures on the microstructure of cement.

Some insight into the effects of admixtures on the microstructure of cement might be gained by the following. Cement pastes must be preslurried before the addition of certain retarders. Bruere (23) explains that this is necessary in order to allow the gypsum to dissolve and coat the  $C_3A$ , leaving a large amount of retarder in solution to retard the silicate hydration. Otherwise, the retarder would adsorb on the  $C_3A$  taking most of the retarder out of solution before the gypsum had a chance to dissolve, thus preventing the retardation of the silicate hydration.

Blank, Rossington and Weinland (24) investigated the adsorption of admixtures on portland cement and its constituents. Salicylic acid and calcium lignosulfonate were investigated. They concluded that the additives were adsorbed primarily by the hydration products of  $C_3A$  and  $C_4AF$ ,



rendering them inactive, while allowing  $C_3S$  and  $C_2S$  to control the reaction.

This theory does not agree with Bruere's conclusion in so far as the adsorption of admixtures by  $C_3A$  is concerned. However, Blank, Rossington and Weinland failed to consider the effects of gypsum and preslurring on the adsorption of admixtures by  $C_3A$ .

Whatever the mechanisms through which glycolic acid and latex are able to achieve substantial strength increases, it is believed that a study of the microstructures of portland cement and its constituents, with and without the additives, will reveal a good insight into the solution of the problem.



## CHAPTER 3 - EXPERIMENTAL PROCEDURE

This chapter includes discussion of the development of a test program, the materials and equipment used, methods of specimen preparation, manner of specimen identification, and a discussion of the strength tests and microstructure studies conducted.

### 3.1 DEVELOPMENT OF TEST PROGRAM

In order to study the effects of the two admixtures, glycolic acid and Latex 464 (Saran), upon neat cement paste on the macroscopic level, five cement paste mixes were investigated. These included a control mix without any admixture, mixes of 150cc and 300cc of glycolic acid per sack of cement, and mixes of 5 per cent and 15 per cent of latex solids by weight of cement. Antifoam B was used in the latex mixes to limit the air content (5). The additions of 300cc glycolic acid and 15 per cent latex conform to the manufacturers' recommendations (4, 5). Since these amounts should have the most beneficial effects on the cement paste, smaller amounts were used to study the effects occurring to a lesser degree, particularly in the microstructure. A summary of the proportions of materials used in each mix is shown in Table 3.1.





TABLE 3.1

MIX PROPORTIONS

MIX NUMBER	1	2	3	4	5
NET L/C RATIO BY WEIGHT	1/3	1/3	1/3	1/3	1/3
CEMENT(GMS)	8400	8400	8400	8400	8400
WATER(GMS)	2800.0	2741.0	2770.4	2369.0	1506.0
GLYCOLIC ACID(CC)	--	59.0	29.5	--	--
% LATEX SOLIDS BY WT CEMENT	--	--	--	5	15
LATEX SOLIDS(GMS)	--	--	--	420	1260
LATEX SOLUTION(GMS) -- (INCLUDING LATEX SOLIDS)	--	--	--	840	2520
ANTIFOAM B SOLIDS(GMS)	--	--	--	1.26	3.88
ANTIFOAM B SOLUTION(GMS)	---	--	--	12.6	38.8



This table shows that all mixes have the same net liquid/cement ratio. This was done to give a basis for comparing the resulting strengths of the different mixes. For each mix compressive and flexural tests were performed at curing ages of three, seven, and twenty-eight days. Four to eight specimens were tested at each age.

For study of the microstructure of the cement two types of specimens were prepared. In the first case finely ground specimens were prepared from hardened cement paste at each curing age tested on the macroscopic level. These specimens were prepared for viewing on the electron microscope. In the second case studies were made on the electron microscope of the microstructure of bottle-hydrated preparations made from the four individual compounds of portland cement and from portland cement itself. Using the method of bottle-hydration provides a looser and more well-dispersed internal structure. Such a specimen can be more readily studied (14) than can specimens taken from hardened cement paste. Additional studies were carried out using the bottle-hydration method with 300cc glycolic acid and 15 per cent latex to investigate their effects on the hydration process of the four compounds and portland cement. Other studies were made



using bottle-hydration with an excessive amount of glycolic acid (to magnify its effect on the four compounds and portland cement) and gypsum (to study its effect alone on  $C_3A$  and its effect on  $C_3A$  in the presence of the glycolic acid). A description of specimen preparation will be given later in this chapter.

Table 3.2 gives a summary of the proportions used in each preparation made for study on the electron microscope. There were twenty-three different preparations in all. For each preparation observations on the electron microscope were made at three hours, six hours, twenty-four hours, and seven days. Each specimen taken was viewed both on the Philip's 100 electron microscope and the Philip's 200 electron microscope for a minimum total of eight observations per preparation. When specimens were unsatisfactory or observations inconclusive, additional specimens were studied. With twenty-three different preparations this gave a minimum total of 184 observation times. An additional twenty observations were made of powdered paste specimens at three, seven, and twenty-eight days of age.



TABLE 3.2

BOTTLE HYDRATED SPECIMEN PROPORTIONS

MAIN CON- STITUENT (GMS)	WATER (GMS)	LATEX SOLUTION (GMS)	ANTIFOAM B SOLUTION (GMS)	ACID (GMS)	GYPSUM (GMS)
P C 5.0	45.0				
5.0	44.0	1.5	.225		
5.0	45.0			.035	
5.0	44.0			1.0	
-----					
C <sub>3</sub> A 2.5	22.5				
2.5	22.0	.75	.113		
5.0	45.0			.035	
2.5	22.0			.50	
2.5	22.5				.96
2.5	22.0			.50	.96
2.5	22.5			.017	.96
-----					
C <sub>4</sub> AF, 2.5	22.5				
C <sub>3</sub> S, 2.5	22.0	.75	.113		
C <sub>2</sub> S 5.0	45.0			.035	
2.5	22.0			.50	
-----					





### 3.2 MATERIALS AND EQUIPMENT

The following materials were used in conducting the experiments related to this thesis:

1. Type I Portland Cement. The major constituents of the cement and their percentages by weight were:  $C_3S$  (54%),  $C_2S$  (16.8%),  $C_3A$  (11.2%),  $C_4AF$  (7.6%), and  $CaSO_4 \cdot 2H_2O$  (4.3%).
2. Water. This was taken directly from the tap and assumed to be of good enough quality for use in cement mixes.
3. Dow Latex 464 (Saran). This was used in solution form with 50% latex solids and 50% water by weight. Additional information can be found in Reference (5).
4. Glycolic Acid. Its chemical formula is  $HOCH_2COOH$ . The manufacturer is Eastman Kodak. E. I. Dupont de Nemours & Co. markets the same product under the trade name, Hydroxyacetic Acid, which is sold specifically as an admixture.
5. The four major compounds of portland cement as listed:

	<u>Surface Area</u>
Tricalcium Silicate ( $3CaO \cdot SiO_2$ ) - $C_3S$	3310
Dicalcium Silicate ( $2CaO \cdot SiO_2$ ) - $C_2S$	3670
Tricalcium Aluminate ( $4CaO \cdot Al_2O_3$ ) - $C_3A$	3018
Tetracalcium Alumino-ferrite ( $4CaO \cdot Al_2O_3 \cdot Fe_2O_3$ ) - $C_4AF$	3350



6. Gypsum ( $\text{CaSO}_4 \cdot 2\text{H}_2\text{O}$ ) used in powdered form.
7. Dow Corning Antifoam B used in solution of 10% solids and 90% water by weight.

Standard laboratory equipment was used for mixing, curing, and testing of the hardened cement paste specimens. For the microscopic studies the Philips 100 and 200 electron microscopes were utilized.

### 3.3 SPECIMEN PREPARATION

The cement paste for the control specimens was mixed according to the procedure contained in ASTM C305-65. For cement paste mixes containing admixtures the mixing procedures were those recommended by the manufacturers of the admixtures. Complete details of these procedures can be found in References (4) and (5). After mixing of the cement pastes, cylinders and beams were cast. For each cement paste mix, twelve to twenty-four cylinders of two inch diameter and four inch height and twelve to twenty-four beams of one inch by one inch cross section and twelve-inch length were made. The specimens were rodded according to ASTM C109-64. Then a small electric-powered vibrator was used to vibrate the specimens in order to eliminate as much as possible any air voids that existed after rodding. All specimens were then cured in their



forms for twenty-four hours in a moist room of 95-100 per cent humidity. After twenty-four hours the forms were stripped, and the specimens submerged in water until such time as they were required for testing. The curing age at the time of testing the specimens was calculated from the time at which they were cast in their forms.

For study of the microstructure of the hardened cement paste mixes, samples were taken from specimens which had been tested on the macroscopic level at curing ages of three, seven, and twenty-eight days. These hardened cement samples were finely ground using a bowl and pestle. The resulting powder was then immersed in ethyl alcohol (9, 14) and ultrasonically vibrated for two minutes to give a better dispersion of the suspended material. A drop of the suspension was then placed on a 200 mesh test grid covered by a carbon subtrait. The alcohol was allowed to evaporate leaving behind the solid material on the carbon subtrait. The carbon subtrait served two main purposes. It absorbed some of the heat of the electron beam and gave a supporting film for better dispersion of the material to be viewed on the electron microscope (6, 9). Other specimens were prepared from the twenty-eight day mixes only, by dispersing the powder in



water for five minutes and then ultrasonically vibrating the suspension for two minutes. Some of these specimens were allowed to rehydrate for up to thirty minutes for further study.

For investigating the microstructure of the bottle-hydrated preparations, specimens were also prepared using copper grids with a carbon substraat. The preparations were ultrasonically vibrated for thirty seconds to disperse the material. Thirty seconds' time gave a good dispersion and did not cause heat generation, which can speed up the hydration process, according to Grudemo (6). Then a few drops of the preparations were dispersed in ethyl alcohol. Using alcohol made preparation of the test grids easier and better due to the lower surface tension of the alcohol as compared to that of water. As was done with the ground paste specimens, a drop of the suspension was placed on the test grid, and the alcohol was allowed to evaporate.

#### 3.4 SPECIMEN IDENTIFICATION

For purposes of identification, the macroscopic test specimens of the five different mixes investigated are simply referred to by the numbers 1 through 5. Mix 1 is the control





mix without any admixtures. Mixes 2 and 3 contain glycolic acid in amounts of 300cc and 150cc per bag of cement, respectively. Latex was added to mixes 4 and 5. Mix 4 contains 5 per cent latex solids by weight of cement and mix 5 contains 15 per cent latex solids by weight of cement. To identify the specimen test age, the letters A, B, and C are used to represent three, seven, and twenty-eight days in that order. For example, a control mix specimen tested at age seven days is referred to as specimen 1B; a 15 per cent latex mix specimen at twenty-eight days as specimen 5C, etc.

Powdered specimens prepared for microscopic studies from hardened cement pastes are identified in the same manner as the corresponding macroscopic specimens, but are preceded by the designation "EM". All of the specimens prepared at age three days (for example, specimen EM1A) were suspended in alcohol. Specimens prepared at age twenty-eight days (for example, specimen EM1C) were rehydrated in water for thirty minutes.

To identify microscopic specimens taken from the bottle-hydrated preparations the symbol for the major constituent



in each preparation is used. To this symbol is added HA if glycolic (Hydroxyacetic) acid is present in the amount of 300cc per bag of cement, HA(EX) if an excessive amount of glycolic acid is present, L if latex is present, and G if gypsum is present. The age of the specimen is given at the end of the specimen identification. For example, a twenty-four hour specimen prepared from bottle hydrated tricalcium aluminate with gypsum and an excessive amount of glycolic acid is referred to as  $C_3A$ -G-HA(EX) - 24 Hours.

### 3.5 MACROSCOPIC TESTING OF SPECIMENS

The macroscopic tests performed on specimens of the hardened cement paste mixes were compressive tests and flexural tests. Both tests were performed at curing ages of three, seven, and twenty-eight days. At each age four to eight specimens of each mix were tested.

The compressive tests were performed on the cement cylinders after they had been capped with quick-set gauging plaster. The cylinders remained in water until just before they were capped and tested. For the three-and seven-day tests only the applied load at failure was measured. From this load the compressive strength was obtained in pounds per



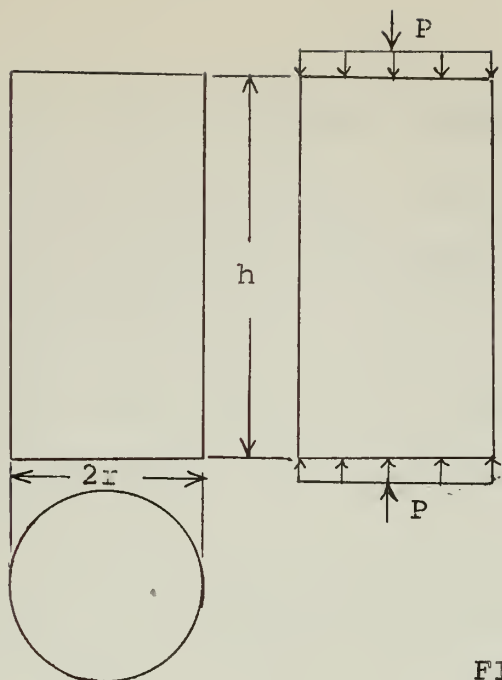
square inch by dividing the load by the cross-sectional area of the cylinder perpendicular to the load. See Figure 3.1 for schematic description. For the cylinders at age twenty-eight days the Instron was used to obtain stress-strain relations under compression loads up to 10,000 pounds. Additional cylinders at age twenty-eight days were tested for determination of failure load.

The flexural tests were performed on the cement beams. Most of the beams were placed as simply supported beams on a ten-inch span and subjected to mid-span loading. A few beams were placed on an eight-inch span. The applied load at failure was measured for each beam. From this load and known values of span length, type of loading, and cross-sectional dimensions, the flexural strength was calculated, based on the structural analysis of simply supported beams. Figure 3.2 gives a detailed description of the analysis.

### 3.6 MICROSCOPIC STUDIES OF SPECIMENS

After preparation of the specimens on the copper grids with carbon substrates, each specimen was viewed on the Philips 100 electron microscope. Observations were recorded, and micrographs were taken of areas which were representative of the specimen. Other micrographs were made of





Cross sectional area  $A = \pi r^2$

Applied Load  $P$  (lbs)

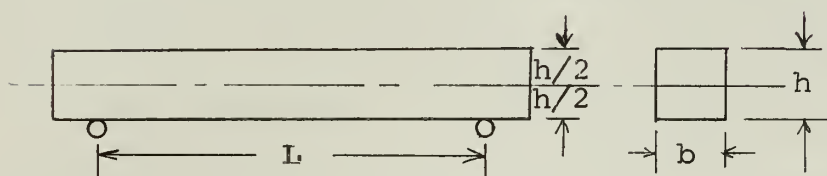
Compressive Strength (psi)

$$= \frac{P}{\pi r^2} \quad (r \text{ in inches})$$

For  $r = 1$  inch

$$\text{Comp. St.} = \frac{P}{3.14} \quad (\text{psi})$$

FIGURE 3.1

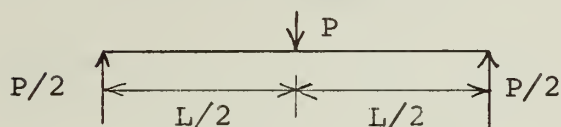


Simply Supported Beam

Flexural Strength (psi)

$$f = \frac{M y}{I}$$

$$y = h/2 \quad I = \frac{b h^3}{12}$$



Mid-Span Loading

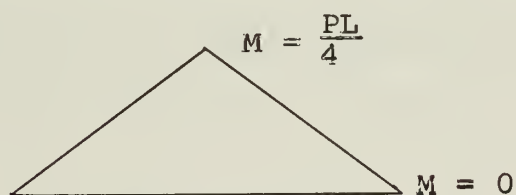
$$f = \frac{PL}{4} \cdot \frac{h}{2} \cdot \frac{12}{b h^3}$$

For  $L = 10$  inches

$b = 1$  inch

$h = 1$  inch

$$f = 15 P \quad (\text{psi})$$



Moment Diagram

FIGURE 3.2





areas which contained anything unusual or unique found while scanning the specimen. The specimens taken from each preparation at the different times were kept on filter paper in plastic petri dishes until a complete series of specimens at three hours, six hours, twenty-four hours, and seven days was obtained. Then the completed series was viewed on the Philips 200 electron microscope and micrographs taken. The reason for viewing the specimens on the Philips 100 electron microscope as soon as they were prepared and viewing only the completed series on the Philips 200 electron microscope was twofold. The availability of each electron microscope was quite different. The Philips 100 was readily available while the Philips 200 was available to only a limited degree. The operating procedures of the two microscopes was the second factor in their use in this thesis work. The Philips 100 was relatively simple to operate while the Philips 200 required an experienced operator. However, in order to build in the simpler characteristics of the Philips 100 some high resolution capability had been sacrificed, while the more complex Philips 200 had excellent high resolution capability. Therefore, the Philips 100 was used primarily for initial investigation of specimen internal structure and



for determination of what was representative in each. The Philips 200 was then used to investigate in greater depth areas not clearly identifiable using the Philips 100. The Philips 200 was also used to obtain clearer and more precise micrographs of the specimens than could be obtained using the Philips 100.

After all micrographs were obtained of specimens of the different preparations, these together with the recorded observations were used to compare the internal structures of the specimens and to relate their internal configurations with the results of tests performed on the macroscopic level.



## CHAPTER 4 - MACROSCOPIC RESULTS

In this chapter the results of macroscopic tests are presented and discussed. The areas of interest include compressive strength, flexural strength and modulus of elasticity.

### 4.1 COMPRESSIVE STRENGTH

The average values of compressive strength were obtained from the testing of from four to eight cylinders of each mix at curing ages of three, seven, and twenty-eight days. These results are presented in Table 4.1 and shown in Figures 4.1 and 4.2.

The test results show an increase in compressive strength of over 20% at all testing ages due to the addition of 300cc glycolic acid per sack of cement (mix 2). Furthermore, the per cent increase in compressive strength remains nearly constant for all testing ages. Test results for mix 3, with 150cc glycolic acid per each of cement, show slight increases in compressive strength, which are insignificant when compared with the strength increases observed in mix 2. Furthermore, test data (4) has shown that amounts of the admixture in excess of 300cc per sack of cement will achieve less than the maximum possible compressive strength increase. Therefore



TABLE 4.1

Average Cylinder Compressive Strength (psi)

Mix No.	Curing Age:			
		3 Days	7 Days	28 Days
1	(Control)	5900	6815	8750
2	(300cc Acid)	7300	8400	10,800
3	(150cc Acid)	6080	7150	8850
4	(5% Latex)	6180	7650	8350
5	(15% Latex)	5220	6500	7400





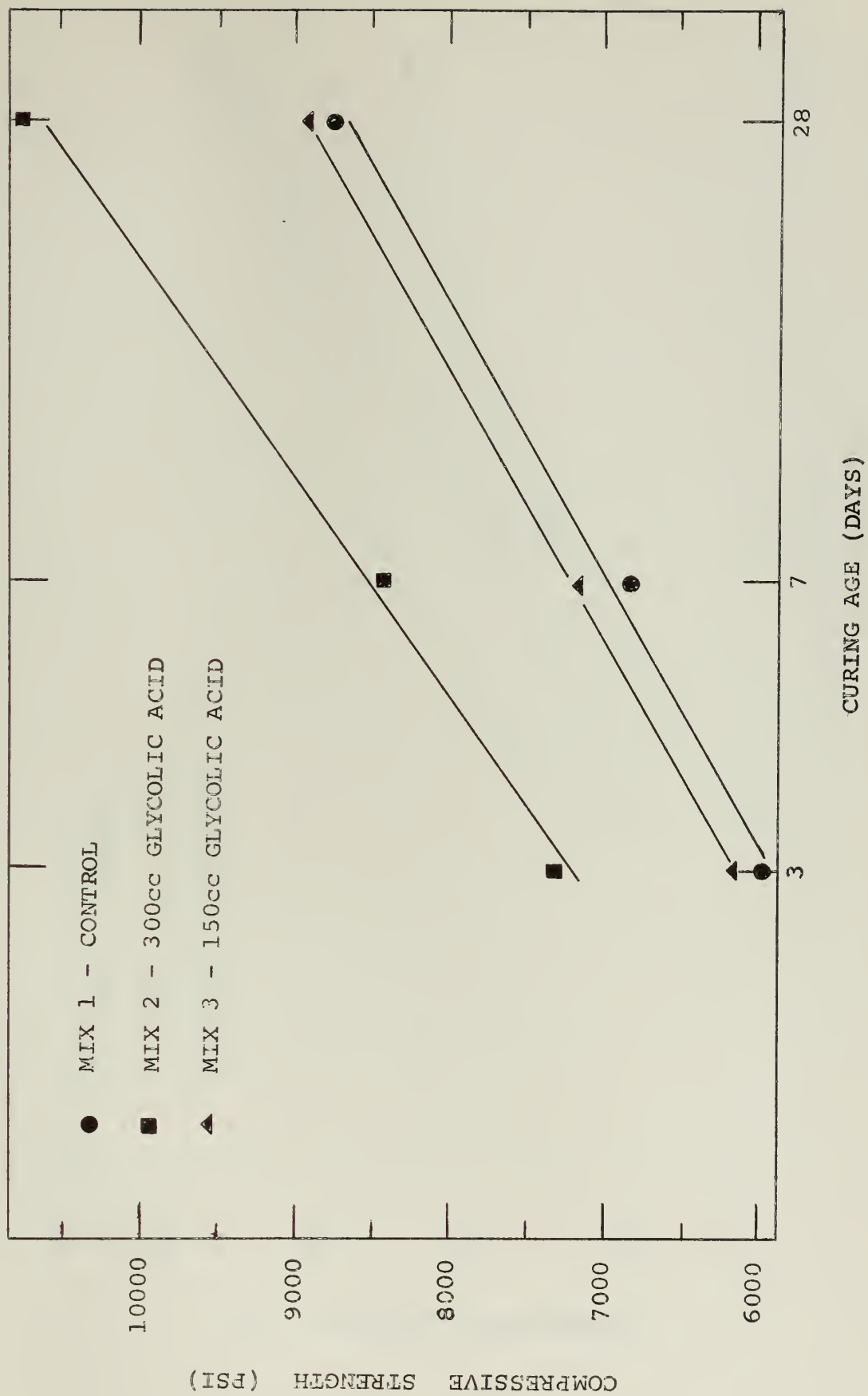


Figure 4.1 COMPRESSIVE STRENGTH VS. CURING AGE FOR GLYCOLIC ACID MIXES



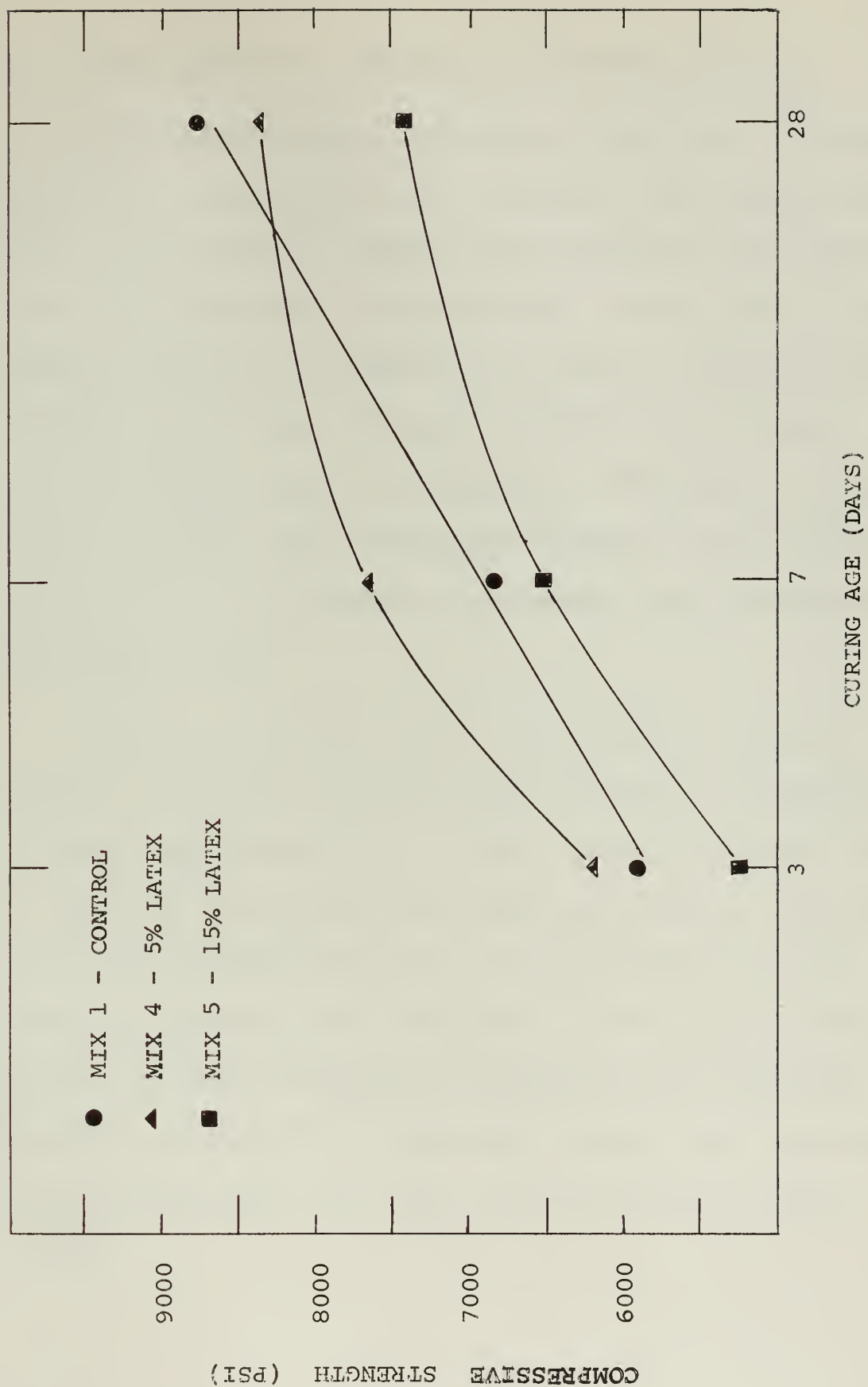


Figure 4.2 COMPRESSIVE STRENGTH VS. CURING AGE FOR LATEX MIXES



the optimum amount of admixture is somewhat critical.

Compressive strength increases on the order of 30% and better have been achieved (4) in concrete with glycolic acid. While such results are somewhat more impressive than the results just presented, it must be borne in mind that the compressive strength of concrete is not only a function of the strength of the cement but also a function of the bond strength between cement and aggregate. Therefore it is not possible to draw valid conclusions relative to the effects of glycolic acid in concrete based solely upon its effects in neat cement paste.

While glycolic acid achieved significant compressive strength increases, no significant increases in compressive strength were observed due to latex. Both latex mixes tend to level off in strength after about seven days. From conversations with Dow personnel it was learned that curing latex mix specimens under water has a deteriorative effect upon the ultimate compressive strengths of the specimens. The curves of Figure 4.2 apparently support this conclusion, since the specimens were cured under water until time of testing.



It has been shown (5) that latex mortar mixes give a considerable increase in compressive strength over that of a control mortar mix. In a control mix without any additives it has been shown (26) that the bond between the aggregate and cement paste matrix is the weakest point. Since the results presented here show no significant increase in the compressive strength of the cement paste mixes with latex, it is concluded that the latex strengthens the bond between the cement paste matrix and the aggregate of the mortar. A similar conclusion was also reached by Gutierrez (27). According to Wagner (22) the most important single variable effecting the compressive strength of latex mortars is the reduction in water requirement. Since the w/c ratio was the same for all mixes tested, these results appear to support in part Wagner's conclusion.

#### 4.2 FLEXURAL STRENGTH

The average values of flexural strength were obtained from the testing of from four to eight beams of each mix at curing ages of three, seven, and twenty-eight days. These results are presented in Table 4.2 and Figures 4.3 and 4.4.





TABLE 4.2

Average Beam Flexural Strength (psi)

Curing Age:		3 Days	7 Days	28 Days
Mix No.				
1	(Control)	810	930	1125
2	(300cc Acid)	540	1060	1280
3	(150cc Acid)	705	940	1170
4	(5% Latex)	987	1038	1080
5	(15% Latex)	1075	1120	1220



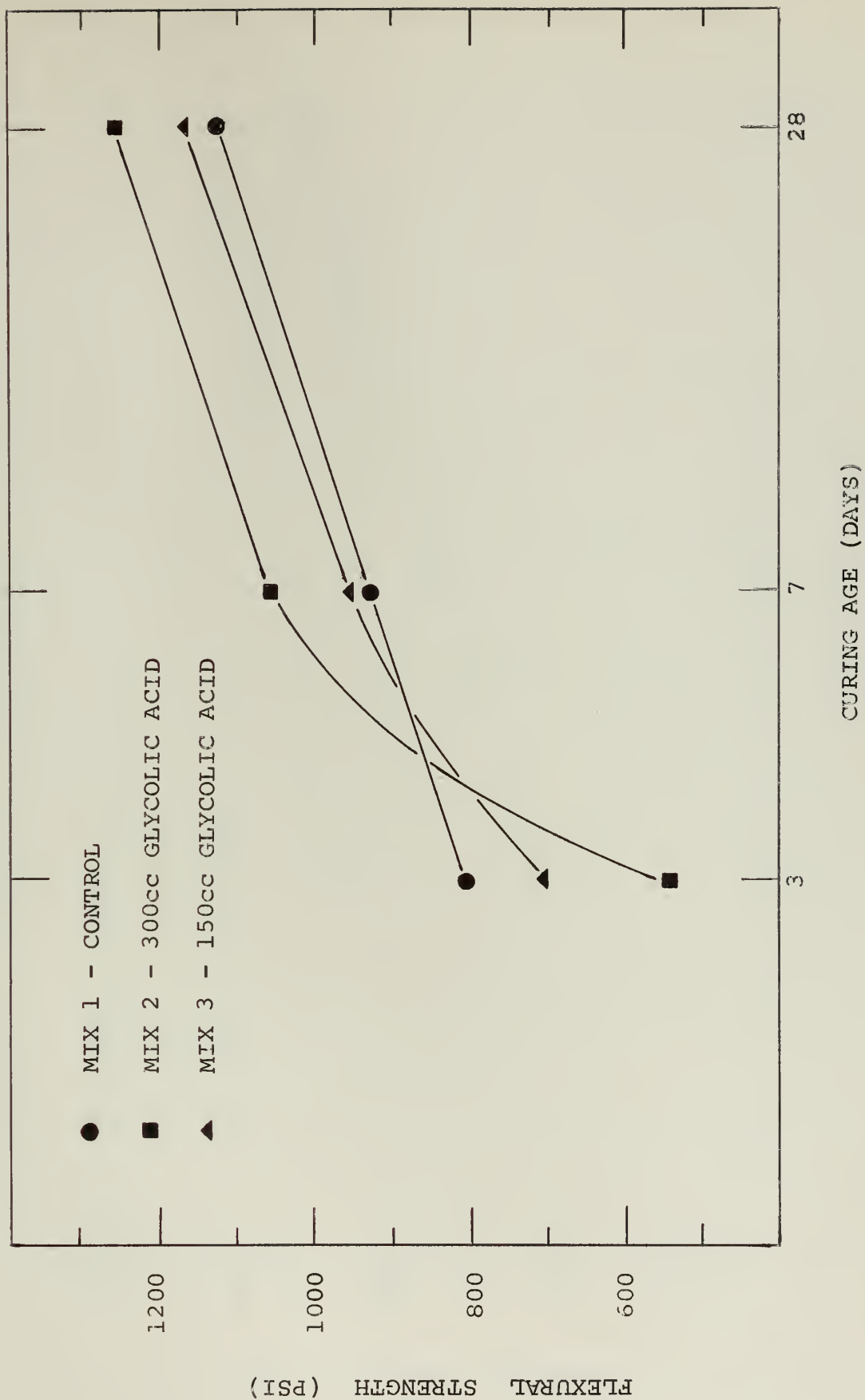


Figure 4.3 FLEXURAL STRENGTH VS. CURING AGE FOR GLYCOLIC ACID MIXES



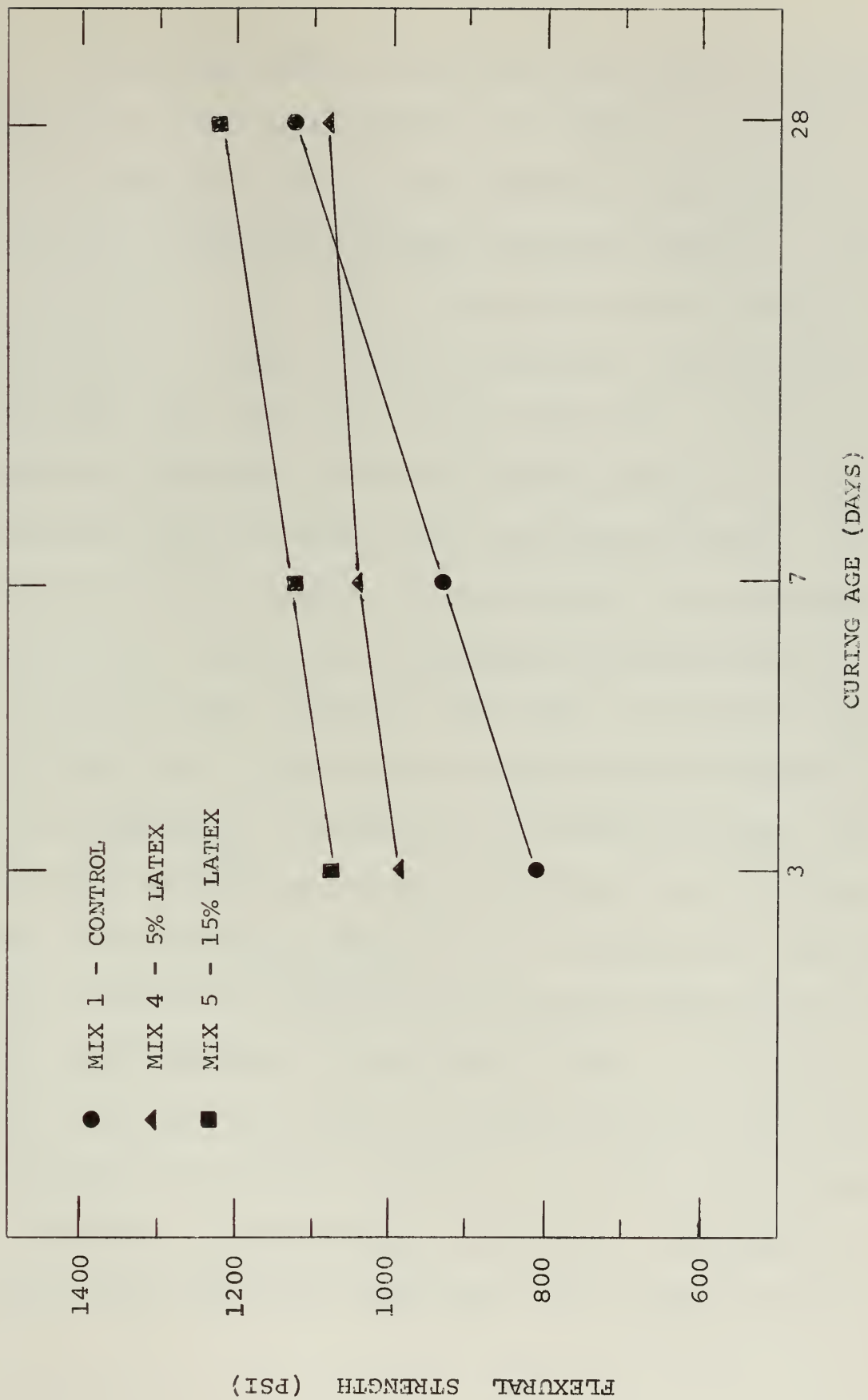


Figure 4.4 FLEXURAL STRENGTH VS. CURING AGE FOR LATEX MIXES



The overall effect of glycolic acid upon the flexural strength of neat cement paste is to increase it on the order of 10% or better, which is not nearly as significant as the comparable compressive strength increases achieved. Comparing Figures 4.1 and 4.3 it is apparent that the compressive and flexural strength curves are similar in appearance at age seven days and later. At age three days, however, the effects of glycolic acid upon flexural strength are markedly different than its effects upon compressive strength. The magnitude of the strength decrease in mix 2 is considered significant. Clearly the development of early flexural strength has been retarded in this case. It does not seem reasonable that an acceleration of compressive strength would be accompanied by a retardation of flexural strength. One plausible explanation for this phenomenon would be the result of preslurrying the mixes in the laboratory. The mixes for the beams and cylinders were prepared separately due to the size limitations of the electric mixer. It has been shown (23) that the effects of preslurrying time upon retardation are extremely critical. It is very possible that a difference in preslurrying time of only a fraction of a minute could have been responsible for delaying the set of





the beams. This effect could reasonably account for the low flexural strength of mix 2 at three days.

The effect of latex upon the ultimate flexural strength of neat cement paste is insignificant. This may be due to the deteriorative effect of curing latex specimens under water as discussed previously. The significant increase in the early flexural strength of mix 5 is probably due to the latex solids forming a continuous network throughout the cement paste, holding the material together as load is applied. Although there is a significant increase in the early flexural strength of mix 4, the increase is not as great as for mix 5. This would seem to indicate that the 5 per cent latex solids are not enough to form a continuous network throughout the mix. The area of latex structure and latex cement paste bond warrants further study.

#### 4.3 MODULUS OF ELASTICITY

The moduli of elasticity for mixes 1, 2, and 5 were determined from the loading of three cylinders of each mix in compression up to 10,000 pounds at curing age twenty-eight days. These results in the form of stress-strain curves are presented in Figure 4.5.



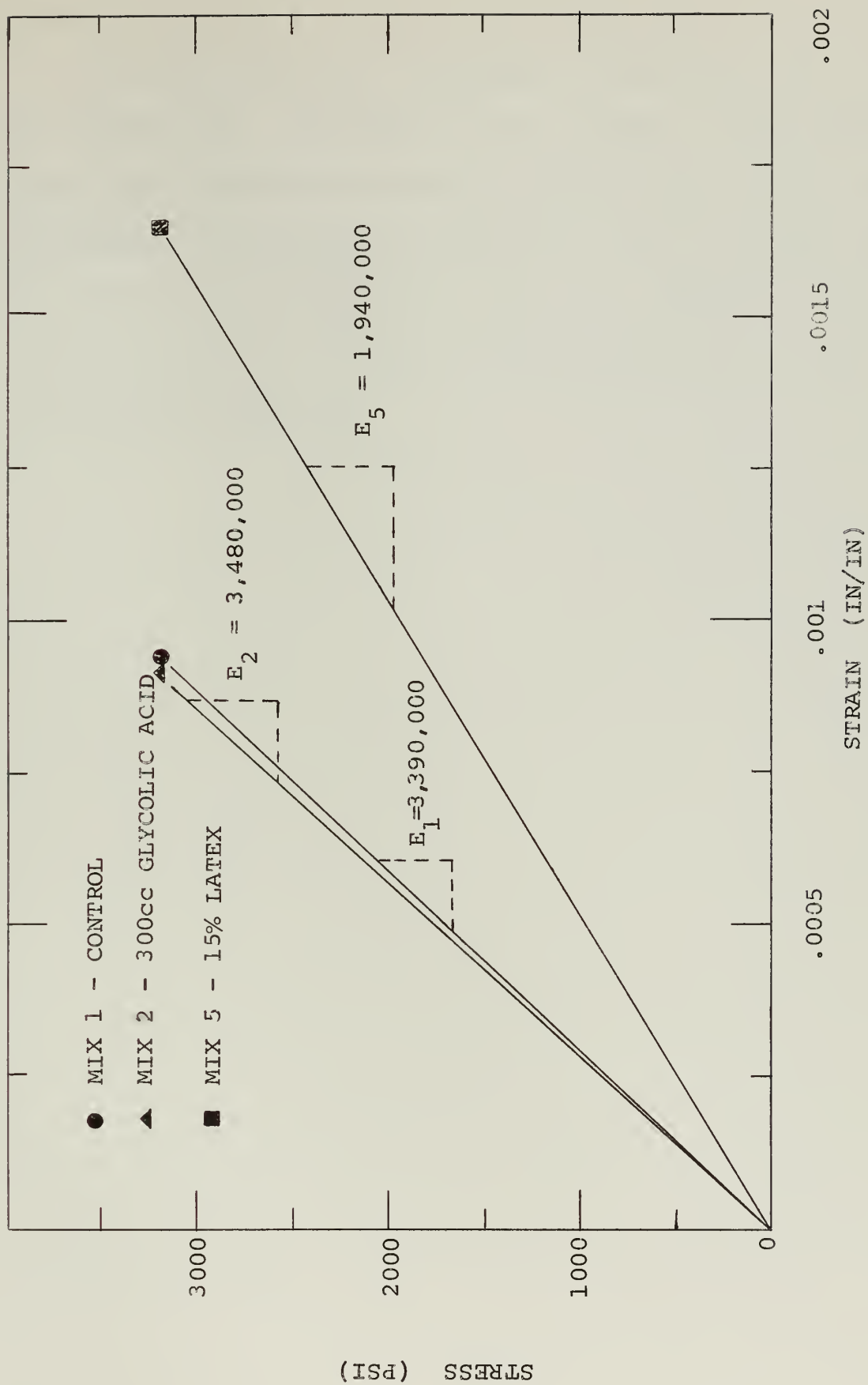


Figure 4.5 STRESS-STRAIN CURVES



The modulus of mix 2 is slightly greater than that of the control mix. The amount of the increase is not significant, but it remained essentially constant for all the tests conducted. The modulus of elasticity of mix 5 is about one half that of the control mix. This lower modulus of elasticity is probably a result of the ductile nature of the latex solids themselves.



## CHAPTER 5 - MICROSCOPIC RESULTS

In this chapter the results of microscopic studies are presented, in the form of electron micrographs, and discussed in detail. The concluding section of the chapter relates the microscopic results with the strength characteristics of the pastes, which were discussed in the previous chapter.

### 5.1 PRESENTATION OF RESULTS

All micrographs are presented in Appendix I. Figures 1 through 92(c) are micrographs of specimens hydrated in excess water. The specimens include tricalcium silicate, dicalcium silicate, tetracalcium aluminoferrite, tricalcium aluminate, and portland cement. Specimens were prepared alone, with latex, with glycolic acid, and in the case of tricalcium aluminate, with gypsum. Figures 93 through 101 are micrographs of specimens prepared from the powder of hardened cement pastes. Specimen preparation is in accordance with Section 3.3 and specimen identification is in accordance with Section 3.4. Micrographs were taken on both the Philips 100 and Philips 200 electron microscopes. Micrographs were selected based upon content and quality, regardless of which instrument was used.





In this chapter five significant groups of micrographs are presented for comparison of the effects of glycolic acid and latex upon the microstructure of portland cement and its major constituents (Figures 5.1, 5.3, 5.4, 5.5 and 5.7). Two additional groups of micrographs are also presented which illustrate the process of hydration in tricalcium aluminate ( $C_3A$ ) with glycolic acid (Figure 5.6) and tricalcium silicate ( $C_3S$ ) with excess glycolic acid (Figure 5.2).

## 5.2 DISCUSSION OF RESULTS

In this section the results of the microscopic studies of both the bottle-hydrated preparations and the hardened cement paste preparations are discussed.

### 5.2.1 GLYCOLIC ACID - BOTTLE HYDRATED PREPARATIONS

The following is a discussion of the effects of glycolic acid upon the microstructure of bottle-hydrated preparations.

a. Hydration of  $C_3S$  - Tricalcium Silicate. At three hours in the hydration process the characteristic hydration products observed were in the form of foils and fibers. The presence of glycolic acid had no significant effects, except that the excess acid might account for the needles seen in the early stages of development



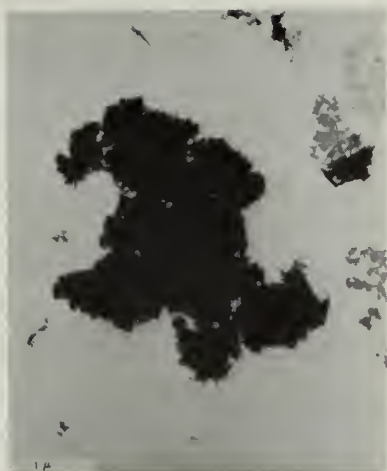
in Figure 9.

At six hours, many tiny needles or fibers formed. No significant effects due to the addition of a normal amount of acid were observed, other than the formation of a few cigar-shaped bundles of fibers. However, the addition of excess acid created numerous cigar-shaped hydration products.

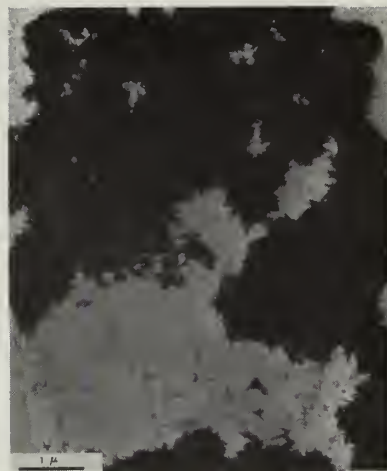
At twenty-four hours a normal addition of acid resulted in the presence of longer and more numerous fibers. In fact, the entire specimen shown in Figure 7(a) could consist of undispersed bundles of fibers in a more advanced stage of development as compared with the untreated  $C_3S$  specimen. The addition of excess acid created remarkably large needles of tobermorite gel, as seen in Figures 11(a) and 11(b). These needles themselves appear to be bundles of smaller needles. The excess acid apparently accelerated the growth of the needles at a rapid rate. See Figure 5.1 for comparison of the effects of glycolic acid at twenty-four hours.

Finally, at seven days, a normal addition of acid gave a slightly more fibrous appearance to the specimen, as seen in Figure 8(a). Once again large needles

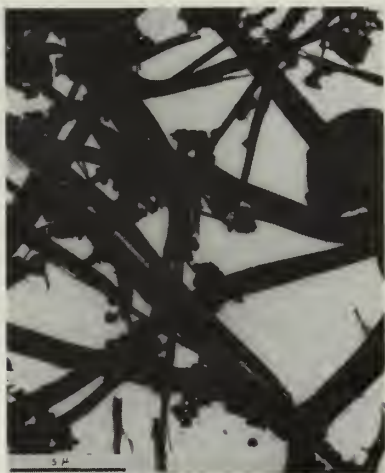




a



b



c



d

Figure 5.1. The Effects of Admixtures on the Microstructure of  $C_3S$  at 24 Hours. (a)  $C_3S$  Alone, (b)  $C_3S$  with Glycolic Acid, (c)  $C_3S$  with Excessive Glycolic Acid, (d)  $C_3S$  with Latex.



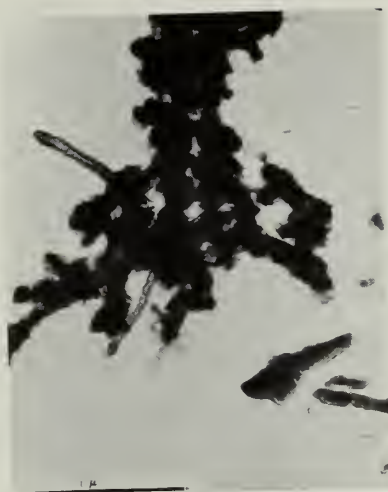
developed in the presence of excess acid, as Figure 12 illustrates. See Figure 5.2 for an illustration of the hydration process in  $C_3S$  with excess glycolic acid:

The results indicate a possible acceleration in the growth of the needles of the tobermorite gel phase due to the addition of a normal amount of acid in excess water. However, the addition of excess acid in order to maintain a water-acid ratio comparable to that of an actual paste results in a most significant acceleration of needle growth. On the basis of these results it appears that glycolic acid does, to a certain extent, accelerate the growth of tobermorite gel needles.

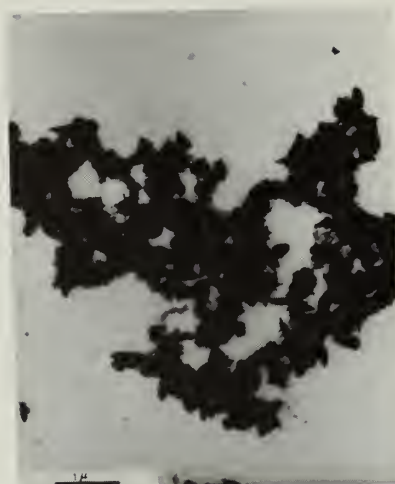
b. Hydration of  $C_2S$  - Dicalcium Silicate. At three hours the microstructure of  $C_2S$  hydrated alone and that of  $C_2S$  hydrated with glycolic acid appear to have about the same hydration products, with the exception of small fibrous particles observed in the acid sample, Figure 21(a). Also, the bundles of fibers observed in both microstructures seem to be more loosely connected in the acid sample, as seen in Figure 21(b). This behavior would seem to indicate some acceleration of the hydration process as the bundles of fibers later break up to become



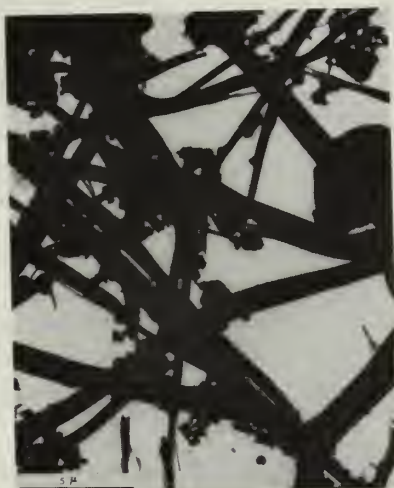




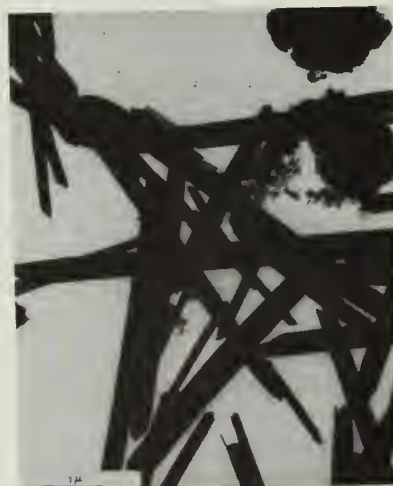
a



b



c



d

Figure 5.2. The Hydration of  $C_3S$  with Excessive Glycolic Acid. (a) The Microstructure at 3 Hours, (b) The Microstructure at 6 Hours, (c) The Microstructure at 24 Hours, (d) The Microstructure at 7 Days.



fibrous foil-like particles.

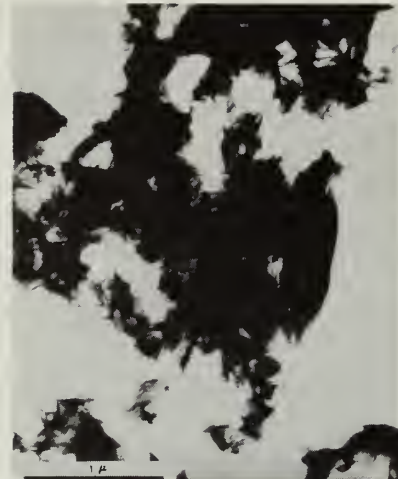
At six hours, the bundles of fibers in  $C_2S$  alone appeared to be composed of long needles, while in  $C_2S$  with a normal amount of acid the bundles were composed of fine fibers. These different bundles can be seen in Figures 18(a) and 22(b). The effect of the excess acid was to give the internal structure the appearance of a foil-like structure as seen in Figures 26(a) and 26(b).

After twenty-four hours of hydration, the internal structure of  $C_2S$  hydrated alone consisted mostly of foils with some needles and bundles of fibers. The addition of a normal amount of acid resulted primarily in foils of a fibrous nature and some bundles of fibers. The excess acid specimen consisted almost entirely of foils. Some foils were fibrous (Figure 27(a) ) and others were of a more open, less distorted texture (Figure 27(c) ). Figure 27(b) shows the open foils as they are beginning to cover the needle. Again, the behavior of the foil formation of the acid samples indicates some acceleration of the hydration process in  $C_2S$ . See Figure 5.3 for a comparison of the effects of glycolic





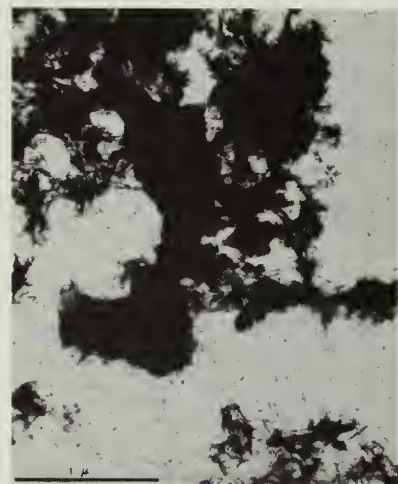
a



b



c



d

Figure 5.3. The Effects of Admixtures on the Microstructure of  $C_2S$  at 24 Hours. (a)  $C_2S$  Alone, (b)  $C_2S$  with Glycolic Acid, (c)  $C_2S$  with Excessive Glycolic Acid, (d)  $C_2S$  with Latex.



acid on the hydration of  $C_2S$  at twenty-four hours.

After seven days the internal structures of all three samples,  $C_2S$ ,  $C_2S$ -HA, and  $C_2S$ -HA(EX), had about the same morphology.  $C_2S$  and  $C_2S$ -HA had a microstructure composed primarily of fine fibrous foils, while  $C_2S$ -HA(EX) had a microstructure of foils of a more open, less distorted texture. For comparison of these foils, see Figures 20(b), 24(a), and 28. However, all the microstructures were nearly the same, indicating that the effect of the acid was mainly to accelerate the hydration process in  $C_2S$ , with the result that the foils developed from excess acid were more open than the foils of the other two samples.

In conclusion, it seems that glycolic acid's main effect on the hydration process of  $C_2S$  is of an accelerating nature, with the excess amount of acid altering somewhat the physical appearance of the foils.

c. Hydration of  $C_4AF$  - Tetracalcium Aluminoferri-ferite. At three hours the effect of a normal amount of glycolic acid on the hydration of  $C_4AF$  was to cause the formation of many more plates (Figure 37) than were formed in  $C_4AF$  hydrated alone (Figure 33). As seen in Figure 41, the







addition of an excess amount of the acid caused the hydration products of  $C_4AF$  to be very irregular in shape and to have a very textured surface.

At six hours the glycolic acid had essentially the same effect on  $C_4AF$  hydration as it did at three hours. The normal amount of acid did cause the hydrogarnet crystals to be much smaller than those in  $C_4AF$  hydrated alone. This behavior indicates a retarding effect of the acid on  $C_4AF$ , since the hydrogarnet crystals are known to form after the plates have formed, until they reach an equilibrium with the plates. Some of the irregularly shaped, textured surface particles, in the excess acid specimens seen at three hours, had hexagonal angles. No hydrogarnet crystals were observed. This behavior indicates some type of chemical reaction by the acid with the plates, either retarding the development of the plates or attacking the plates after they have formed. In Figures 42(a) and 42(b) these effects can be seen.

At twenty-four hours the effect of the normal amount of acid was to retard the formation of the hydrogarnet crystals. The excess acid gave no hydrogarnet crystals



at all and still caused the plates to have a shredded appearance. But at twenty-four hours the plates have a somewhat less textured surface than before. Figure 5.4 shows the twenty-four hour specimens for comparison purposes.

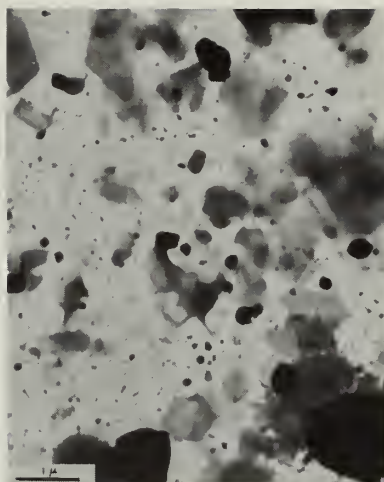
After seven days of hydration, the normal amount of acid still retarded the formation of the hydrogarnet crystals to some extent and gave the plates a more textured surface than before (Figure 40). The excess acid, on the contrary, caused the microstructure to consist of shredded plates with surfaces full of holes. (See Figures 44(a) and 44(b) ).

In summary, it seems that the effect of glycolic acid used in normal amounts is to considerably retard formation of the hydrogarnet crystals in the earlier stages of hydration (up to seven days) and, at about seven days, to attack the plate surfaces, giving them a rough, textured appearance. The excess acid seems to magnify the effects of the normal amount of acid by attacking the surfaces of the plates from the beginning of hydration, and by completely preventing the formation of hydrogarnet crystals up to seven days of hydration.

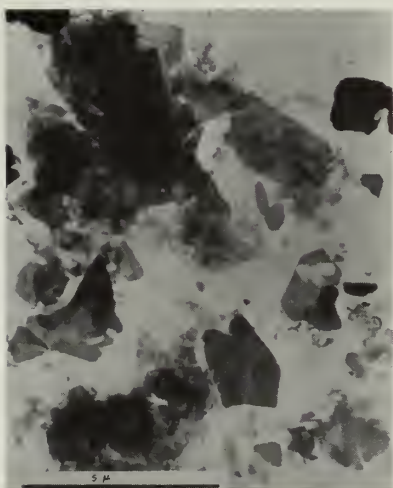




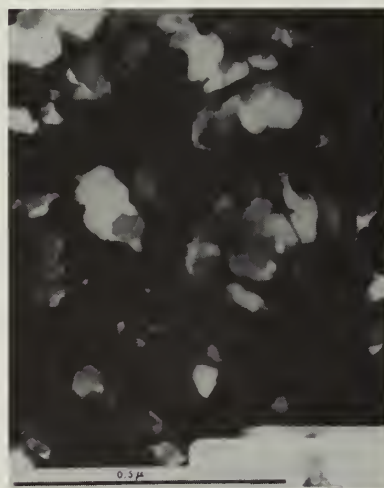
a



b



c



d

Figure 5.4. The Effects of Admixtures on the Microstructure of  $C_4AF$  at 24 Hours. (a)  $C_4AF$  Alone, (b)  $C_4AF$  with Glycolic Acid, (c)  $C_4AF$  with Excessive Glycolic Acid, (d)  $C_4AF$  with Latex.



d. Hydration of  $C_3A$  - Tricalcium Aluminate. At three hours in the hydration process the untreated specimen consisted of sheets or plates, for the most part, and several isometric forms assumed to be hydrogarnet crystals. A normal addition of acid appeared to result in a greater number of plates and to retard the formation of the hydrogarnet phase, although a few small isometric forms were observed. In the presence of excess acid some broken plates were observed, but most of the structure resembled torn or crumpled sheets. In addition, the excess acid completely suppressed formation of the hydrogarnet phase.

At six hours the development of the hydrogarnet phase had advanced considerably in the untreated specimen and to a lesser degree in the presence of a normal amount of acid. The plate phase was still the major constituent of both specimens, however. In the presence of excess acid the hydrogarnet phase continued to be suppressed; nevertheless, more plates and pieces of plates had developed. The major constituent was still in the form of crumpled sheets, as seen in Figure 58(a).





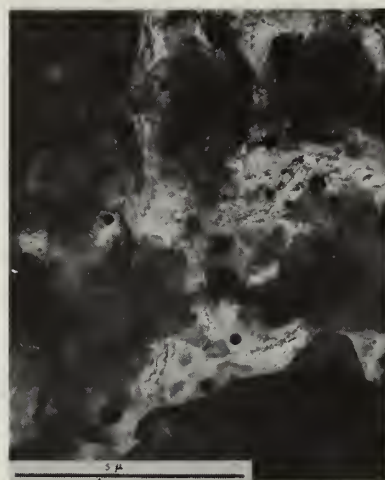
At twenty-four hours the hydrogarnet phase had developed to a greater extent in both the untreated specimen and the specimen containing a normal amount of glycolic acid, as Figure 55 illustrates. However, as shown in Figure 59, in the presence of excess acid the specimen consisted entirely of plates and pieces of plates. The crumpled sheets were no longer present and none of the hydrogarnet phase had developed. Many of the plates were textured, possibly containing holes. For comparison of the effects of the acid on  $C_3A$  at twenty-four hours see Figure 5.5.

Finally, at seven days, the plate phase and the hydrogarnet phase had achieved an equilibrium in the untreated specimen (see Figure 52), while a normal addition of acid reduced the size and number of hydrogarnet crystals (see Figure 56). Furthermore, the plates were more numerous and more textured than in the untreated specimen. The addition of excess acid completely eliminated the hydrogarnet phase. The specimen, as seen in Figure 60, was composed entirely of plates and pieces of plates of various sizes with highly textured surfaces. The plates appeared to be full of small holes, giving the

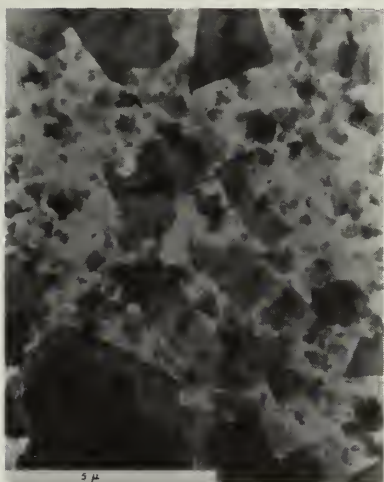




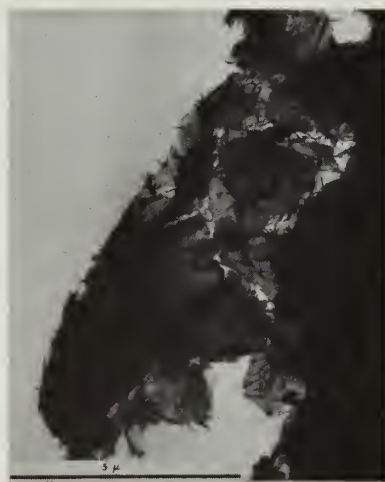
a



b



c



d

Figure 5.5. The Effects of Admixtures on the Microstructure of  $C_3A$  at 24 Hours. (a)  $C_3A$  Alone, (b)  $C_3A$  with Glycolic Acid, (c)  $C_3A$  with Excessive Glycolic Acid, (d)  $C_3A$  with Latex.



textured appearance. See Figure 5.6 for an illustration of the hydration process in  $C_3A$  with glycolic acid.

The results indicate that glycolic acid suppresses the formation of hydrogarnet crystals. In small amounts it reduces them in number and size, while in large amounts it completely eliminates them. In large amounts the acid apparently retards the formation of plates. Furthermore, the acid appears to cause holes or textured surfaces in the plates in proportion to the amount of acid present.

e. Hydration of  $C_3A$  - Tricalcium Silicate and  $CaSO_4$  - Gypsum. At three hours the majority of the hydration products were in the form of broken or irregularly shaped plates as seen in Figure 65(a). A few rods or fibers were observed, but none of the hydrogarnet phase was present. A normal addition of glycolic acid produced the rods or fibers observed in Figure 69(a), leaving the plate phase unaltered. Finally, in the presence of excess acid, a significant change in morphology occurred. In addition to rod and plate phases, a phase of small dark globules formed, as well as a phase resembling shredded or crumpled sheets (see Figure 73(a)).

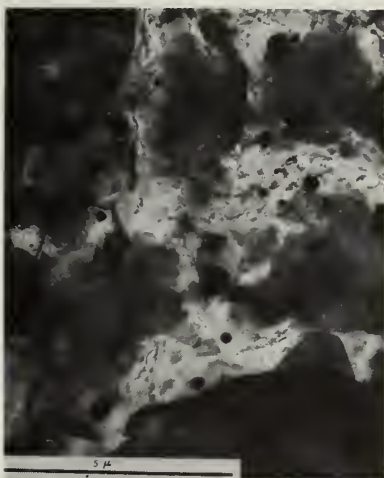




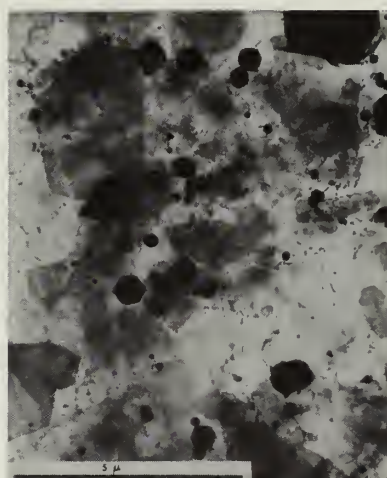
a



b



c



d

Figure 5.6. The Hydration of  $C_3A$  with Glycolic Acid. (a) The Microstructure at 3 Hours, (b) The Microstructure at 6 Hours, (c) The Microsturcture at 24 Hours, (d) The Microstructure at 7 Days.







Figure 73(b) reveals a lacy structure of holes in the rods and dark globules.

At six hours the untreated specimen consisted entirely of plates and pieces of plates. They were much more fully developed with many having distinct hexagonal edges. The specimen containing a normal addition of acid retained only a few rods and consisted almost entirely of the plate phase (see Figure 70(a) ). The lacy structure of some of these plates is shown in Figure 70(b). In the presence of excess acid, the specimen retained much the same structure as was observed at three hours.

At twenty-four hours no significant change could be observed in the untreated specimen. Likewise, a normal addition of acid produced no significant change over the comparable six-hour specimen, except for the fact that the rods had completely disappeared. Once again a lacy structure can be observed in the plates of Figure 71(b). An excessive amount of acid bore results similar to the comparable six-hour specimen (see Figure 75(a) ), except that the number of rods had greatly diminished.



At seven days the untreated specimen shown in Figure 68 again consisted almost entirely of plates, except for the appearance of several tiny black shapes which were probably isometric hydrogarnet crystals. A normal addition of glycolic acid created a similar specimen (see Figure 72), consisting primarily of plates as well as several tiny black shapes. No significant difference in plate texture was apparent. With an addition of excess acid no significant change in morphology was apparent over the comparable six-hour specimen. Plates and pieces of broken plates were visible, as well as crumpled and shredded plates or sheets, perhaps a few rods, and what appeared to be partially rolled plates.

In summary, other investigators (8) have determined that the initial hydration product of  $C_3A$  and gypsum is in the form of rods, which quickly decompose to form plates. A normal addition of acid apparently retarded the hydration of  $C_3A$  and gypsum, in that many rods were observed at three hours with acid present while most rods had apparently decomposed in the untreated specimen taken at three hours. No apparent difference in the morphology of the hydration products could be detected at ages in



excess of six hours. Excess acid, however, was responsible for significant changes in the appearance of the plate phase. Much of the plate phase appeared crumpled or shredded even at seven days. The rods had not completely disappeared and many plates appeared partially rolled up. Thus it is conceivable that the rods unroll to form plates rather than decompose. Finally, as discussed earlier in this section, there is some evidence to indicate that the acid may be partially responsible for the lacy structure observed in some plates. The holes in the plates appeared to be larger in some cases due to the action of the acid, although the evidence is inconclusive.

f. Hydration of Portland Cement. After three hours of hydration the only differences in the internal structures of samples PC, PC-HA, and PC-HA(EX), are the holed surface texture of the plates observed in the PC-HA and PC-HA(EX) samples. These holes are probably due to the effects of the glycolic acid as seen previously in the  $C_3A$  and  $C_4AF$  samples.

At six hours the plates of the sample with the normal amount of acid have taken on a mottled appearance while



the plates in the sample with excess acid still retain a holed, textured surface. Evidence of crumpled foils or plates appeared in portland cement alone. The acid seems to have a definite effect on the plate phases of portland cement. Needles of PC and PC-HA samples appeared about the same in size and number while the needles of the PC-HA(EX) sample appeared to be more numerous and generally thinner in size. Thus the excess acid seems to accelerate the formation of more and finer needles than form in PC alone.

After twenty-four hours the needles seen in the microstructures of the three samples were considerably different. Needles in the PC-HA sample were longer and more numerous than in PC alone while the needles in the PC-HA(EX) sample were much more numerous than seen in either of the other samples. Fibrous foils appeared in samples PC-HA and PC but not in the PC-HA(EX) sample. This would seem to indicate that the excess acid retarded the formation of the foils while accelerating the needle formation. The normal amount of acid seemed to accelerate both the formation of the foils and the needles as seen in Figures 79(a) and 83. See Figure 5.7 for





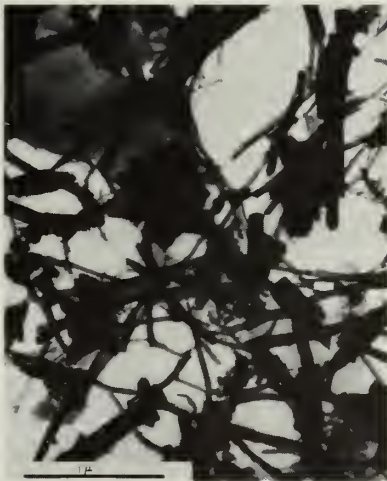




a



b



c



d

Figure 5.7. The Effects of Admixtures on the Microstructure of Portland Cement at 24 Hours.  
 (a) Portland Cement Alone, (b) Portland Cement with Glycolic Acid, (c) Portland Cement with Excessive Glycolic Acid, (d) Portland Cement with Latex.



comparison of the effects of glycolic acid on portland cement at twenty-four hours.

After seven days of hydration approximately the same general differences existed in the microstructures of the three samples as those observed at twenty-four hours. One exception was the appearance of foils in the PC-HA(EX) sample which were not present at twenty-four hours. However, these foils were present to a lesser degree than those seen in PC-HA and PC samples. Again, the foils of the PC-HA sample were more prevalent than those observed in PC alone. The needles in the PC-HA(EX) sample were far more numerous than in either of the other samples. Again, approximately the same conclusions are drawn for seven days as for twenty-four hours. Typical micrographs of these samples are shown in Figures 80(b), 84, and 88(a).

In general, glycolic acid in normal amounts seems to accelerate the formation of needles and foils of the C-S-H phase in portland cement hydration, while in excess amounts it accelerates the needle formation, only to retard the formation of the foils. In either amount the acid seems to have a reaction with the plates of the



C-A-H phase giving them a holed, textured surface or mottled appearance. The texture of the needles appears to remain unaffected by the acid. Needles with textured surfaces are seen in Figures 80(a) and 86(b). Needles with tiny dark spots in their textured surfaces are seen in Figures 79(b), 82, and 88(b).

g. Summary of Results. While an excess amount of acid clearly accelerated growth of needles of the tobermorite gel phase in  $C_3S$ , the accelerating effect of a normal addition of acid was much less conclusive. However, it did appear that glycolic acid accelerated needle growth and development in  $C_3S$  to a certain extent.

Similarly, an accelerating effect was apparent in  $C_2S$ , in that the bundles of fibers formed and began breaking up earlier as a result of the acid. Furthermore, the acid modified to a certain degree the appearance of the foils, the final product of hydration observed in  $C_2S$ .

The effects of glycolic acid on  $C_3A$  and  $C_4AF$  were similar. The acid retarded or completely suppressed the formation of the hydrogarnet phase in proportion to the amount used. Furthermore, in large amounts it



appeared to retard the formation of distinct hexagonal plates. In addition it appeared to impart a lacy structure of holes to many of the plates when used in larger amounts, although these results are not considered conclusive.

Probably of greater importance was the effect of the acid upon  $C_3A$  in the presence of gypsum, since gypsum reacts with  $C_3A$  in portland cement. Gypsum alone has been seen to suppress formation of the hydrogarnet phase and to cause the formation of rods as the initial product of hydration. These rods later decompose and plates begin to form. Glycolic acid retarded the development of the plate phase and extended the duration of the rod phase. In larger amounts it extended the duration of the rod phase even longer and retarded the development of distinct hexagonal plates, leaving much of the plate phase crumpled or shredded.

Finally, all of the previous results were observed to a greater or lesser degree in portland cement. The acceleration of the growth and development of the needles due to excess acid was readily apparent. And in the presence of excess acid the plates of the C-A-H phase appeared







shredded and torn as observed in the hydration of  $C_3A$  with gypsum. Normal additions of acid appeared to accelerate the development of both needles and foils. And, in general, addition of acid appeared to impart a textured surface of holes to the plates of the C-A-H phase.

Blank, Rossington and Weinland (24) concluded that certain retarding admixtures adsorb on the hydration products of  $C_3A$  and  $C_4AF$  with negligible adsorption, initially at least, on  $C_3S$  and  $C_2S$  in water. However, Bruere (23) has shown that when a portland cement paste is preslurried before the addition of a retarding admixture the  $C_3A$  is unable to adsorb the admixture due to the action of gypsum. As a result much of the admixture is available to react with the silicate components. The effects of glycolic acid have been observed to a greater or lesser degree in all of the components of portland cement including  $C_3A$  with gypsum, although this preparation was preslurried for only a short time - on the order of 10 seconds. Thus, it would appear that some adsorption of admixture does occur on all the component phases of portland cement.



### 5.2.2 DOW LATEX 464 - BOTTLE HYDRATED PREPARATIONS

The following is a discussion of the effect of latex upon the microstructure of bottle-hydrated preparations.

a. Hydration of  $C_3S$  - Tricalcium Silicate. At three hours in the hydration process, as seen in Figure 13, a coating of latex covered the characteristic foils and fibers observed in the untreated specimen. At six hours the latex coating was not so dense and revealed more of the structure of the specimen as seen in Figure 14(a). In general, no changes could be observed in the morphology of the hydration products. The cause of the mottled texture of the fibers seen in Figure 14(b) is not clear. At twenty-four hours the fibrous structure of Figures 15(a) and 15(b) strongly resembled that of the untreated specimen (see Figure 5.1). Only small amounts of latex could be detected in this specimen. Finally, at seven days, the fibrous nature of the hydration products remained unchanged in the presence of latex when compared with the untreated specimen.

b. Hydration of  $C_2S$  - Dicalcium Silicate. At three hours of hydration nothing was visible in the latex



preparation except the structured latex throughout the sample. The hydration products that did exist were coated with latex and not visible on the electron microscope.

After six hours the latex sample contained foils, probably of the C-S-H[I] phase, and latex as seen in Figure 30. Some of these foils were observed in  $C_2S$  hydrated alone (Figure 18(c) ), but most of the internal structure of  $C_2S$  alone consisted of long needles and bundles of needles (see Figure 18(a) ). Since the foils form later in the hydration of  $C_2S$  as the needles break up, this would seem to indicate an acceleration of the hydration process in the  $C_2S$  sample with latex.

After twenty-four hours the microstructure of  $C_2S$  with latex was still primarily made up of foils and latex (see Figure 5.3). In  $C_2S$  alone foils were beginning to form, but bundles of fibers and needles still existed as seen in Figures 19(a) and 19(b). As at six hours, this would seem to indicate some acceleration of the hydration process.

After seven days of hydration, the microstructures of both  $C_2S$  hydrated alone (see Figures 20(a) and 20(b) )



and  $C_2S$  hydrated with latex (see Figure 32) appeared to have about the same hydration products present. The products consisted mainly of foils and some rectangular block crystals with structured latex visible in the latex preparation.

In general, it seemed that latex accelerated the formation of the foils in the hydration of  $C_2S$  until about seven days when the microstructures of both  $C_2S$  hydrated alone and  $C_2S$  hydrated with latex were similar.

c. Hydration of  $C_4AF$  - Tetracalcium Aluminoferrite. At three hours of hydration the microstructures of the preparations of  $C_4AF$  alone and of  $C_4AF$  with latex can be observed in Figures 33 and 45. The primary hydration products in both were the hexagonal plates of the C-A-H phase. However, in Figure 45 the latex structure which predominated in the microstructure can be seen.

After six hours of hydration, the hexagonal plates seen at three hours were still present in both microstructures as seen in Figures 34(a) and 46. However, after six hours small, dark isometric shaped particles appeared in both microstructures. These particles were probably hydrogarnet crystals. Again, as at three hours,





the only apparent difference in the two microstructures was the latex structure seen throughout the latex specimen.

After twenty-four hours of hydration the dark isometric shaped particles had increased in number and size in the  $C_4AF$  sample hydrated alone. However, due to the latex structure in  $C_4AF$  with latex it was impossible to distinguish anything about the isometric shapes. Hexagonal plates appeared in both microstructures. Micrographs of the samples are presented in Figure 5.4.

By seven days of hydration the microstructure of  $C_4AF$  hydrated alone had developed into fifty per cent thin hexagonal plates of the C-A-H phase and fifty per cent dark isometric shaped hydrogarnet crystals. Figure 36 shows this microstructure. Again, as at twenty-four hours, the latex structure of  $C_4AF$  with latex prevented any recognition of the relative amounts of the plates and isometric shapes. The plates are visible in Figures 48(a) and 48(b) with some isometric shapes visible in Figure 48(b).

In conclusion the addition of latex to  $C_4AF$  seemed to have no effect on the hydration products of  $C_4AF$ ,



either by type or amount. Due to the latex structure obscuring many of the hydration products, difficulty in distinguishing the hydration products did arise, but nothing other than plates and isometric shapes were observed in more dispersed areas. In general, the only effect latex seems to have is to coat everything and form a network of latex throughout the internal structure of  $C_4AF$ .

d. Hydration of  $C_3A$  - Tricalcium Aluminate. At three hours the only discernible hydration products were plates and many small rods or fibers as seen in Figure 61, all of which are coated with latex. None of the hydrogarnet phase observed in the untreated specimen was observed at three hours. Of great significance were the presence of the rods which were not observed in any of the untreated specimens and which have been observed by other researchers only in the presence of gypsum (8).

At six hours the morphology of the latex specimen is not significantly changed, except that the number of rods present has diminished considerably as seen in Figure 62. The undispersed dark masses may contain hydrogarnet crystals, but none of them were clearly observed in the specimen.



At twenty-four hours numerous rods and plates were seen. Once again none of the hydrogarnet phase observed in the comparable untreated specimen could be observed (see Figure 5.5). Its presence in the undispersed dark areas remains a possibility.

Finally, at seven days, the hydrogarnet phase appeared in the latex specimen and the rods completely disappeared. The specimen, as seen in Figure 64(a), is well coated with latex. The plate phase appeared to predominate in this specimen, while in the comparable untreated specimen the plates and hydrogarnet crystals were present in about equal amounts.

In summary, the latex was apparently responsible for a change in the morphology of the hydration products, indicating some sort of a chemical interaction with tri-calcium aluminate, in addition to the obvious physical coating action of the latex. Rods and fibers of the C-A-H phase have been observed (8) as the first product of hydration when a small amount of gypsum is added to  $C_3A$ . In a short time the rods decompose and plates begin to form. The latex has apparently caused a similar reaction. However, the fibrous phase retained its morphology in excess of twenty-four hours in the presence of



latex, while it quickly decomposed in the presence of gypsum. Furthermore, in the presence of latex the development of the hydrogarnet phase appeared to be considerably retarded.

e. Hydration of Portland Cement. At three hours of hydration the only noticeable difference between the microstructures of portland cement hydrated alone and portland cement hydrated with latex, other than the latex structure, was the presence of longer needles in the latex sample.

After six hours, the microstructures of the two samples appeared about the same in terms of hydration products. In the latex sample the latex structure seemed to coat everything. Some evidence of crumpled foils appeared in portland cement alone and a few isometric shaped particles were observed in portland cement with latex.

After twenty-four hours no significant differences in the two microstructures were observed. More hexagonal plates seemed to be present in the latex sample, but otherwise both microstructures consisted of needles, foils, hydrogarnet crystals, and hexagonal plates. Representative micrographs are presented in Figure 5.7.







Again, after seven days, both microstructures appeared the same, consisting of plates, fine fibrous foils, and long needles. See Figures 80(a), 80(c), and 92(a), 92(b), 92(c) for micrographs of the internal structures.

In conclusion, no significant differences in microstructure, other than the physical coating of latex, were observed at any stage of hydration.

f. Summary of Results. For the most part the effect of latex seems to be physical in nature with the latex coating the hydration products as seen in the microstructures of the specimens. This type of physical behavior was observed in samples taken from the preparations of latex with portland cement and its four major compounds. However, in the preparations of latex with  $C_2S$  and  $C_3A$  the latex apparently was responsible for a change in the morphology of the hydration products in addition to the previously mentioned coating action.

In the case of  $C_2S$ , latex appeared to have accelerated the formation of the final hydration product of the C-S-H phase. However, at seven days of hydration both the microstructure of  $C_2S$  with latex and  $C_2S$  alone



were composed of the same hydration products. These included foils and some rectangular block crystals. Thus, the latex effect was still a physical one, responsible for acceleration of the hydration of  $C_2S$  probably due to the latex solids retaining water needed for hydration.

In  $C_3A$  the latex was responsible for a change in the morphology of the hydration products, which was due to some sort of chemical reaction with  $C_3A$ . In the  $C_3A$  samples latex caused the formation of a fibrous phase similar to the first hydration products produced when gypsum is added to  $C_3A$ . However, the fibrous phase formed by gypsum quickly decomposes, but the fibrous phase produced in the presence of latex retained its morphology in excess of twenty-four hours. In addition to the fibrous phase, latex also seemed to be responsible for retarding the development of the hydrogarnet phase.

### 5.2.3 HARDENED CEMENT PASTE PREPARATIONS

The following is a discussion of the microscopic results obtained by means of dispersing powdered cement pastes in alcohol and water.



a. Powdered Paste Dispersed in Alcohol. In general, the specimens prepared from powdered paste dispersed in alcohol consisted of "exceedingly ill-formed colloidal products, in which it is...difficult to discern any definite morphology" (18). A comparison of Figures 93(a), 95(b), 97, 98 and 100(a) revealed little discernible difference in the morphology of the five mixes at age three days. Micrographs of similar specimens prepared at later ages appeared the same and are not included. Other investigators have met with only limited success using this method of sample preparation (18), and it was therefore decided not to pursue this phase of the research to a greater extent.

b. Powdered Paste Dispersed in Water. By dispersing powdered paste in water, hydration of the sample begins anew, presumably from previously unhydrated grains of cement. While this was not a valid approach to studying the actual microstructure of the original specimens, the results observed are nevertheless interesting enough to be included here.

Powdered paste samples from mixes 1, 2, 4, and 5 at age twenty-eight days were dispersed in water for exactly



thirty minutes and then ultrasonically vibrated for two minutes before preparation of the specimen for viewing. Figure 94 is a micrograph of the control mix showing several needles of various sizes which have formed after only thirty minutes in water. However, Figure 96 revealed that many more needles have formed in the same length of time in mix 2, most of which appeared to be thin and of medium length. Glycolic acid had apparently accelerated the development of needles in the rehydrated specimen.

In mix 4, as shown in Figure 99, more needles of various sizes were observed than in the control mix, possibly as a result of the 5% latex addition to the mix. Similarly, mix 5 with 15% latex shown in Figure 101, revealed a greater abundance of needles than the control mix, though most of the needles appeared to be rather short. The reason for this apparent acceleration of needle development in the rehydrated specimens in the presence of latex is not clear.

### 5.3 RELATION OF MICROSCOPIC RESULTS TO STRENGTH CHARACTERISTICS

In this section the microscopic results, based upon the effects of glycolic acid and latex, are related to the strength





characteristics of the pastes.

### 5.3.1 EFFECTS OF GLYCOLIC ACID

As discussed in the previous chapter, the addition of glycolic acid to neat cement paste results in significant increases in the strength of the cement. In an earlier section of this chapter, the significant changes in the microstructures of portland cement and its major constituents in the presence of glycolic acid were discussed. In this section the objective is to analyze and relate the previous results in an attempt to explain the reasons for the significant strength increases obtained in terms of the changes which have taken place in the microstructure.

The most significant changes were observed in the microstructures of  $C_3A$ ,  $C_4AF$  and  $C_3S$ . Blank, Rossington, and Weinland (24) concluded that adsorption of salicylic acid by the hydration products of  $C_3A$  and  $C_4AF$  rendered them inactive, allowing  $C_3S$  and  $C_2S$  to control the reaction. Similar effects appear to have occurred in the presence of glycolic acid. Normal additions of acid were seen to significantly retard development of the hydrogarnet phase, while excessive amounts of the acid eliminated this phase and retarded development of the C-A-H plate phase, imparting a



ragged appearance to the normally hexagonal shaped plates. The  $C_3A$  and  $C_4AF$  phases in portland cement do not contribute beneficially to the development of ultimate strength, and the stacked plates which are characteristic of these phases are known to possess inherently poor strength properties. If the addition of glycolic acid renders these phases inactive, as the significant changes in their microstructures would seem to indicate, then quite possibly some of the poor strength characteristics of these phases have been at least partially eliminated, allowing  $C_3S$  and  $C_2S$  to contribute more significantly to the development of strength in portland cement.

Significant changes were also observed in the microstructure of  $C_3S$ . In general, the calcium hydroxide (C-H) phase was not observed due to carbon contamination. However, x-ray diffraction studies of similar specimens, recently undertaken, indicate that a normal addition of glycolic acid significantly reduces the amount of the C-H phase present in  $C_3S$ , while an excessive amount of the acid completely eliminates this phase. The plates of the C-H phase, like those of the C-A-H phase, have poor strength properties. Hence their reduction or elimination could reasonably be expected to contribute somewhat to the strength increases realized in the presence of



glycolic acid. Furthermore, it is likely that a similar effect takes place in  $C_2S$ , since calcium hydroxide is a hydration product of  $C_2S$  also.

Another significant change observed in the microstructure of  $C_3S$  was the apparent increase in quantity and size of the needles or fibers of the tobermorite phase. While the changes observed in the presence of a normal addition of glycolic acid were noticeable, they were not considered extremely significant. However, it is felt that the addition of excess acid has magnified its effect upon  $C_3S$ . The presence of extremely large needles, presumably related to the tobermorite phase, would seem to indicate that glycolic acid accentuates the growth of this needle-like phase, which is believed to contribute most significantly to the strength of cement. Further investigation into this area of research by means of x-ray diffraction is now underway in order to positively identify the phases present. While excess acid is known to be detrimental to the development of maximum strength potential, it is felt that optimum quantities of the acid slightly accelerate the growth of the tobermorite phase to produce a cement of higher strength. Such a phenomenon could improve the bond within cement by producing a more



strongly interlocking needle-like structure. The exceedingly large needles which result from the use of excessive quantities of acid probably reduce the strength of the cement as a result of their low unit surface area and may set up stresses within the cement due to their microscopically enormous size.

Effects similar to those just discussed were also observed to a degree in the microstructure of portland cement. While the hydration of portland cement is more complex chemically due to the presence of all component phases, no significant physical differences were observed in its microstructure when compared with that of its major constituents. Therefore it is concluded that the same strength mechanisms observed in the microstructure of its component phases contribute to the development of higher strength in portland cement.

#### 5.3.2 EFFECTS OF DOW LATEX 464

As discussed in the previous chapter, the addition of 15% latex solids by weight of cement to neat cement paste results in significant increases in the early flexural strength of the cement paste. No significant increases in compressive strength were encountered. However, the 15% latex mix had a





modulus of elasticity about one half that of neat cement paste without latex. Discussed earlier in this chapter were the significant differences in the microstructures of portland cement and its major constituents in the presence of latex. This section will analyze and relate the previous results in an attempt to explain the macroscopic results in terms of what was observed in the microstructure.

The most significant difference observed in the microstructure of portland cement and its major constituents was a physical one in nature with the latex coating the hydration products and stretching throughout the microstructure. The initial increased flexural strength of the 15% latex mix is possibly the result of a continuous latex network throughout the cement paste. The microscopic studies appear to support this possibility. Also, the significant reduction of the modulus of elasticity of the 15% latex mix is probably a result of the ductile nature of the latex which is dispersed throughout the paste.

There were no significant differences in the compressive strengths of the latex mixes as compared to the control mix indicating that the bond between the cement paste matrix and



the aggregate must be improved in order to achieve the higher strengths in mortars. Since the microscopic studies were performed on the cement paste alone, nothing significant was able to be concluded in this area.

No relationship between the apparent retardation of the hydration of  $C_3A$  or the initial acceleration of the hydration of  $C_2S$  by the addition of latex and the macroscopic results could be deduced by the authors.



## CHAPTER 6 - SUMMARY OF RESULTS AND CONCLUSIONS

In this chapter is presented a summary of macroscopic and microscopic results, followed by the conclusions of the authors based upon these results.

### 6.1 SUMMARY OF RESULTS

1. An addition of 300cc glycolic acid per sack of cement increased the compressive strength of neat cement paste on the order of 23% at all testing ages, and increased the ultimate flexural strength on the order of 13%. An addition of 150cc glycolic acid had no significant effects upon the compressive or flexural strengths of the paste.

2. Glycolic acid had no significant effect upon the modulus of elasticity of neat cement paste.

3. Glycolic acid retarded the initial set of the paste, but accelerated the development of strength once setting had taken place.

4. An addition of 5% latex to neat cement paste had no significant effect upon the ultimate compressive or flexural strength. An addition of 15% latex significantly increased the early flexural strength of neat cement paste, had no



significant effect upon its ultimate flexural strength, and significantly decreased the ultimate compressive strength of the paste.

5. Additions of latex on the order of 15% result in a modulus of elasticity on the order of one half the modulus of neat cement paste alone.

6. Glycolic acid accelerated the hydration of tricalcium silicate and dicalcium silicate. The hydration of tricalcium aluminate and tetracalcium aluminoferrite was retarded by glycolic acid approximately in proportion to the amount of acid used. Glycolic acid in the presence of gypsum retarded the hydration of tricalcium aluminate to a much greater extent than did either the acid or gypsum individually.

7. In excessive amounts glycolic acid imparted a lacy structure of holes to numerous plates in the C-A-H phase. Similar structures were observed in untreated specimens, but to a much lesser degree.

8. The addition of latex was responsible for a change in the morphology of the early hydration products of tricalcium aluminate, as well as for retardation of the full development of its ultimate hydration products. The latex appeared





to accelerate the early hydration of dicalcium silicate but had no significant effect upon the final hydration products.

## 6.2 CONCLUSIONS

Since glycolic acid has been shown to have significant effects upon the morphology of all component phases of portland cement, it is believed that the acid is adsorbed to a certain degree by all phases or their hydrates. The retarding effect of the acid upon tricalcium aluminate, as observed in microscopic studies, is believed to be responsible for the substantial retardation of initial and final setting times of macroscopic test specimens. The acceleration observed in the hydration of dicalcium silicate and tricalcium silicate is believed to be partially responsible for the strength increases achieved. Furthermore, the observed deteriorative effects of the acid upon tricalcium aluminate and tetracalcium aluminoferrite is believed to render these phases inert, further enhancing the strength characteristics of neat cement paste. Since preliminary x-ray diffraction studies have shown that the calcium hydroxide phase in  $C_3S$  is substantially reduced or eliminated in the presence of glycolic acid, it is concluded that the reduction or elimination



of this phase may be partially responsible for strength increases achieved. This conclusion is further supported by the work of Dr. Copeland of the Portland Cement Association, who recently indicated at M.I.T. that the abundance of calcium hydroxide crystals observed on fracture surfaces may be an indication of a weak point in the matrix.

It is believed that the change in morphology of the early hydration products of tricalcium aluminate in the presence of latex is a result of a chemical interaction between the latex and tricalcium aluminate. However, this change in morphology can not be related to any macroscopic result. It is believed that the flexural strength variations in the latex mixes can be accounted for by the formation of a latex network in the mixes. In mixes containing 15% latex a continuous latex network could account for the increased flexural strength. However, in 5% latex mixes the formation of a non-continuous latex network could account for the apparent lack of effectiveness of the admixture. This conclusion is further supported by the microscopic studies which revealed a physical coating of latex on all hydration products. Because latex does not significantly increase the compressive strength of neat cement paste, it is believed



that it apparently strengthens the bond between the cement paste and aggregate in order to achieve increases in the compressive strength of mortars.



## CHAPTER 7 - RECOMMENDATIONS

1. Further studies in the area of powdered pastes dispersed in alcohol are desirable. This would allow studying the microstructure developed in a mix using normal water-cement ratios. Satisfactory results may be obtainable very early in the hydration process, at least for curing ages not in excess of forty-eight hours. Further research is necessary in the area of specimen preparation of powdered paste samples, especially as affected by the mode and severity of the grinding of the paste.

2. Latex has been shown to modify the hydration products of tricalcium aluminate. An electron microscopy study of the effects of latex upon tricalcium aluminate and gypsum should be made in order to determine its effects upon this phase in portland cement.

3. Other investigators (26) have shown that preslurrying of a mix reduces the amount of retarder which is capable of being adsorbed by the hydration products of tricalcium aluminate. Further electron microscopy studies in this area should be made to determine the effects of glycolic acid upon tricalcium aluminate and gypsum as influenced by variations in preslurrying time.





4. It has been shown (23) that when using retarders the time of preslurrying affects the initial and final setting times, as well as the amount of adsorption of the admixture by the various phases. Further research should be conducted to determine the effects of preslurrying time upon early strength development and upon the ultimate strength developed in mixes containing glycolic acid.

5. Glycolic acid has apparently altered the surface texture of plates in the C-A-H phase. The effects of the acid upon the surface texture seen in needles of the C-S-H phase was not noted. Further electron microscopy research into the effects of the acid, if any, upon the lacy surface texture of the plate and needle phases should be conducted.

6. Latex-cement paste specimens cured underwater have shown poor strength properties, whereas latex used in cement mortars has achieved marked strength increases. Further research into this area is desirable in order to determine the effects upon compressive strength of allowing latex-cement paste specimens to dry cure completely, or to dry cure for a period of time before re-immersing them in water.



## BIBLIOGRAPHY

1. R. F. Blanks, H. L. Kennedy, The Technology of Cement and Concrete, Vol. I, Wiley and Sons, Inc., New York, 1955.
2. D. F. Orchard, Concrete Technology, Vol. I, Wiley and Sons, Inc., New York, 1962.
3. D. R. MacPherson and H. C. Fischer, "The Effect of Water-Reducing Admixtures and Set-Retarding Admixtures on the Properties of Hardened Concrete". ASTM STP No. 266, ASTM, Philadelphia, Pa., 1960.
4. Reports of tests of E.I. DuPont Concrete Admixture-Hydroxyacetic Acid by Law Engineering Testing Company, Atlanta, Georgia, Seven Reports from March 28, 1963 to December 10, 1965.
5. "Latex Modified Cement Mortars" Pamphlet published by the Dow Chemical Company, Midland, Michigan.
6. Ake Grudemo, "The Microstructures of Cement Gel Phases", Swedish Cement and Concrete Institute at the Royal Institute of Technology, Stockholm, 1965.
7. C. M. Sliepcevich, L. Gildart, and D. L. Katz, "Crystals from Portland Cement Hydration", Industrial and Engineering Chemistry, Vol. 35, No. 11, November 1943.
8. H. F. W. Taylor, The Chemistry of Portland Cement, 2nd ed., Reinhold Publishing Corp., New York, 1964.
9. L. E. Copeland and E. G. Schulz, "Electron Optical Investigation of the Hydration Products of Calcium Silicates and Portland Cement", Journal of the PCA Research and Development Laboratories, Vol. 4, No. 1, January 1962.
10. S. Brunauer and L. E. Copeland, "The Chemistry of Concrete", Scientific American, Vol. 210, No. 4, April 1964.
11. H. S. Kurczyk and H. E. Schwiete, "Concerning the Hydration Products of  $C_3S$  and Beta  $-C_2S$ ", Chemistry of Cement-Proceedings of the Fourth International Symposium, Washington, D. C., 1960.



12. J. A. Gard, J. W. Howison, and H. F. W. Taylor, "Synthetic Compounds Related to Tobermorite: An Electron-Microscope, X-ray, and Dehydration Study", Magazine of Concrete Research, Vol. 11, No. 33, November 1959.
13. S. Brunauer, "Tobermorite Gel - The Heart of Concrete", American Scientist, Vol. 50, March, 1962.
14. Ake Grudemo, "The Microstructure of Hardened Cement Paste", Chemistry of Cement-Proceedings of the Fourth International Symposium, Washington, D. C., 1960.
15. J. F. Young, "Hydration of Tricalcium Aluminate with Lignosulphonate Additives", Magazine of Concrete Research, Vol. 14, No. 42, November 1962.
16. H. E. Davis and G. E. Troxell, Composition and Properties of Concrete, McGraw-Hill Book Co., Inc., New York, 1956.
17. T. C. Hansen, "Strength, Elasticity, and Creep as Related to the Internal Structure of Concrete", Chemistry of Cement-Proceedings of the Fourth International Symposium, Washington, D. C., 1960.
18. R. H. Bogue, The Chemistry of Portland Cement, 2nd ed., Reinhold Publishing Corp., New York, 1955.
19. L. H. Tuthill, R. F. Adams, and J. M. Hemme, Jr., "Observations in Testing and Use of Water-Reducing Retarders", ASTM STP No. 266, ASTM, Philadelphia, Pa., 1960.
20. A. M. Rosenberg, "Study of the Mechanism Through Which Calcium Chloride Accelerates the Set of Portland Cement", Journal of the ACI, Proceedings, Vol. 61, No. 10, October 1964.
21. O. G. Herrell and A. E. Smith, Term Project Report, Course 1.46, Massachusetts Institute of Technology, Cambridge, Mass., May 1966.
22. H. B. Wagner, "Compressive Strength of Polymer-Modified Hydraulic Cements", Ind. Eng. Chem. Prod. Res. Develop., Vol. 5, June 1966.
23. G. M. Bruere, "Importance of Mixing Sequence When Using Set-Retarding Agents with Portland Cement", Nature, No. 4888, July 6, 1963.



24. B. Blank, D. R. Rossington, and L. A. Weinland, "Adsorption of Admixtures on Portland Cement", Journal of the American Ceramic Society, August 1963.
25. "Instruction Manual for Philips 100A Electron Microscope", Dept. of Civil Eng., Materials Division, M.I.T., Cambridge, Mass.
26. A. M. Neville, Properties of Concrete, John Wiley and Sons, Inc., New York, 1963.
27. Arturo Jorge Gutierrez Alvarez, "Strengthening Mechanisms in Latex Modified Concretes", M.S. Thesis, C.E. Dept., M.I.T., 1964.





## APPENDIX I

### ELECTRON MICROGRAPHS

This appendix presents the micrographs taken of both the bottle hydrated preparations and the hardened cement paste preparations. The following is a list of the micrographs of portland cement and its four major constituents.

#### Bottle Hydrated Preparations:

#### Figures:

Tricalcium Silicate	1(a) - 16(b)
Dicalcium Silicate	17(a) - 32
Tetracalcium Aluminoferrite	33 - 48(b)
Tricalcium Aluminate	49 - 76
Portland Cement	77 - 92(c)

#### Hardened Cement Paste Preparations:

Mixes 1, 2, 3, 4, and 5	93(a) - 101
-------------------------	-------------



## APPENDIX I

### ELECTRON MICROGRAPHS

This appendix presents the micrographs taken of both the bottle hydrated preparations and the hardened cement paste preparations. The following is a list of the micrographs of portland cement and its four major constituents.

#### Bottle Hydrated Preparations:

#### Figures:

Tricalcium Silicate	1(a) - 16(b)
Dicalcium Silicate	17(a) - 32
Tetracalcium Aluminoferrite	33 - 48(b)
Tricalcium Aluminate	49 - 76
Portland Cement	77 - 92(c)

#### Hardened Cement Paste Preparations:

Mixes 1, 2, 3, 4, and 5	93(a) - 101
-------------------------	-------------



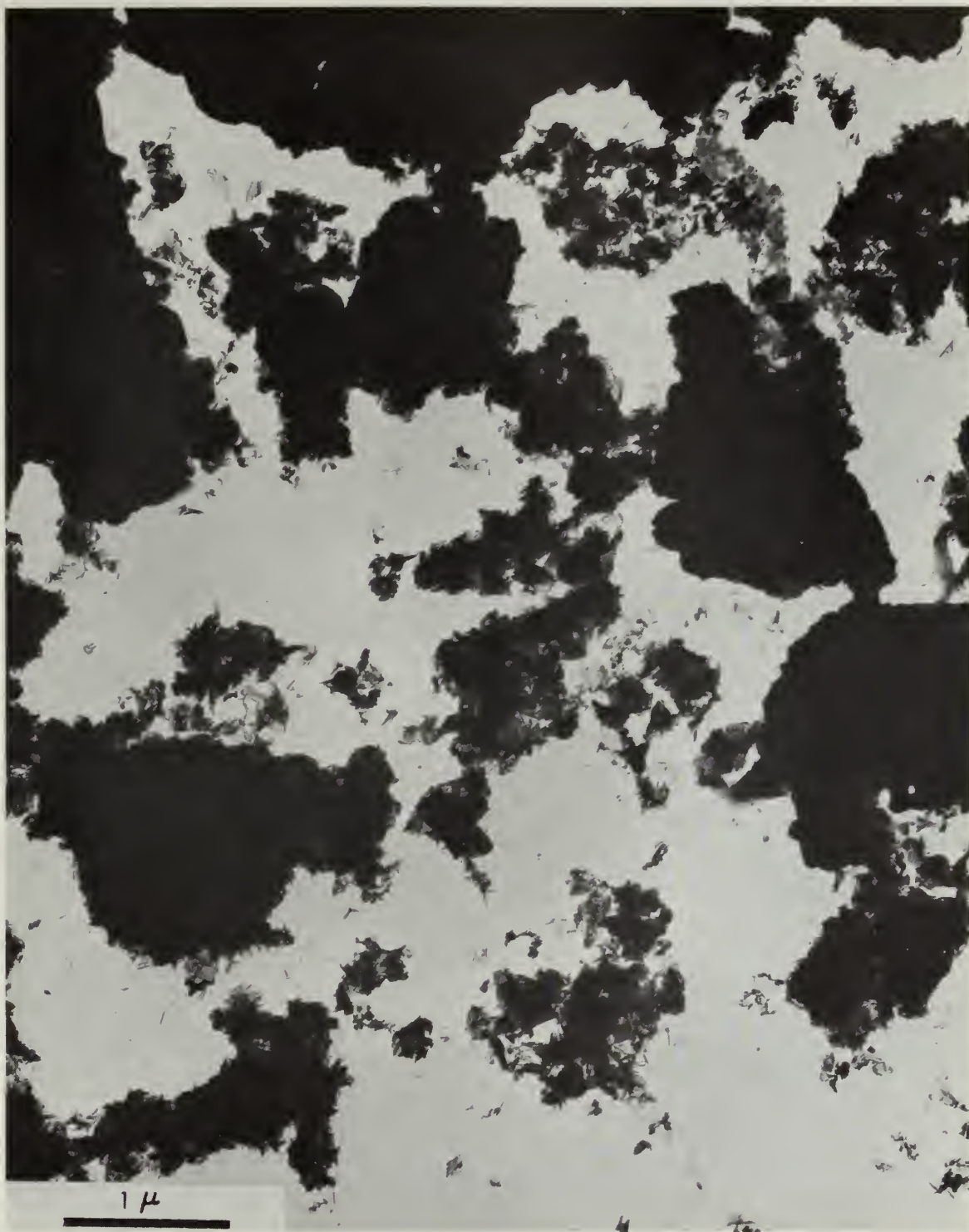


Figure 1(a). Sample C<sub>3</sub>S - 3 Hours. C<sub>3</sub>S particles covered with foils and fibers are characteristic of the early development of the C-S-H phase in the hydration of C<sub>3</sub>S. This micrograph is representative of what was generally observed.







Figure 1(b). Sample  $C_3S$  - 3 Hours. In this micrograph, bundles of fibers are observed in addition to the characteristic foils observed in the previous figure. These bundles of fibers resemble the C-S-H (II) phase, but are not generally representative of the specimen.







Figure 2. Sample  $C_3S$  - 6 Hours. Here the foils which were observed at three hours have taken on the appearance of fibers or needles, resembling the C-S-H (I) phase. This micrograph is representative of what was observed at six hours.





Figure 3. Sample  $C_3S$  - 24 Hours. At twenty-four hours, the characteristic fibers of the C-S-H phase project out from the edges of the dark masses as in the previous specimen. However, a few longer rods or fibers have now appeared lying on edge. The transparent areas in the background are apparently the  $CO_2$  contaminated C-H phase.





Figure 4(a). Sample C<sub>3</sub>S - 7 Days. Here hydration has essentially completed. The undispersed dark masses are covered with the characteristic foils or fibers observed in earlier specimens of this series. In the well dispersed areas, about 50% of the hydration products observed were in the form of foils or fibers resembling the C-S-H (I) phase.







Figure 4(b). Sample C S - 7 Days. Another area of the same specimen is seen in this<sup>3</sup> micrograph. Here the characteristic bundles of fibers resembling the C-S-H (II) phase are observed. These constituted about 50% of the observable hydration products in well dispersed areas.







Figure 5(a). Sample  $C_3S$ -HA - 3 Hours. The characteristic foil-like structure of the C-S-H phase is observed in this micrograph, which is representative of the specimen and which resembles the specimen of Figure 1(a).





Figure 5(b). Sample  $C_3S$ -HA - 3 Hours. An enlarged view of the previous specimen reveals the foil-like structure of the C-S-H phase in greater detail. It appears that a few rods or needles are present beneath or between the foils.



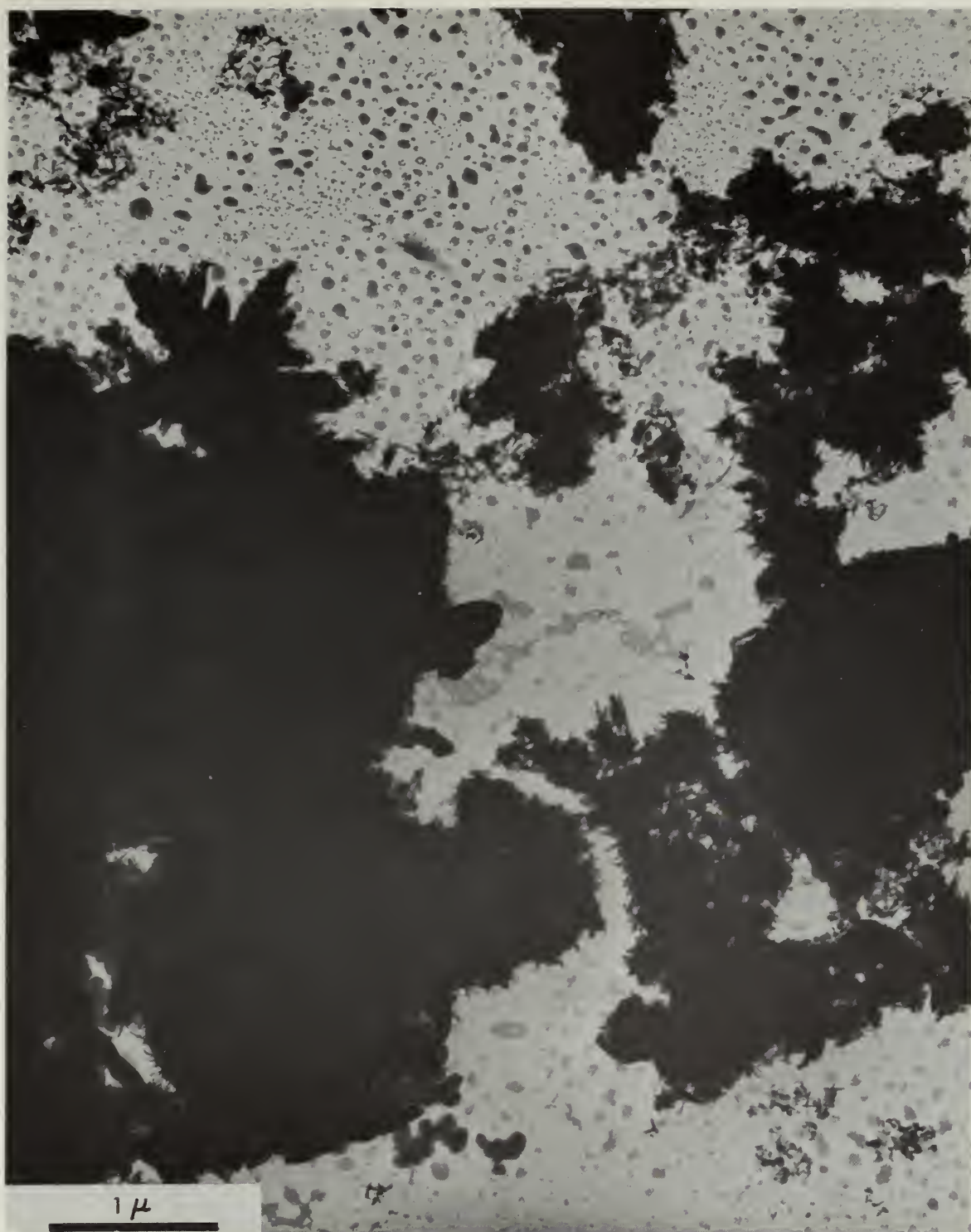


Figure 6(a). Sample  $C_3S$ -HA - 6 Hours. In this micrograph small needles or fibers are seen projecting outward from the dark masses. This type of structure is representative of the six hour specimen with glycolic acid. In the upper left-hand corner, bundles of fibers are observed, but are not considered representative of the specimen. In the background is the  $CO_2$  contaminated C-H phase.





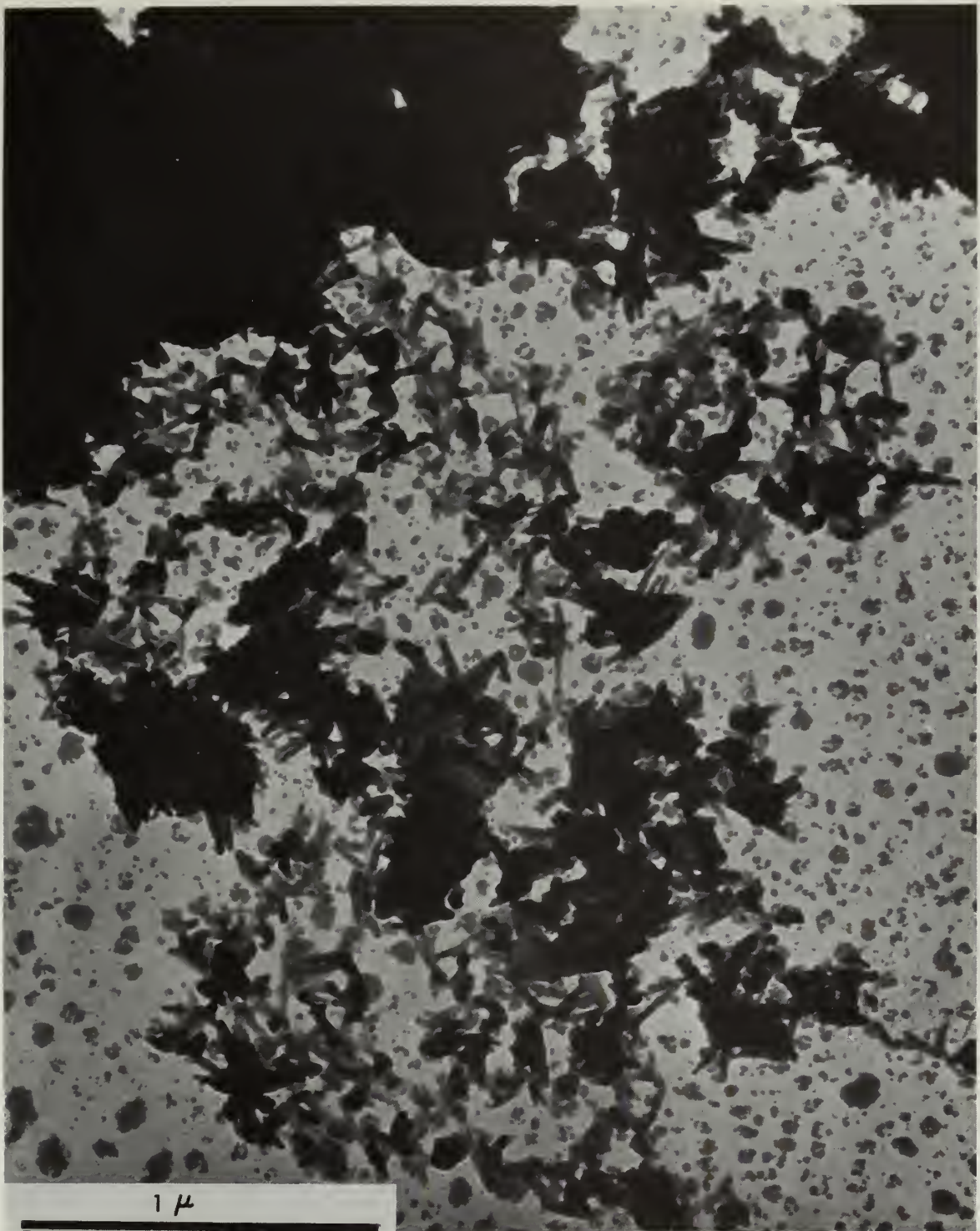


Figure 6(b). Sample  $C_3S$ -HA - 6 Hours. A well dispersed area of small needles or fibers can be observed in this micrograph. The needles appear similar to those seen projecting from the dark clusters in the previous figure, but most areas observed were not this well dispersed. Again,  $CO_2$  contamination is observed in the background.





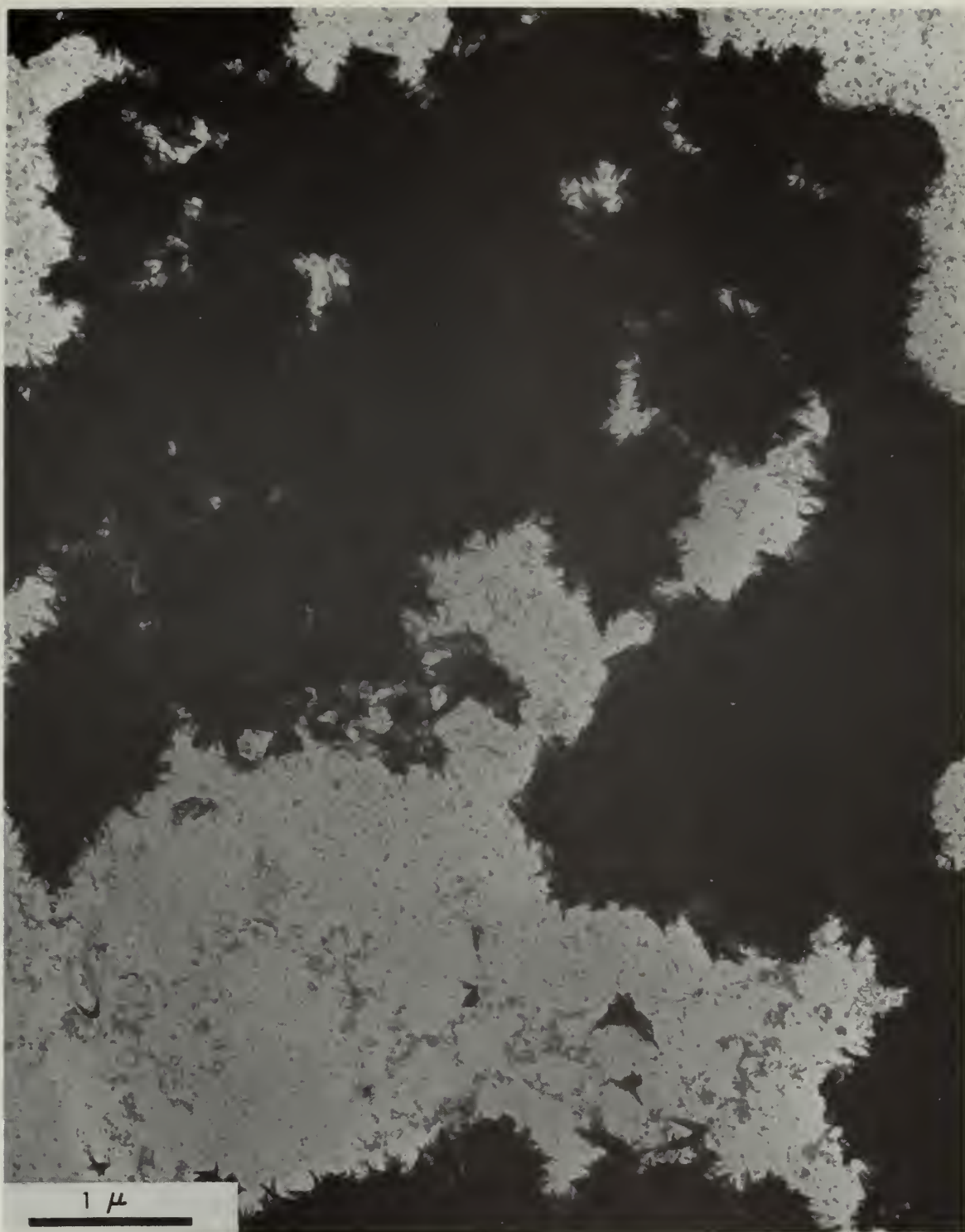


Figure 7(a). Sample C<sub>3</sub>S-HA - 24 Hours. The needles or fibers seen here at twenty-four hours appear longer and more numerous than in either the previous specimen or the twenty-four hour specimen without acid. This micrograph is considered representative of what was observed at twenty-four hours.





Figure 7(b). Sample  $C_3S$ -HA - 24 Hours. While the micrograph is not representative of the specimen, it is nevertheless an excellent example of the bundles of fibers resembling the C-S-H (II) phase. Note how the bundles appear to be breaking up, revealing the individual needles or fibers. The white band across the upper half of the micrograph is simply a crack in the carbon substrait.





Figure 8(a). Sample  $C_3S$ -HA - 7 Days. In this well dispersed specimen, the needles or fibers again appear to be slightly longer than in the comparable specimen without acid. The foils and fibers comprised about 60% of the hydration products observable in the dispersed areas.







Figure 8(b). Sample C<sub>3</sub>S-HA - 7 Days. In this micrograph the morphology of the hydration products is not completely clear. In general, about 40% of the specimen resembled the cigar shaped bundles of fibers observed in micrograph 4(b). However, the ends are smooth and not fibrous, and thus do not truly resemble the C-S-H (II) phase.







Figure 9. Sample C<sub>3</sub>S-HA(EX) - 3 Hours. Sheets or foils are seen in this micrograph outlining the edges of the dark masses. This structure closely resembles that observed in Figure 5(b). The most interesting feature of this micrograph is the presence of needle-like particles, apparently in the early stages of growth, projecting out of the dark masses.





Figure 10. Sample  $C_3S$ -HA(EX) - 6 Hours. The predominant structure observable in this specimen is once again the foil-like structure observed in other  $C_3S$  specimens. However, numerous small cigar shaped hydration products, presumably bundles of fibers, have now appeared throughout the dark structure of the specimen.





Figure 11(a). Sample  $C_3S-HA(EX)$  - 24 Hours. Extremely long needles or fibers predominate in this specimen. This startling effect is clearly the result of excessive glycolic acid which has caused a complete change in morphology over comparable twenty-four hour specimens as seen in Figures 3 and 7.







Figure 11(b). Sample  $C_3S$ -HA(EX) - 24 Hours. An enlarged view of the end of a needle reveals that it is composed of many smaller needles or fibers. This structure is similar to that of the cigar shaped bundles of fibers, except that the needles are relatively long and slender. The acid may have caused elongation of the bundles of fibers or perhaps large bundles of fibers may have broken up into more slender bundles of fibers.







Figure 12. Sample  $C_3S-HA(EX)$  - 7 Days. The structure of the needles appears unchanged, but the needles observed are considerably shorter than at twenty-four hours. This could be due to the smaller needles separating from the larger ones and/or to the larger needles breaking up as a result of ultrasonic vibrations. Also present in this specimen are small quantities of foils.





Figure 13. Sample C<sub>3</sub>S-L - 3 Hours. In this specimen, most of the hydration products are coated with latex, but along the edges the foils or fibers characteristic of comparable specimens without latex can be clearly observed.





Figure 14(a). Sample  $C_3S-L$  - 6 Hours. This representative specimen is well coated with latex, and the morphology of the hydration products can not be clearly determined. However, from the apparent transparency of the dispersed areas, it appears the hydration products consist largely of the characteristic foils and fibers as would be expected.







Figure 14(b). Sample C<sub>3</sub>S-L - 6 Hours. Bundles of fibers having a mottled texture were observed in very small quantities in the specimen and are not considered representative of what was seen on the whole. The clarity of the fibers is notable, considering the effects of latex in previous micrographs.







Figure 15(a). Sample  $C_3S-L$  - 24 Hours. The characteristic fibers or needles and foils of the C-S-H phase are clearly visible on the edges of the dark masses. This representative specimen strongly resembles  $C_3S$  alone as seen in Figure 3, except that the edges appear slightly more fibrous. The scarcity of latex in this micrograph is unusual.





Figure 15(b). Sample  $C_3S-L$  - 24 Hours. In this micrograph the structure is similar to that observed in the previous specimen, but the effect of the latex stretching between the fibers can be observed more clearly.





Figure 16(a). Sample  $C_3S-L$  - 7 Days. The predominant hydration products readily identifiable are foils and fibers. The micrograph is similar to Figure 4(a), except that the foils and fibers are not nearly as distinct due to the presence of latex coating the hydration products. The fibrous structure is representative of the specimen.







Figure 16(b). Sample C<sub>3</sub>S-L - 7 Days. Bundles of fibers and broken bundles of fibers were observed in small quantities. These are apparently covered with latex. Note the similarity to Figure 7(b), except for the latex coating.





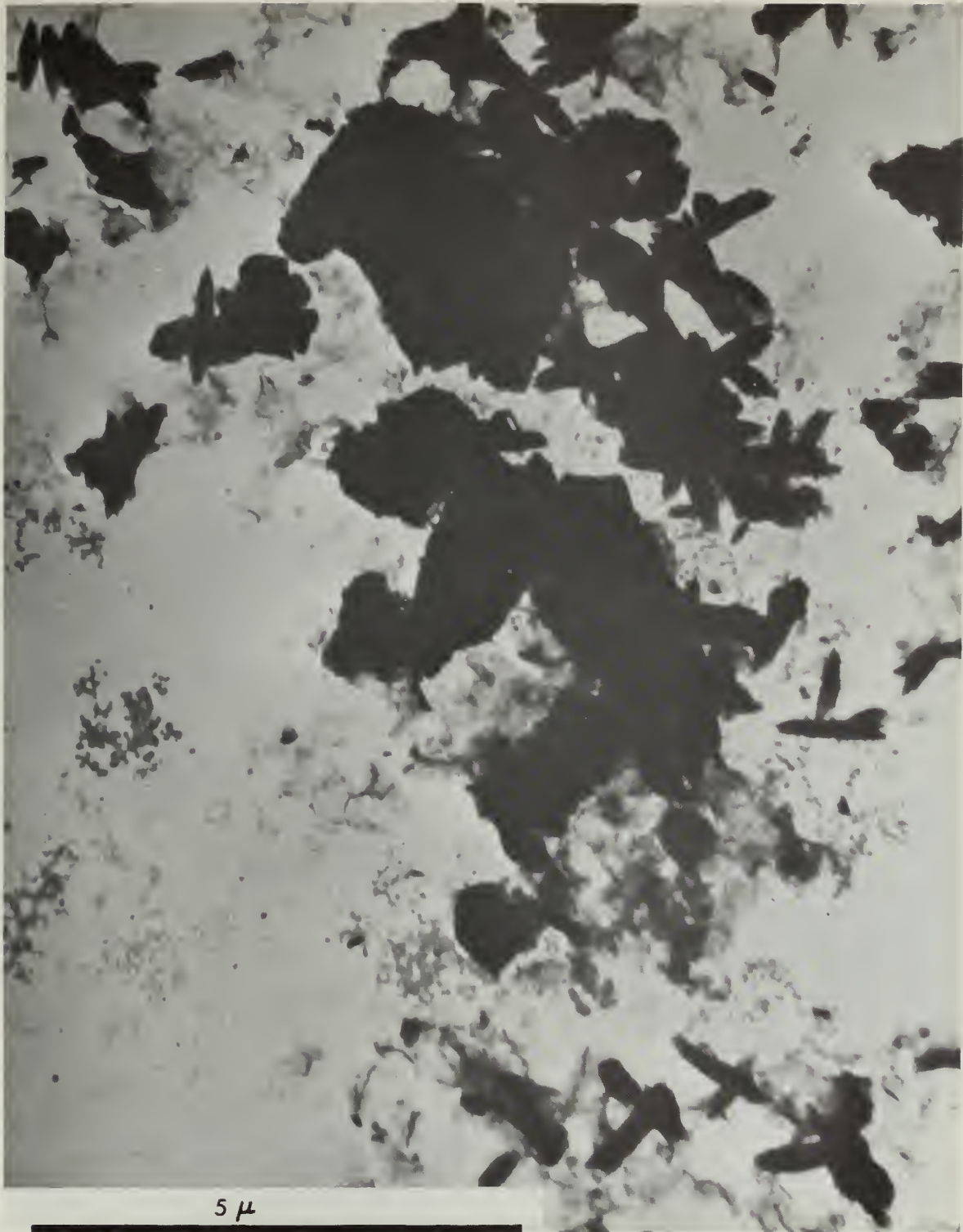


Figure 17(a). Sample  $C_2S$  - 3 Hours. The microstructure consists mainly of bundles of fibers and dark particles of unhydrated  $C_2S$ . The bundles of fibers are probably C-S-H (II) hydration products. The transparent particles chained together in the micrograph are carbon contamination.





Figure 17(b). Sample C<sub>2</sub>S - 3 Hours. This is an enlarged view of one of the bundles of fibers seen in the previous micrograph. Note the textured surface of the bundle.







Figure 18(a). Sample  $C_2S$  - 6 Hours. This micrograph shows the representative internal structure of the sample. It consists of many long needles and bundles of needles growing outward from the dark particles of  $C_2S$ . Note that the bundles of needles mentioned here appear to be separating into individual needles.





Figure 18(b). Sample C<sub>2</sub>S - 6 Hours. This is an enlarged view of an area where a bundle of needles has separated leaving a network of individual needles.







Figure 18(c). Sample  $C_2S$  - 6 Hours. Shown here are some of the bundles of fibers or cigar shaped particles, which are just beginning to break up at their ends. Also, there are areas which appear as crumpled foils.





Figure 19(a). Sample C<sub>2</sub>S - 24 Hours. This micrograph shows the needles which predominated in the microstructure of the sample. Again, there appear to be areas of crumpled foils.





Figure 19(b). Sample  $C_2S$  - 24 Hours. Cigar shaped particles and a foil like structure which could be C-S-H (I) are shown in this micrograph.







Figure 20(a). Sample  $C_2S$  - 7 Days. In this micrograph is seen the representative microstructure of the sample consisting of areas of C-S-H(I) foils and some fibrous particles. Also, there exist two rectangular block crystals of unknown composition.







Figure 20(b). Sample  $C_2S$  - 7 Days. This is an enlarged view of the C-S-H (I) foils. Note the fibrous make-up of the foils.





Figure 21(a). Sample C<sub>2</sub>S-HA - 3 Hours. Bundles of fibers are seen here along with dark particles whose edges appear to have small needles growing irregularly outward from them. Note the ends of the bundles of fibers. The bundles are representative of the C-S-H (II) hydration products.





Figure 21(b). Sample  $C_2S$ -HA - 3 Hours. This is an enlarged view of the bundles of fibers. They appear here as very small fibers which are beginning to separate from each other.







Figure 22(a). Sample  $C_2S$ -HA - 6 Hours. As in the sample  $C_2S$ -HA - 3 Hours, the microstructure consists primarily of bundles of fibers. In this micrograph, the bundles have separated considerably into areas of many needles. Also, some bundles have retained their relatively smooth shape, indicating they have not yet begun to break up.







Figure 22(b). Sample  $C_2S$ -HA - 6 Hours. In this enlarged view of some of the bundles of fibers they are seen as they begin to break up into the many separate needles.





Figure 22(c). Sample  $C_2S$ -HA - 6 Hours. This is another view of the thick bundles which appear to be made up of rolls of sheet-like elements or many fibers as mentioned earlier.





Figure 23. Sample  $C_2S$ -HA - 24 Hours. This representative micrograph shows the internal structure of the sample as foils and bundles of fibers.







Figure 24(a). Sample C<sub>2</sub>S-HA - 7 Days. Shown here is the fine fibrous make-up of the internal structure of the sample.







Figure 24(b). Sample C<sub>2</sub>S-HA - 7 Days. This is not representative of the sample,<sup>2</sup> but is one area that was observed showing an internal structure made up of short needle-like particles and foil-like particles.





Figure 25. Sample  $C_2S$ -HA(EX) - 3 Hours. In this micrograph are dark particles connected in chains which could be carbon contamination. The transparent areas among the darker particles could be the formation of foils. In general, the sample was poor and not much was visible.





Figure 26(a). Sample  $C_2S$ -HA(EX) - 6 Hours. Shown here is the foil-like internal structure of the sample with a few small needles also present. The dark circular particles are  $CO_2$  contamination.







Figure 26(b). Sample  $C_2S$ -HA(EX) - 6 Hours. This is an enlarged view showing the foil-like structure of an aggregate in the microstructure of the sample.







Figure 27(a). Sample  $C_2S$ -HA(EX) - 24 Hours. Shown here is the fibrous like C-S-H (I) foil. As indicated by the parallel striations of the foil at the top right of the picture, the structure was probably formed from a rod-like aggregate.





Figure 27(b). Sample  $C_2S$ -HA(EX) - 24 Hours. This is an enlarged view of one of the needles observed in the microstructure of the sample. Note the aggregates of more open foils and of a less distorted texture than the foils of the previous micrograph beginning to cover the needle.





Figure 27(c). Sample  $C_2S$ -HA(EX) - 24 Hours. In this micrograph is shown an enlarged view of the foils with a more open, less distorted texture as observed in Figure 27(b).





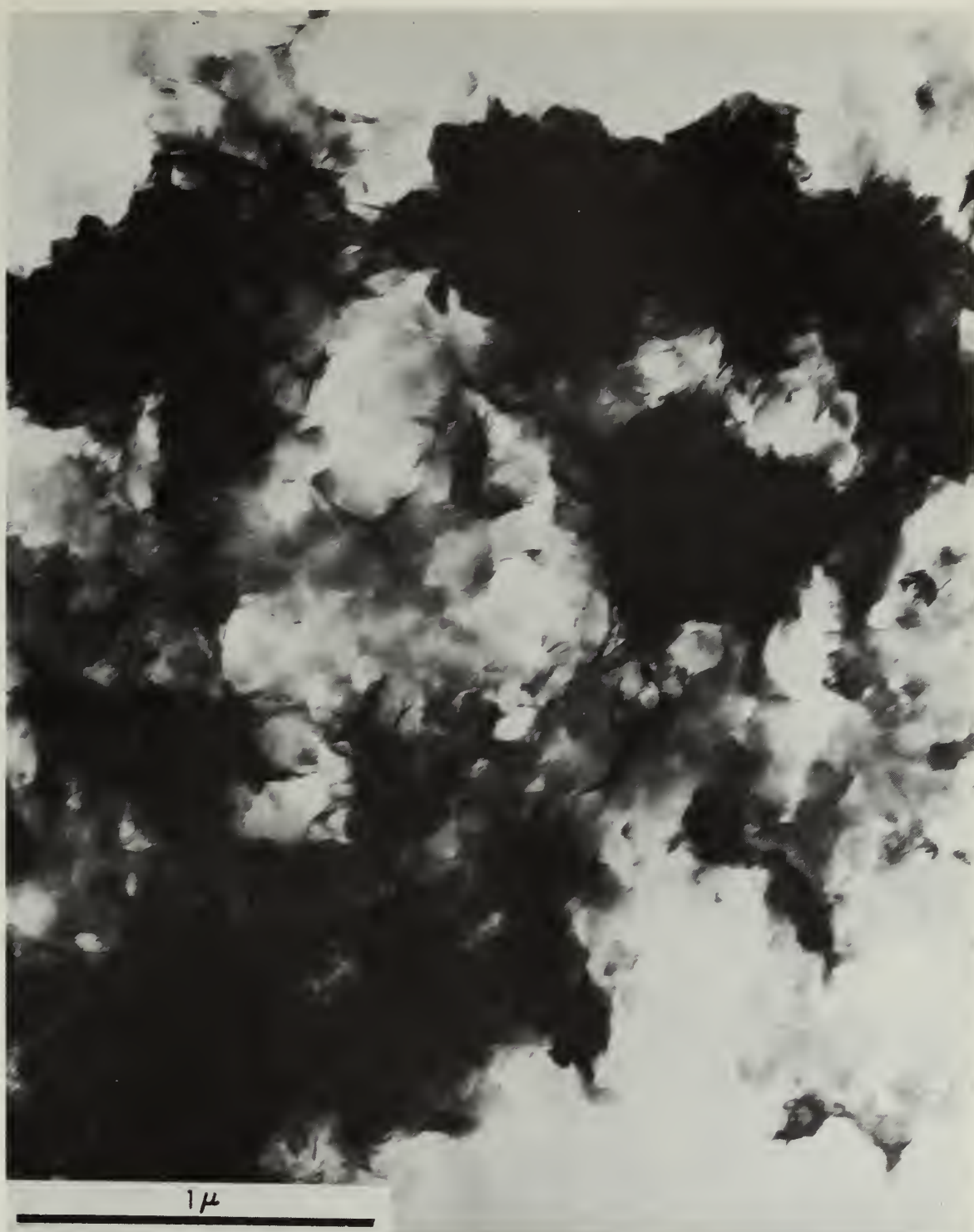


Figure 28. Sample  $C_2S$ -HA(EX) - 7 Days. In this representative micrograph is shown the foil-like internal structure of the sample. The foils are primarily the same as described in Figures 27(b) and 27(c).







Figure 29. Sample C<sub>2</sub>S-L - 3 Hours. Due to the overabundance of latex, no detail of the internal structure of the sample was visible. Shown here is the latex structure which covered everything.



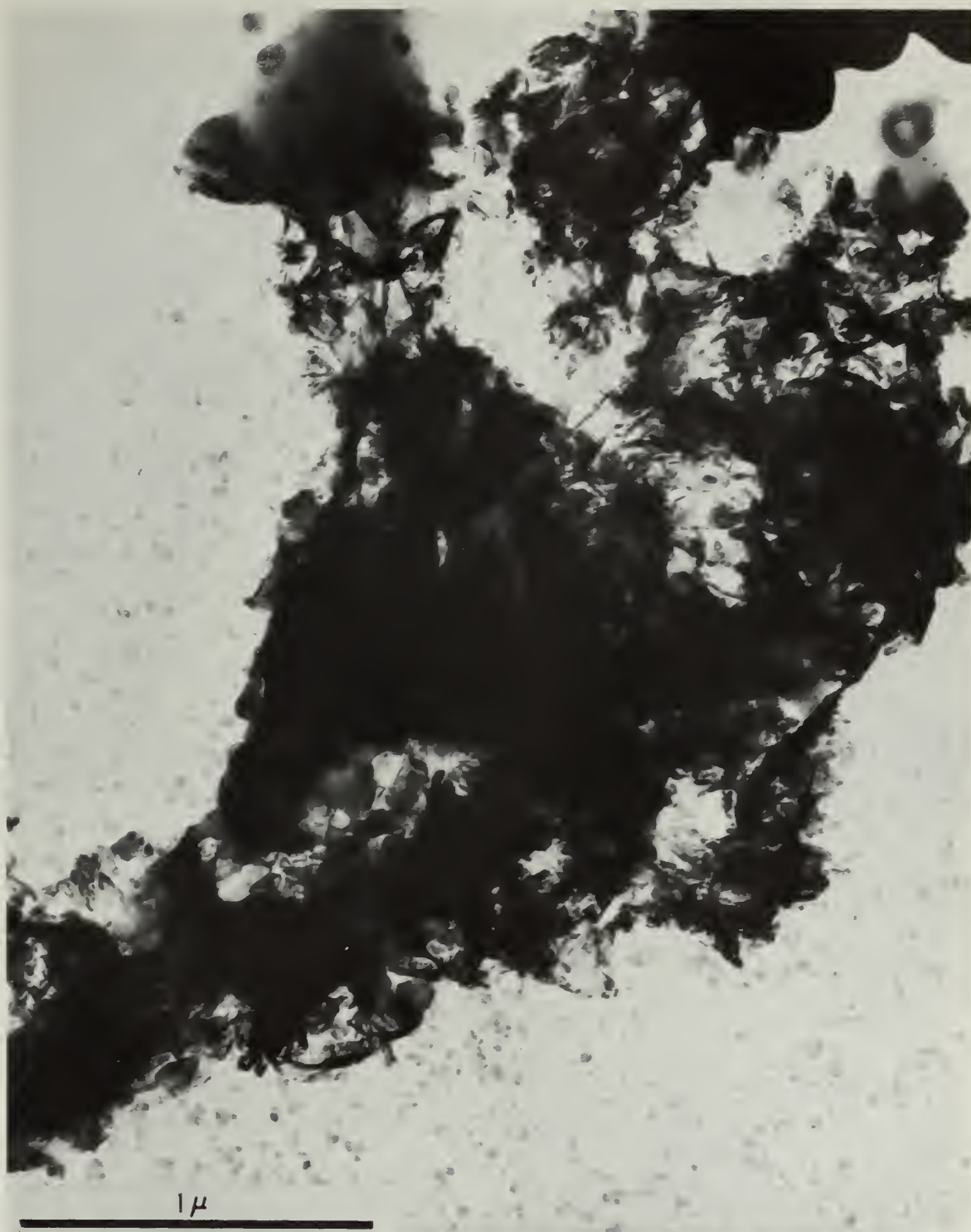


Figure 30. Sample  $C_2S-L$  - 6 Hours. Shown here is the representative internal structure of the sample consisting of foil-like particles partly coated with latex. The foils are fibrous and appear the same as seen in sample  $C_2S$  - 6 Hours, Figure 18(c).





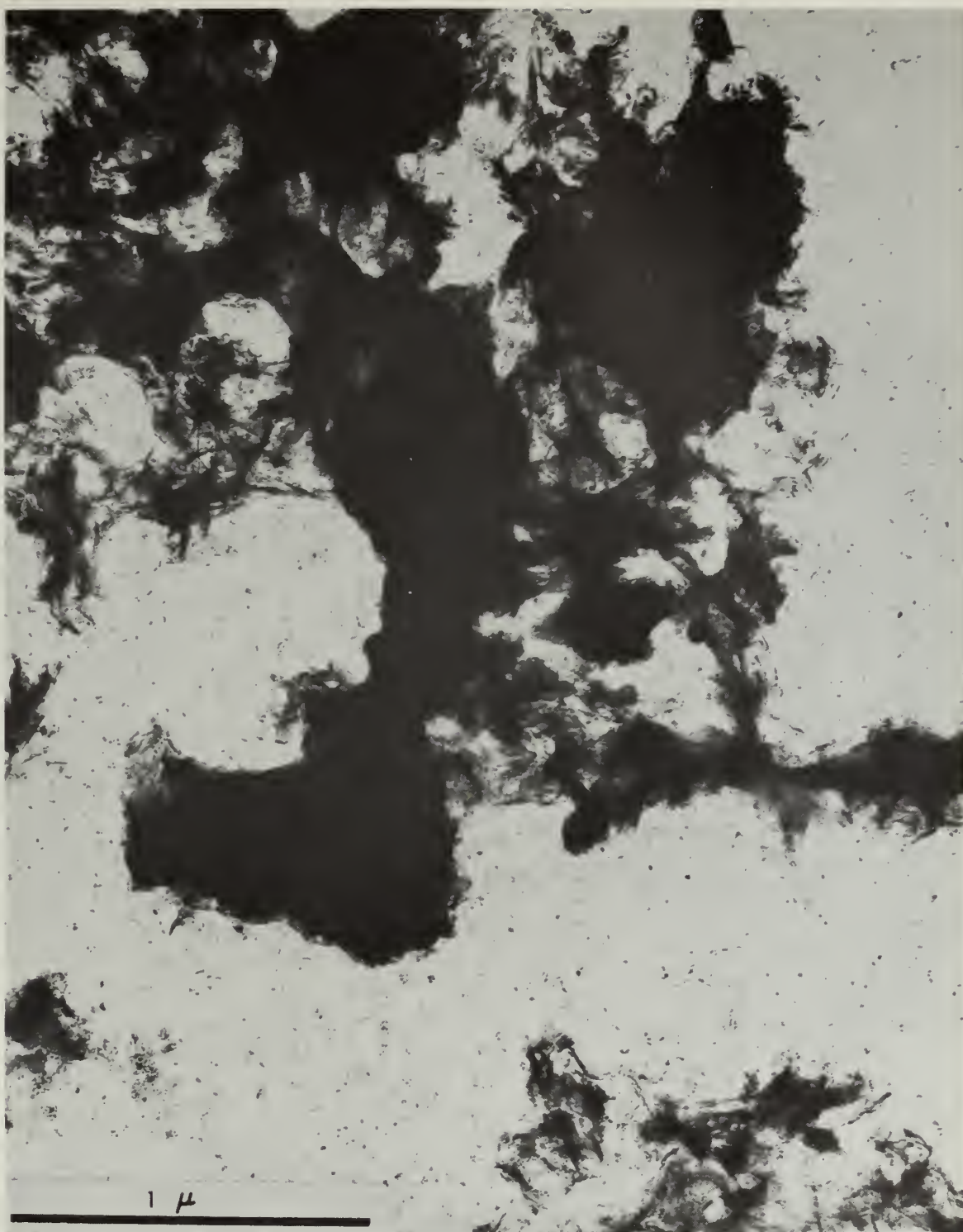


Figure 31. Sample C<sub>2</sub>S-L - 24 Hours. The microstructure appears about the same as for the sample at six hours, consisting primarily of foil-like particles coated in part with latex.





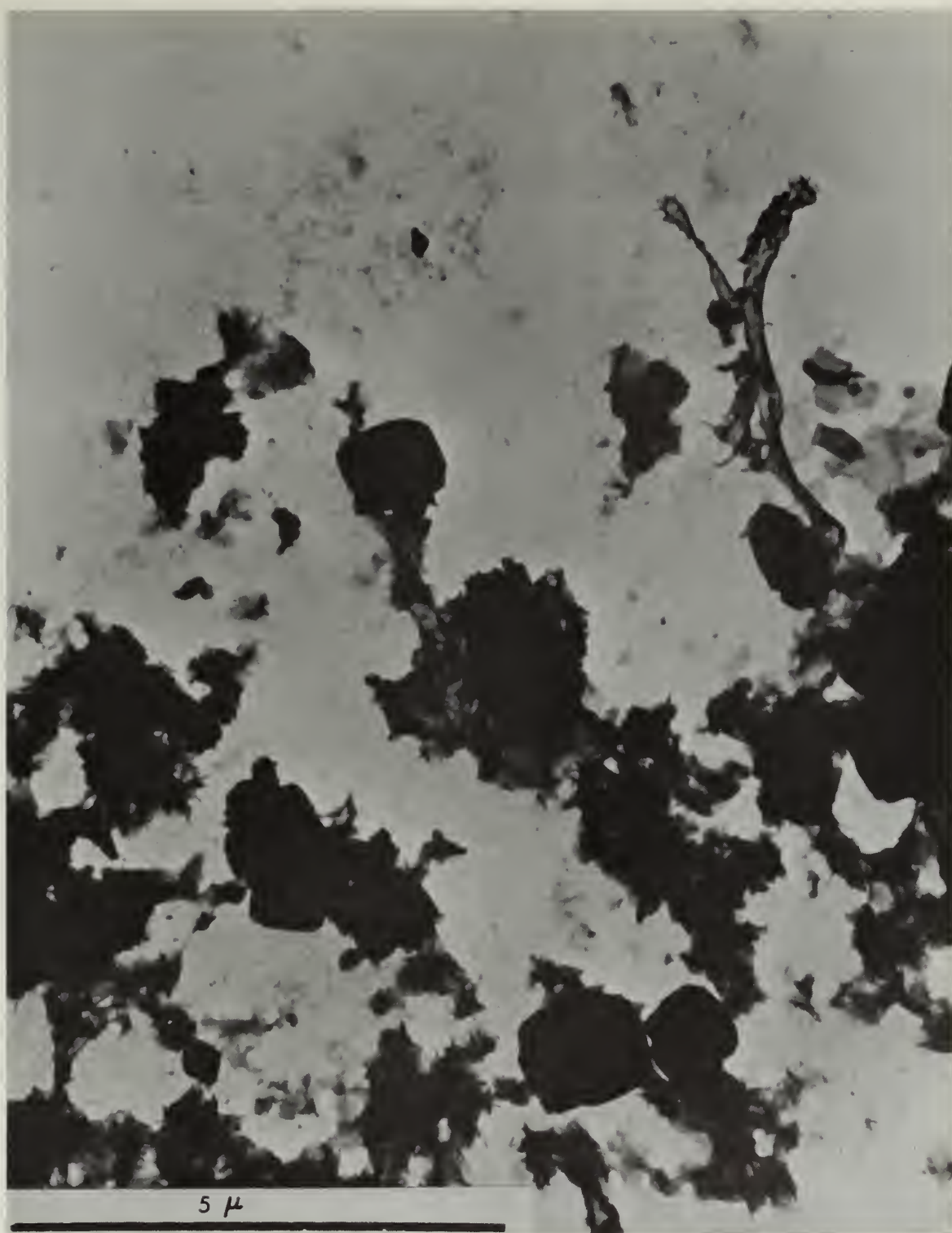


Figure 32. Sample C<sub>2</sub>S-L - 7 Days. The microstructure consists again primarily of foils, except in this sample the foils appeared more open than did the foils seen at six hours and twenty-four hours. Also, a few rectangular block crystals were seen as shown here.



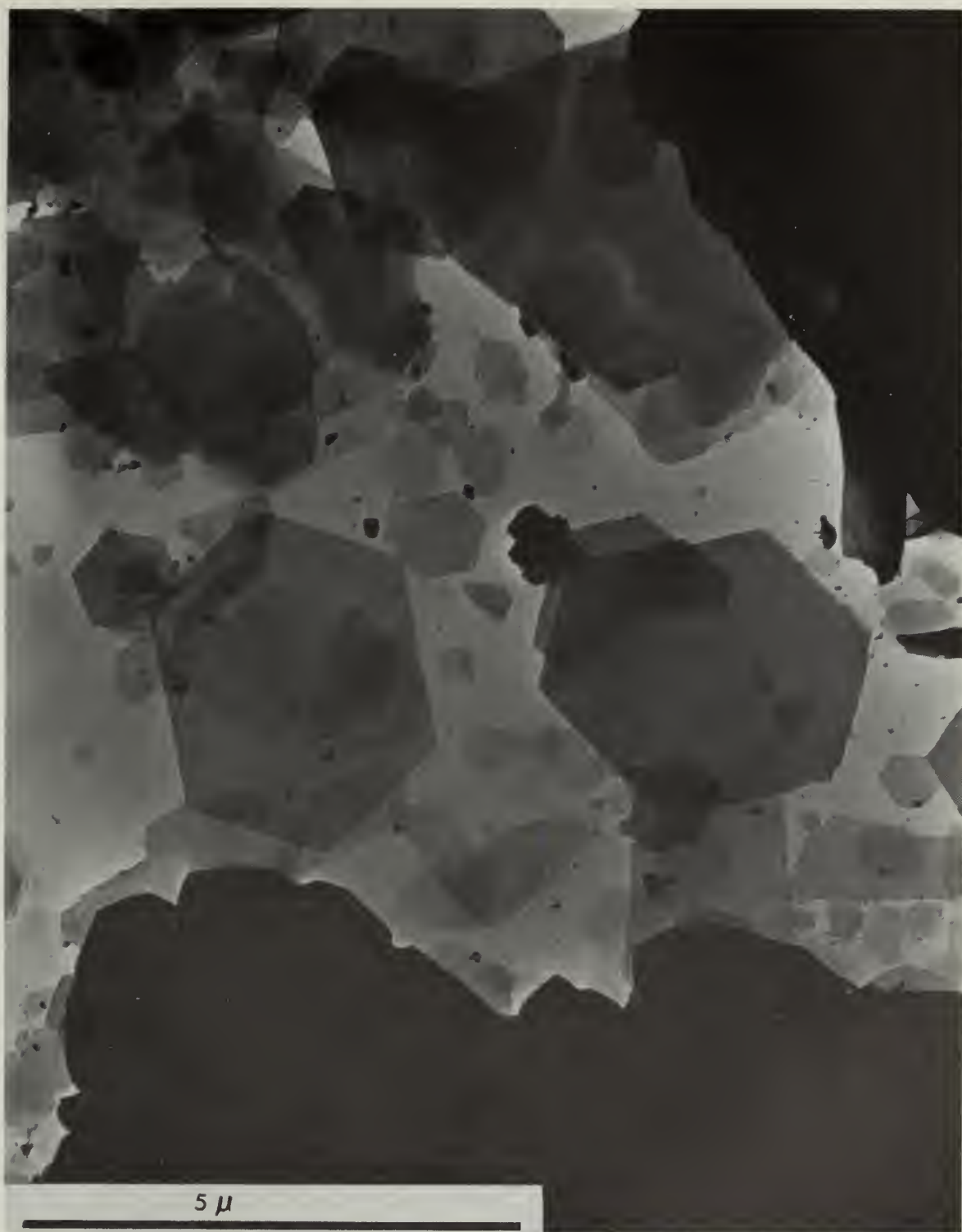


Figure 33. Sample  $C_4AF$  - 3 Hours. Thin plates of various sizes with hexagonal angles can be seen in this representative micrograph. Some plates have broken apart and pieces of plates are also present. The irregular shaped, dense particles at the bottom and upper right of the micrograph are probably unhydrated  $C_4AF$  particles with some plates crumpled along the edges of the particles.



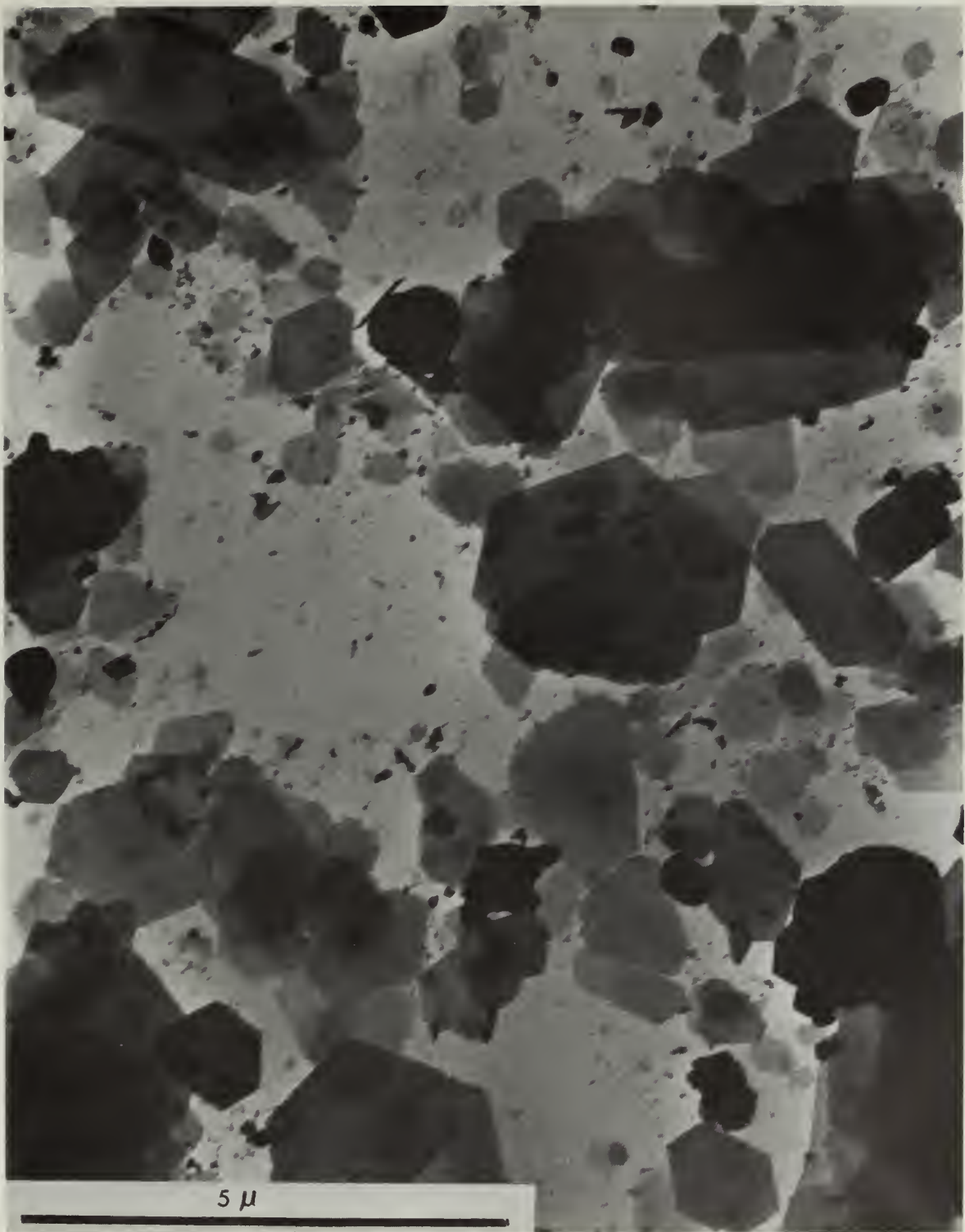


Figure 34(a). Sample  $C_4AF$  - 6 Hours. Seen in this representative micrograph are many thin plates of various sizes with hexagonal angles and a few small, dark, irregular shaped particles which are probably hydrogarnet crystals beginning to form. Some large, irregular shaped particles of unhydrated  $C_4AF$  are present.







Figure 34(b). Sample  $C_4AF$  - 6 Hours. This micrograph shows the textured surface of one of the thin plates observed in the previous micrograph. Also is shown one of the dark particles with a hexagonal outline which is probably a hydrogarnet crystal.







Figure 35. Sample  $C_4AF$  - 24 Hours. As seen in  $C_4AF$  samples at three and six hours, there are thin plates with hexagonal angles. As seen at six hours, there are also darker particles of various shapes and sizes. However, here the darker particles appear to have increased in size and number over those observed at six hours.





Figure 36. Sample C<sub>4</sub>AF - 7 Days. In this micrograph, one sees thin plates with hexagonal angles and a few plates which appear broken. The plates and dark particles appeared to exist in a 50-50 ratio in observations made at seven days. However, in this micrograph, the plates appear to predominate slightly over the dark particles.





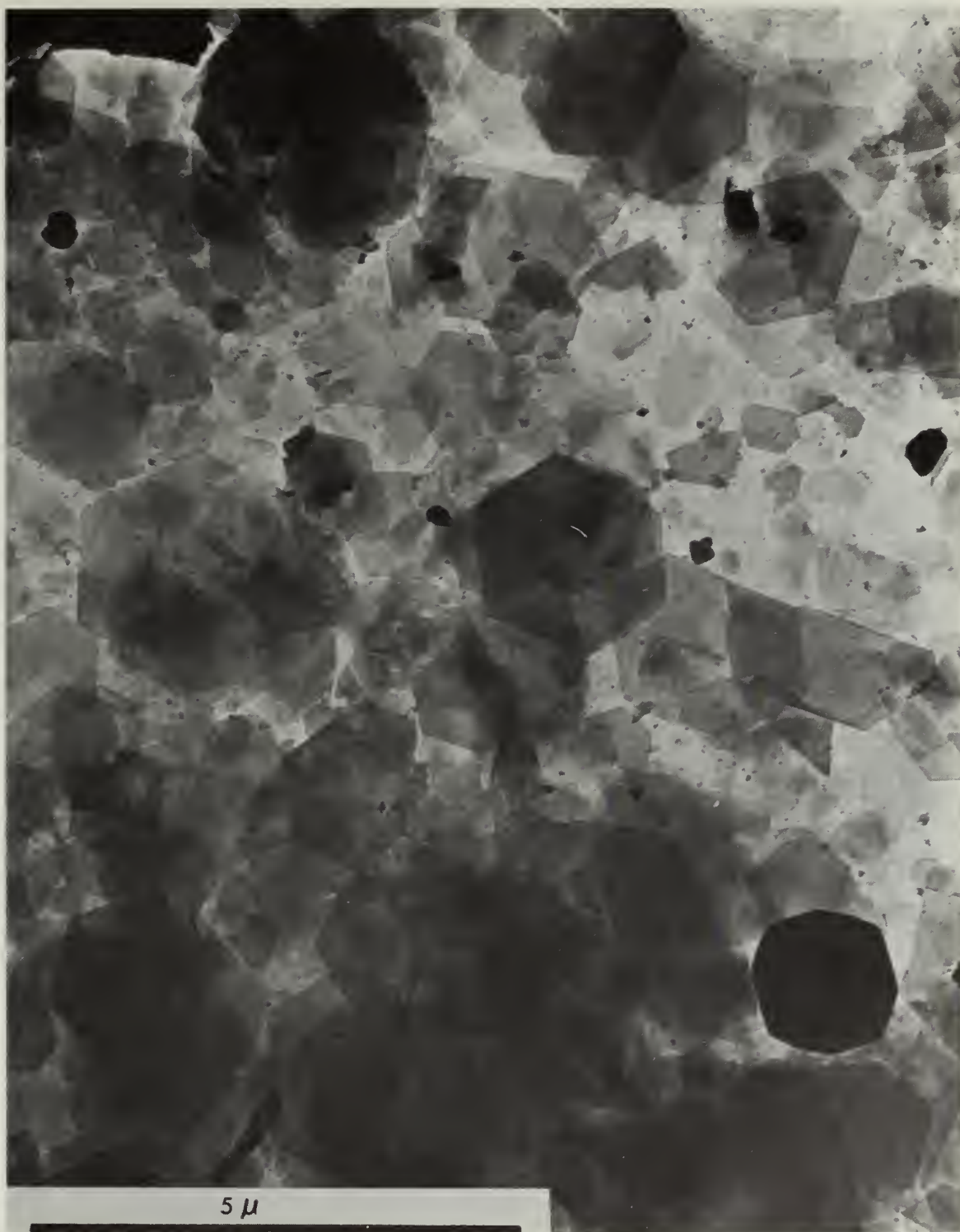


Figure 37. Sample C<sub>4</sub>AF-HA - 3 Hours. The layers of thin plates are representative of the microstructure of C<sub>4</sub>AF with the addition of glycolic acid. Most plates are distinctly hexagonal in shape and are of various sizes. In the lower right corner of the micrograph appears an octagonal shaped dark particle, probably a hydrogarnet crystal.





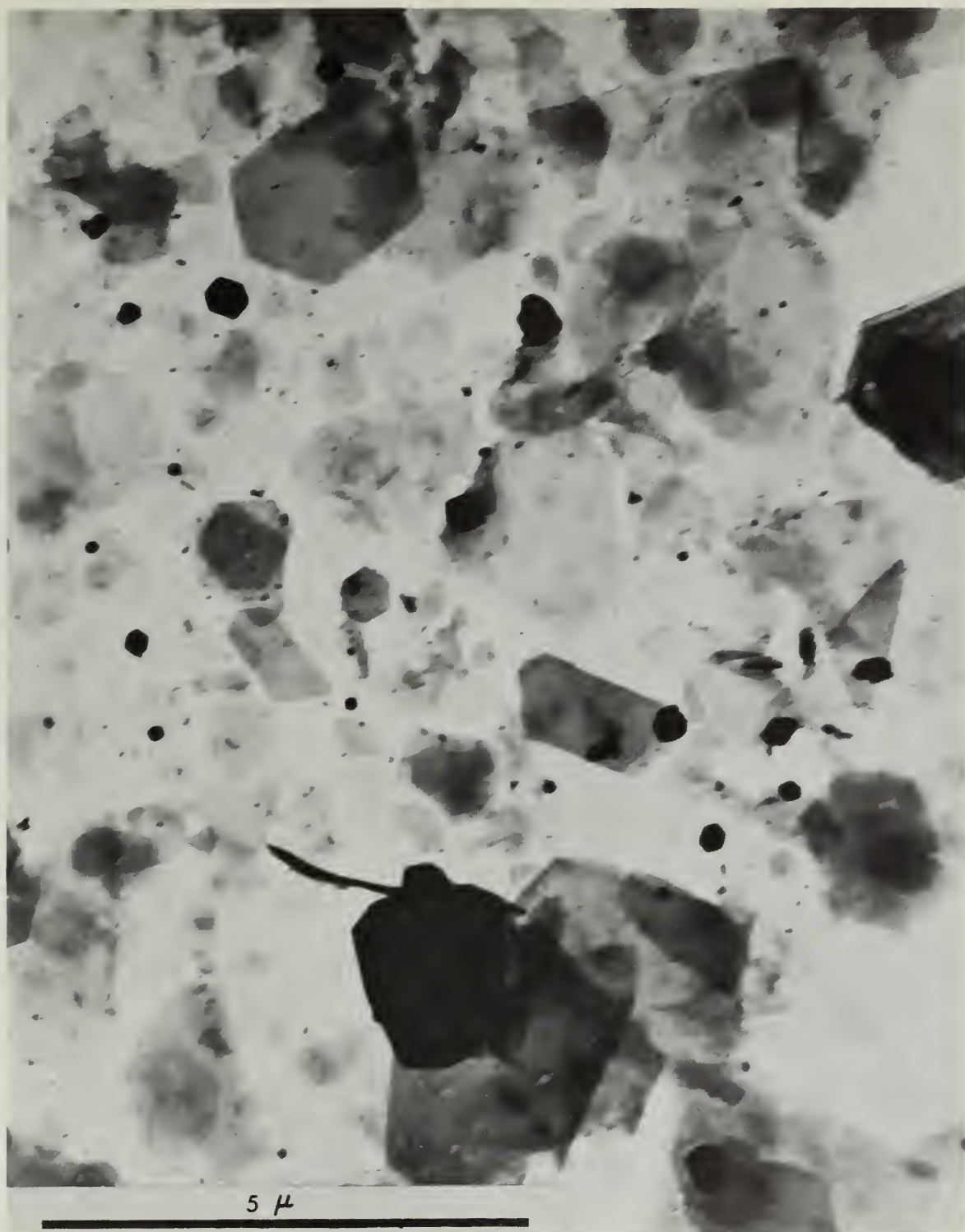


Figure 38. Sample  $C_4AF$ -HA - 6 Hours. The micrograph consists almost entirely of plates. More plates were observed here than in the  $C_4AF$  - 6 Hour sample as seen in Figure 34. Scattered throughout this micrograph are very small dark, isometric shaped particles, probably hydrogarnet crystals. These appear much smaller than did those observed in the  $C_4AF$  - 6 Hour sample.



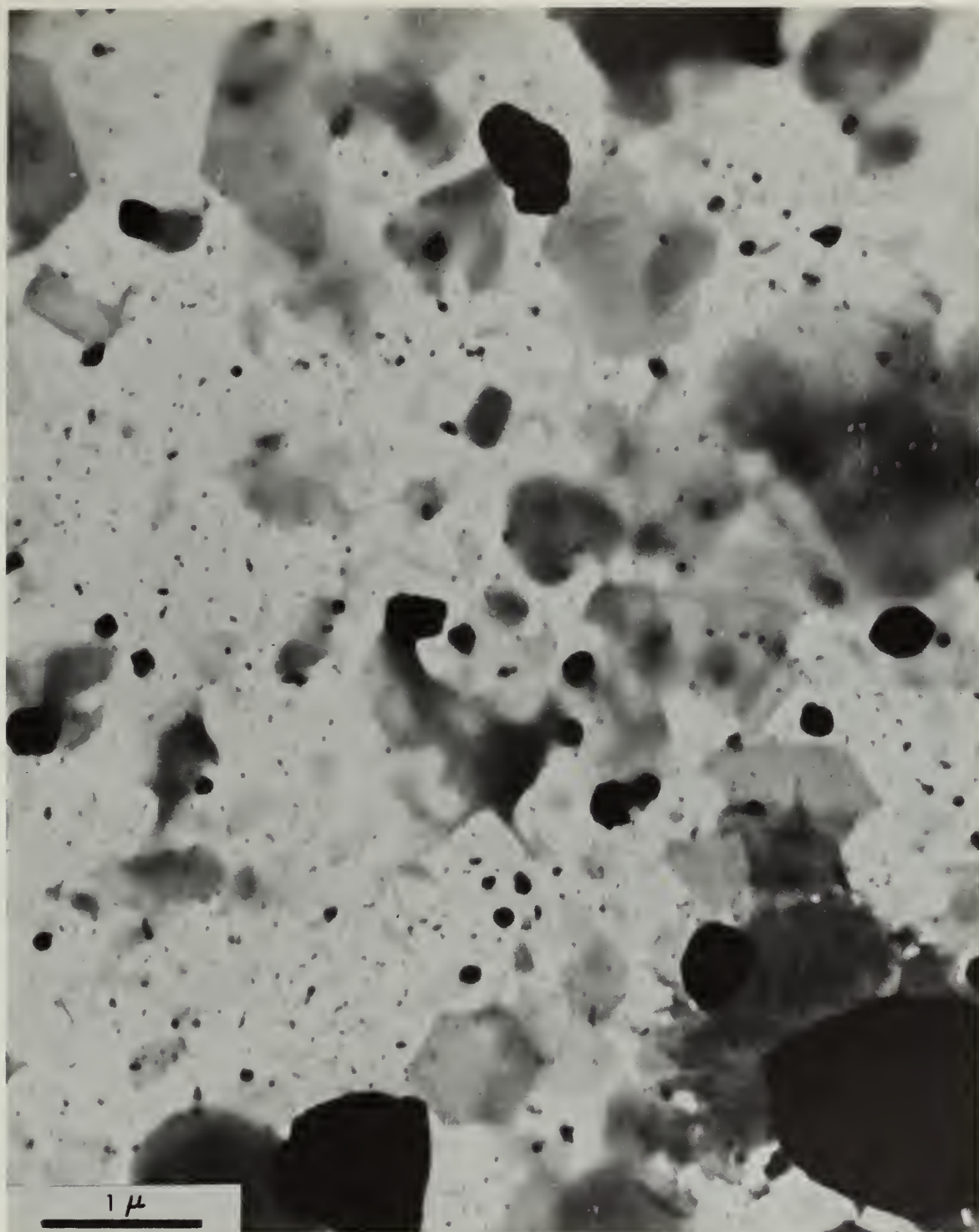


Figure 39. Sample C<sub>4</sub>AF-HA - 24 Hours. Many layers of thin plates are seen which dominated the microstructure of the sample. Some small, dark, isometric shapes of hydrogarnet crystals appear on and between the plates. The appearance of the microstructure is about the same as for the C<sub>4</sub>AF-HA - 6 Hour sample seen in the previous micrograph.







Figure 40. Sample  $C_4AF$ -HA - 7 Days. Layers of thin plates predominate in the microstructure of the sample. However, the dark isometric shapes appear somewhat larger than before. From observations made of the entire specimen, plates appeared to occupy 75% and dark isometric shapes 25% of the areas which were not large dark masses of unhydrated  $C_4AF$ .





Figure 41. Sample  $C_4AF-HA(EX)$  - 3 Hours. Seen in this micrograph are transparent, shapeless particles resembling crumpled foils or shredded plates which predominated the microstructure. Compare this micrograph with the plates of sample  $C_4AF-HA$  - 3 Hours. In other observations of the sample, all that was seen were large, dark masses which were probably unhydrated  $C_4AF$ .





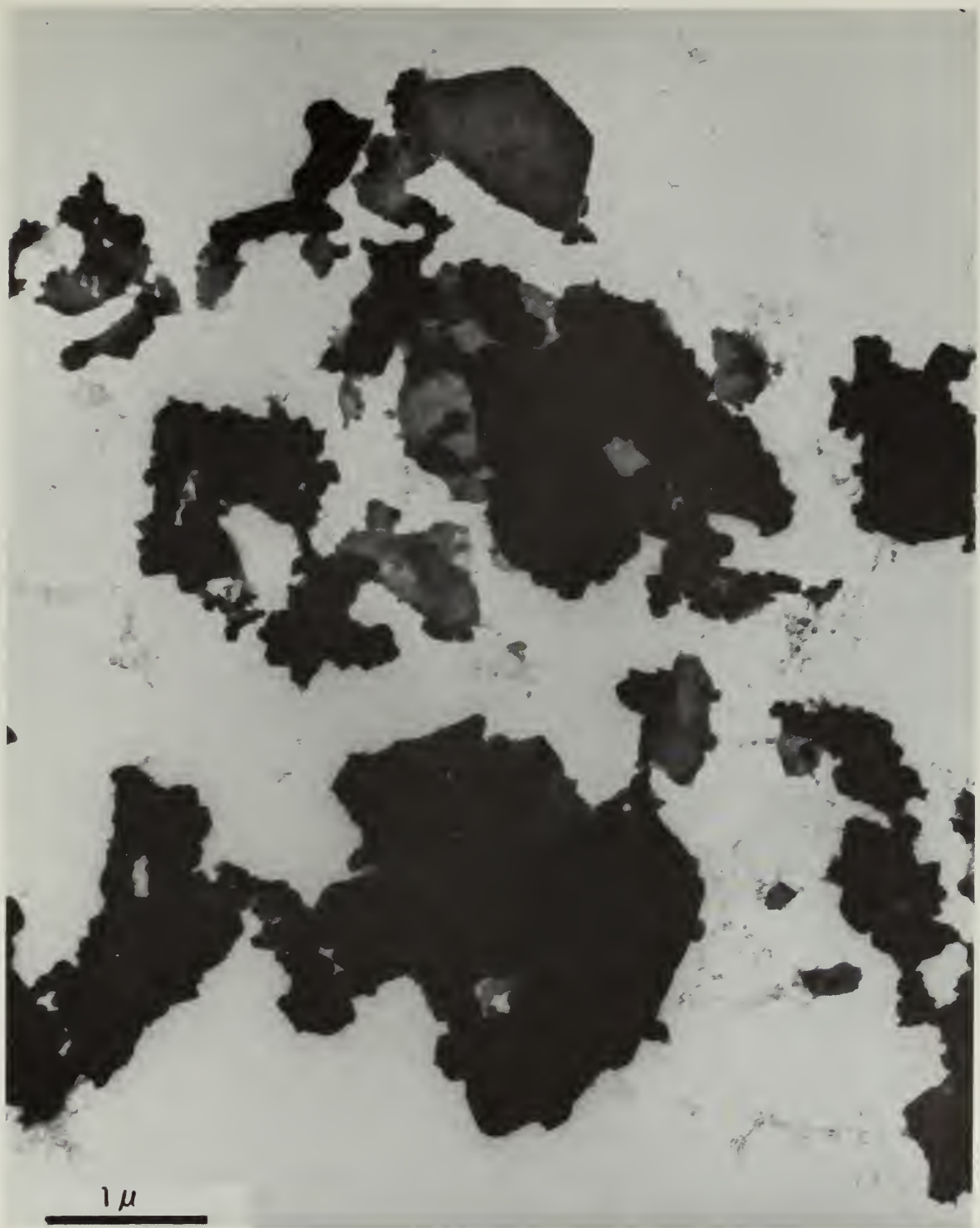


Figure 42(a). Sample C<sub>4</sub>AF-HA(EX) - 6 Hours. This micrograph is representative of the transparent shapeless particles that predominated in the microstructure of the sample. Note in the upper center of the micrograph the hexagonal angles of the particle resembling possibly a plate of very rough surface.





Figure 42(b). Sample  $C_4AF$ -HA(EX) - 6 Hours. Shown in this micrograph is a higher magnification view of one of the shapeless particles observed in the microstructure. Note the shredded appearance of the edges and texture of the surface.



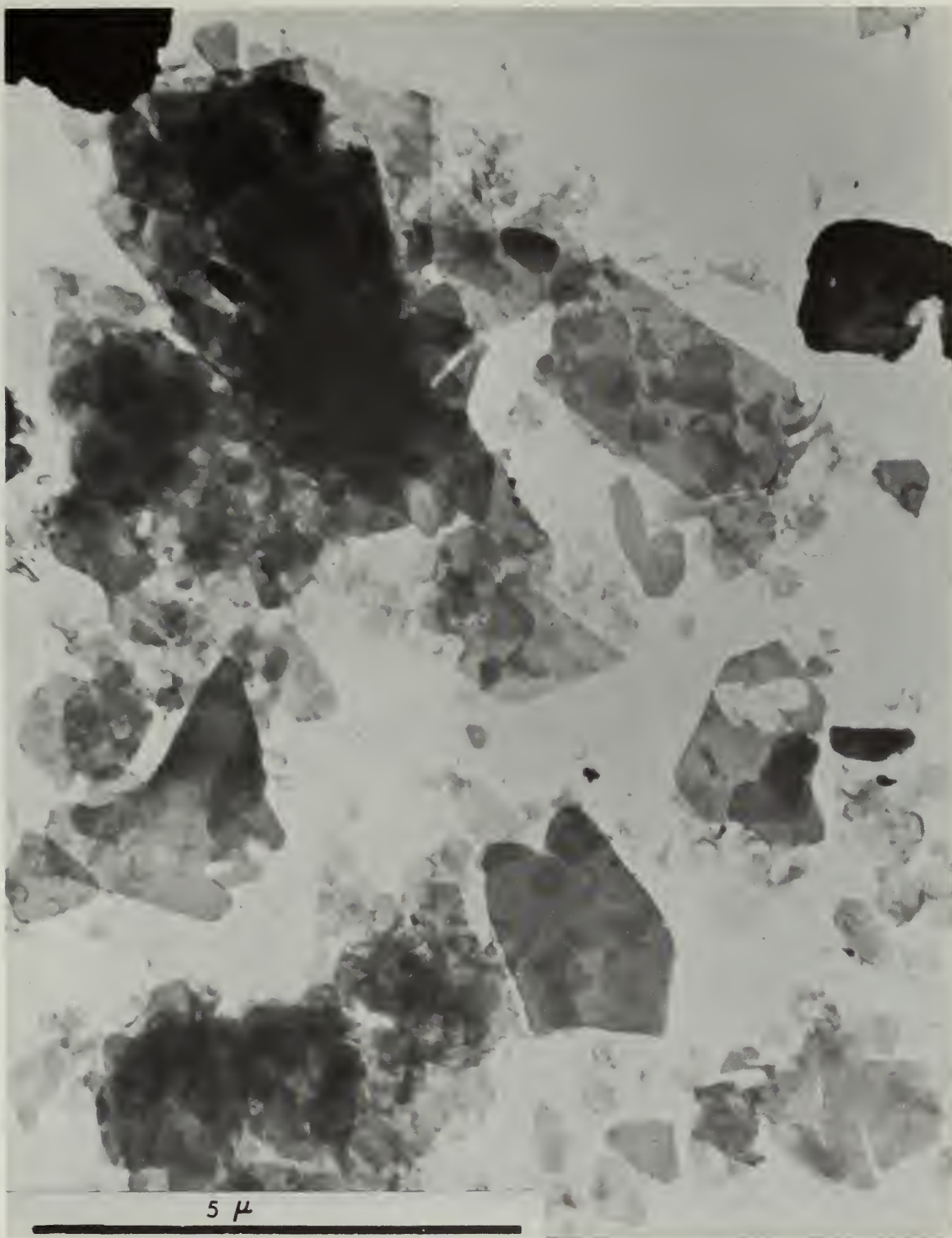


Figure 43. Sample  $C_4AF$ -HA(EX) - 24 Hours. The transparent, shapeless particles dominated the microstructure. Also observed were areas of dark, shapeless masses which were either layers of the shredded plate-like particles or unhydrated  $C_4AF$ . In the micrograph note some of the distinct edges in the transparent mass which could possibly be plates or pieces of plates.







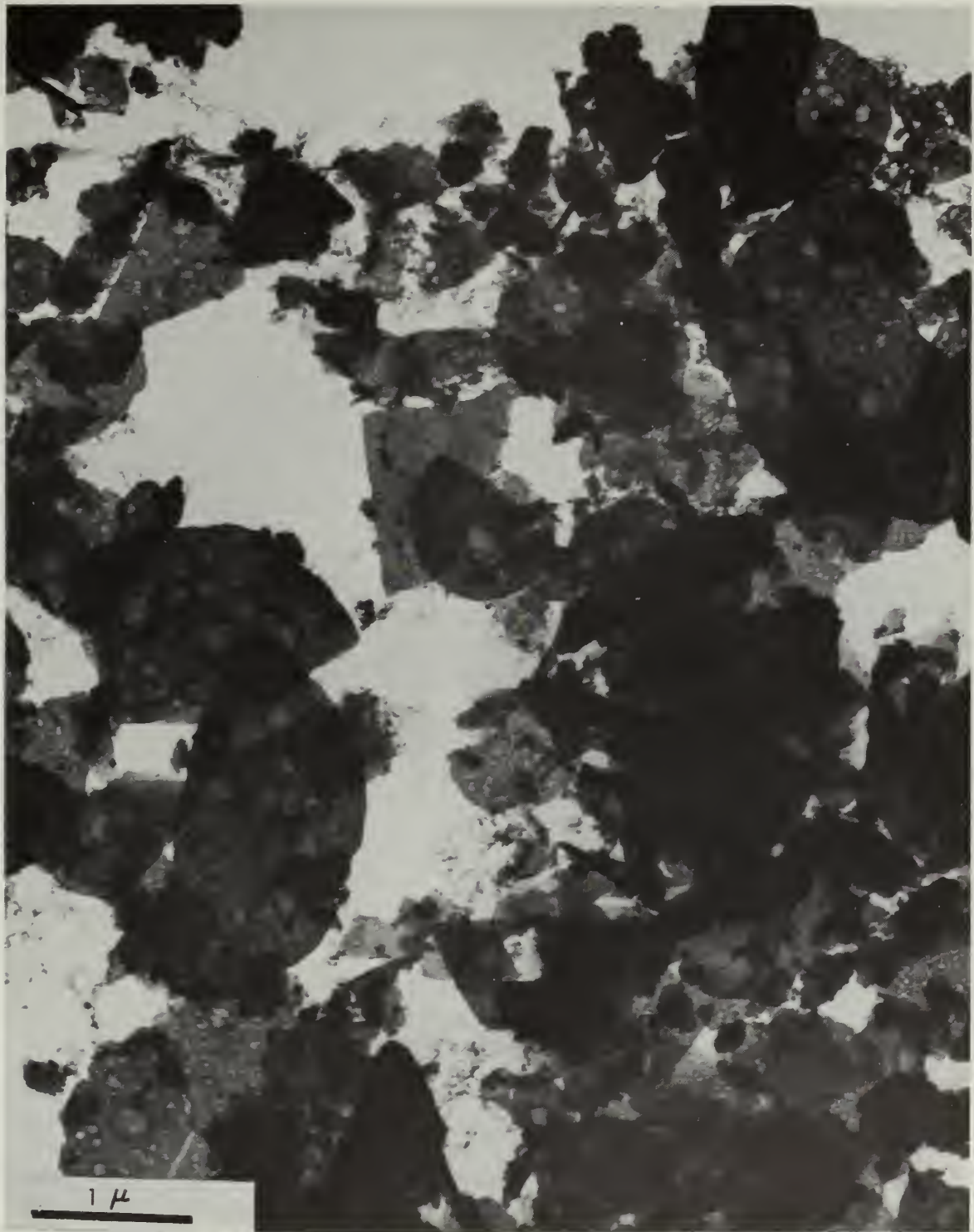


Figure 44(a). Sample C<sub>4</sub>AF-HA(EX) - 7 Days. Again the shapeless, transparent particles were predominant. A few, as seen in this micrograph, had distinct edges. In other observations the edges of some of these particles were definitely hexagonal shaped. Note in this micrograph the texture of the darker particles indicating that they might possibly be thicker shredded plates.



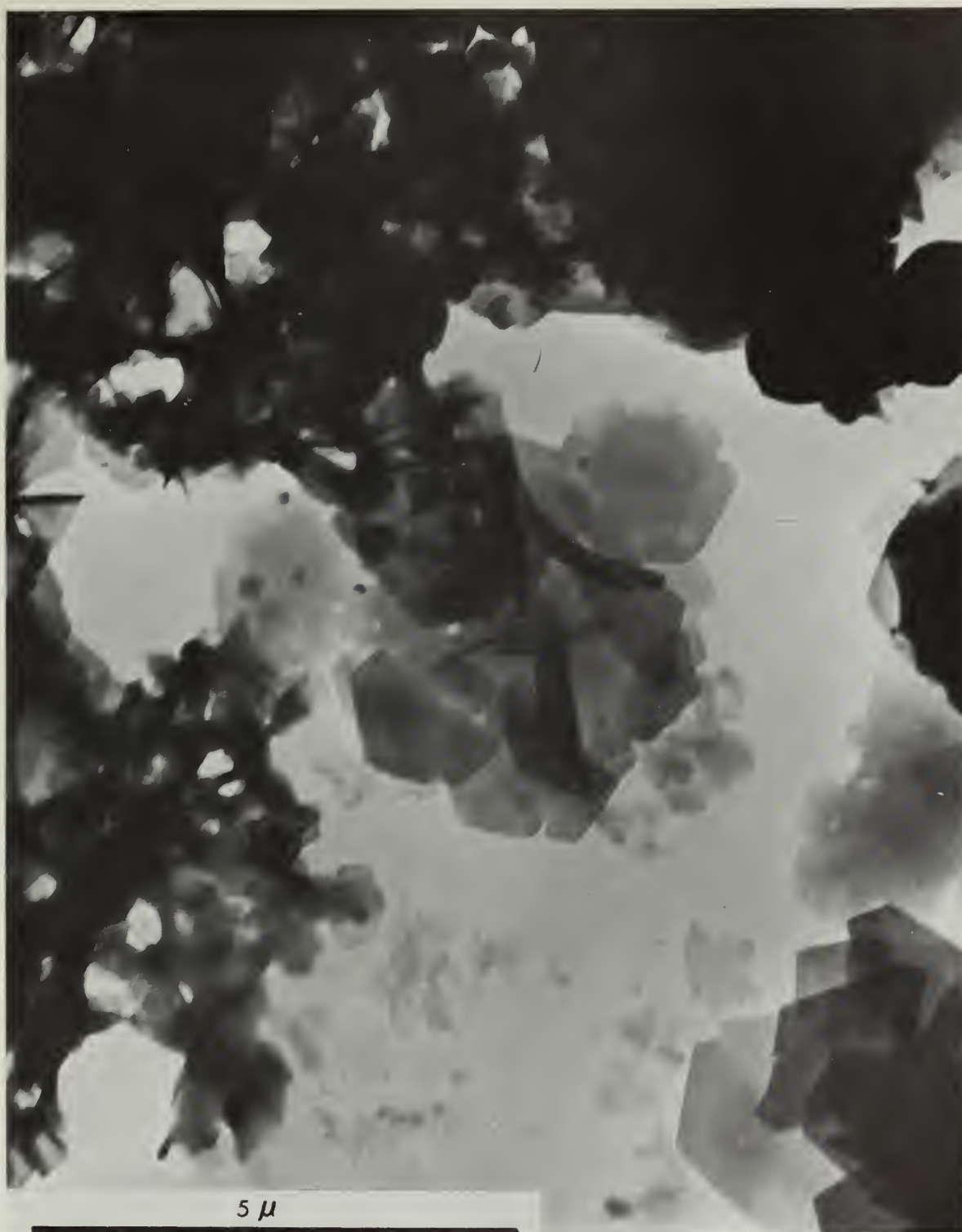


Figure 45. Sample C<sub>4</sub>AF-L - 3 Hours. Thin hexagonal plates can be observed in the center of the micrograph and behind the darker latex structure at the top of the micrograph. In other observations of this specimen there were a few octagonal shaped, dark particles seen which were probably hydrogarnet crystals.







Figure 46. Sample C<sub>4</sub>AF-L - 6 Hours. Again, the latex structure can be seen stretched throughout the micrograph with hexagonal plates behind the structure. From observations of the sample, the plates and dark, octagonal shapes appeared to be in almost the same proportions as seen in the C<sub>4</sub>AF sample at six hours.



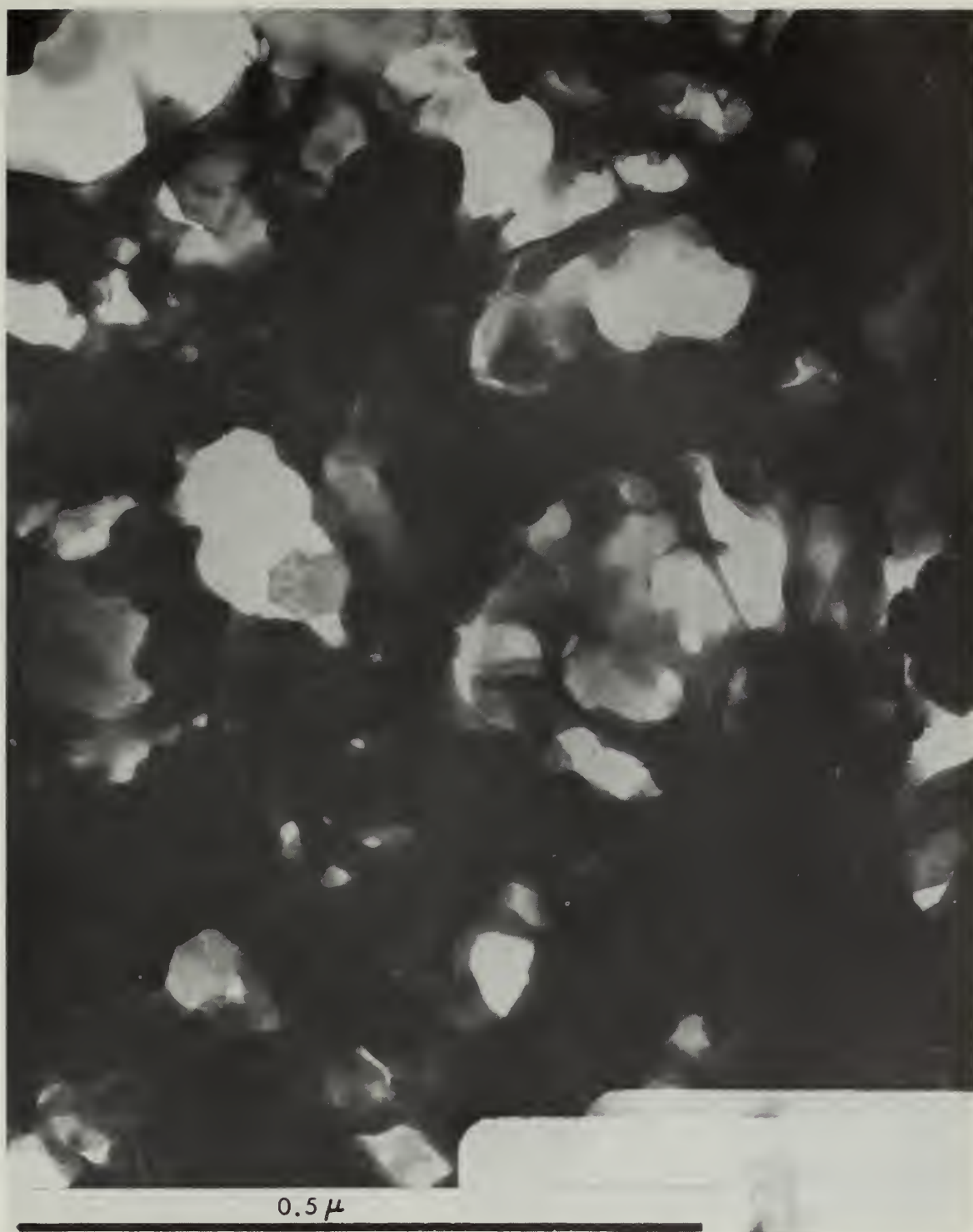


Figure 47. Sample C<sub>4</sub>AF-L - 24 Hours. A few plates can be seen behind some areas of the latex structure in this micrograph. But the latex structure appeared throughout the specimen, and made it impossible to distinguish if plates or dark particles predominated.







Figure 48(a). Sample C<sub>4</sub>AF-L - 7 Days. The latex structure with many hexagonal<sup>4</sup> shaped plates visible behind the structure is shown in this micrograph.





Figure 48(b). Sample C<sub>4</sub>AF-L - 7 Days. The latex structure is not as predominant in this micrograph, and the hexagonal plates and a few of the dark, isometric particles are visible.





Figure 49. Sample C<sub>3</sub>A - 3 Hours. In the center of this specimen prepared without a carbon subtrait, the distinct edges of hexagonal plates can be seen, but near the edges plates are torn or rolled in the absence of a supporting film. Dark areas appear to be composed of isometric hydrogarnet crystals. Most such crystals observed were of an octagonal shape.







Figure 50. Sample C<sub>3</sub>A - 6 Hours. This specimen prepared without a carbon substra<sup>3</sup>it is less dispersed than the previous one. It consists almost entirely of dark masses, presumably hydrogarnet crystals. Around the edges and in the lower left corner can be seen pieces of plates. The percentage of plates present has apparently diminished as hydration has progressed.





Figure 51. Sample C<sub>3</sub>A - 24 Hours. This poorly dispersed specimen prepared without a carbon subtrait is quite similar to the last one. The only apparent difference is that fewer pieces of plates are observable around the edges of the specimen. As a result, the edges of the hydrogarnet crystals are more distinct.



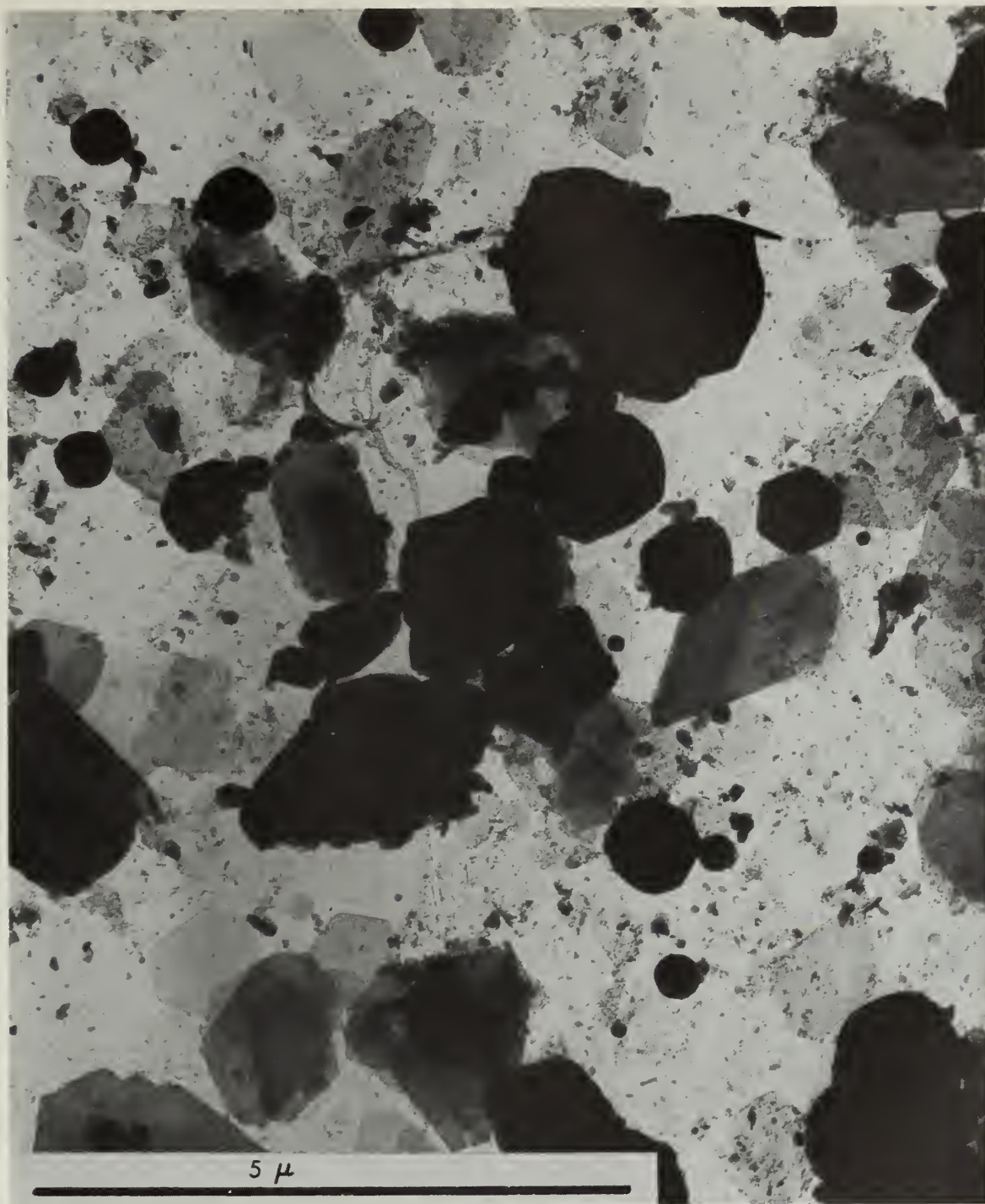


Figure 52. Sample C<sub>3</sub>A - 7 Days. In this specimen, a carbon substrait has been used to achieve a good dispersion. Distinct plates, pieces of plates, and isometric hydrogarnet crystals can be observed. The mottled background apparently consists of tiny fragments of plates. The plates and hydrogarnet crystals exist in about a 50-50 ratio.







Figure 53. Sample C<sub>3</sub>A-HA - 3 Hours. This specimen prepared without a carbon substrait consists almost entirely of plates, although a few small isometric shapes can be observed. Many of the plates or sheets are torn and rolled or wrinkled. The acid has apparently suppressed the formation of the hydrogarnet phase.







Figure 54. Sample C<sub>3</sub>A-HA - 6 Hours. This specimen appears similar to the previous one with the exception of an apparent increase in the number of isometric hydrogarnet crystals present. Nevertheless, the plate phase predominates as contrasted with the comparable untreated specimen seen in Figure 50 where the plate phase was in the minority.



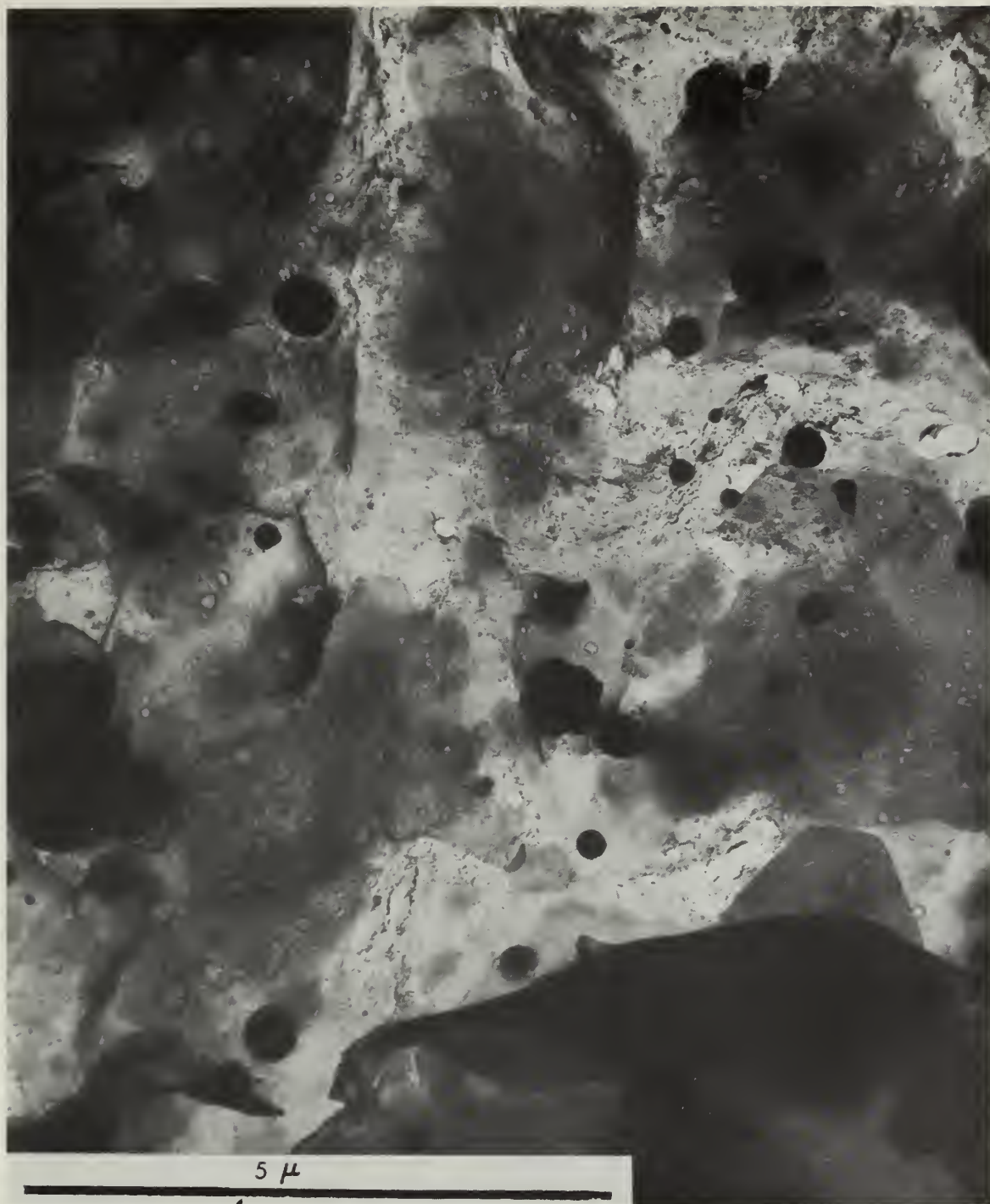


Figure 55. Sample  $C_3A$ -HA - 24 Hours. Here again, the plates of the C-A-H gel phase dominate the sample. The plates are seen to have a mottled or wrinkled texture, perhaps due to the absence of a supporting carbon film. The hydrogarnet crystals of the C-A-H gel phase do not appear to have increased in number as compared with the previous specimen.





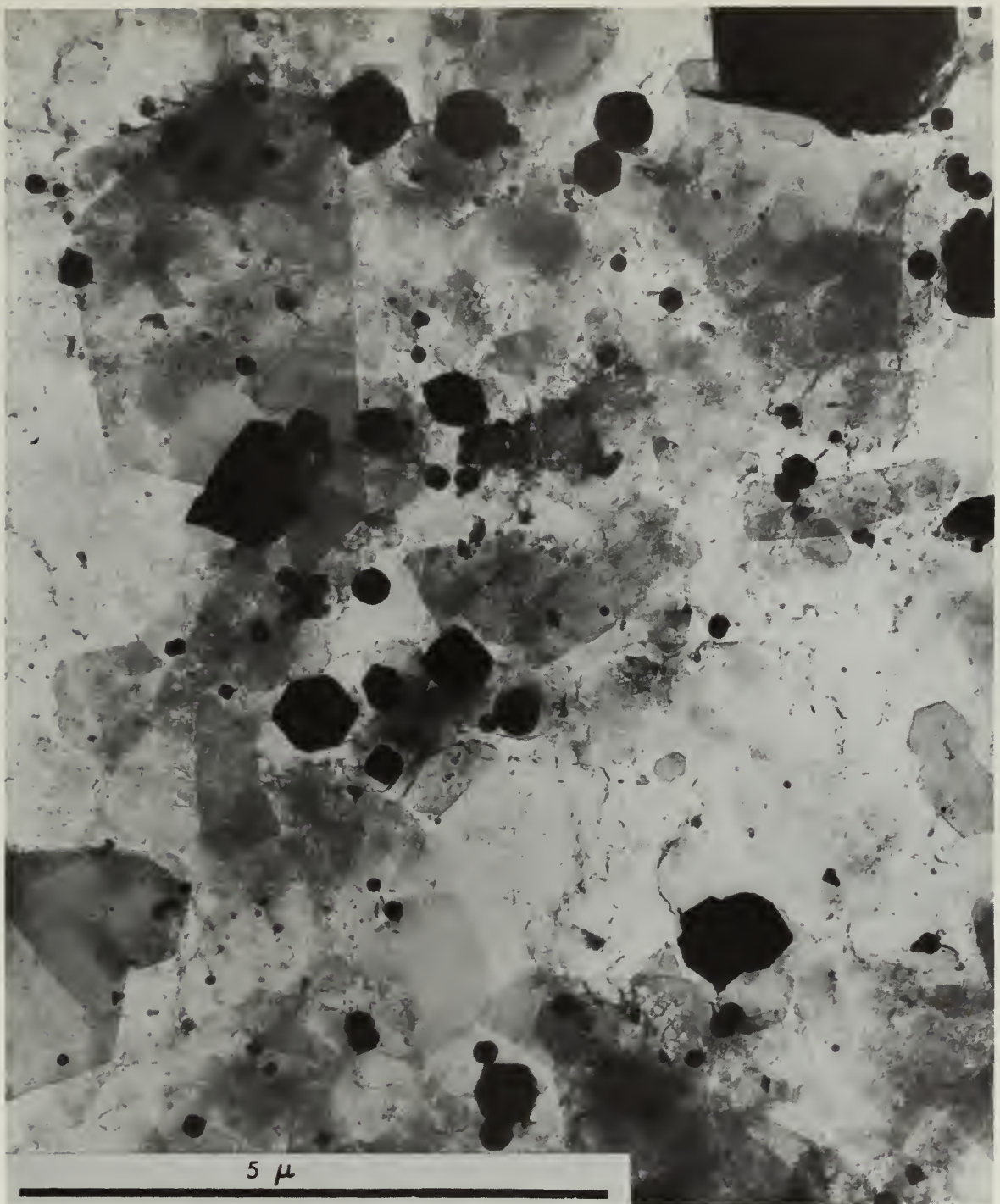


Figure 56. Sample  $C_3A$ -HA - 7 Days. With hydration essentially completed, the plate phase still predominates in the specimen. Plates, pieces of plates, and tiny fragments cover the carbon subtrait. Several small to medium size hydrogarnet crystals are shown here as well, but they are clearly in the minority.





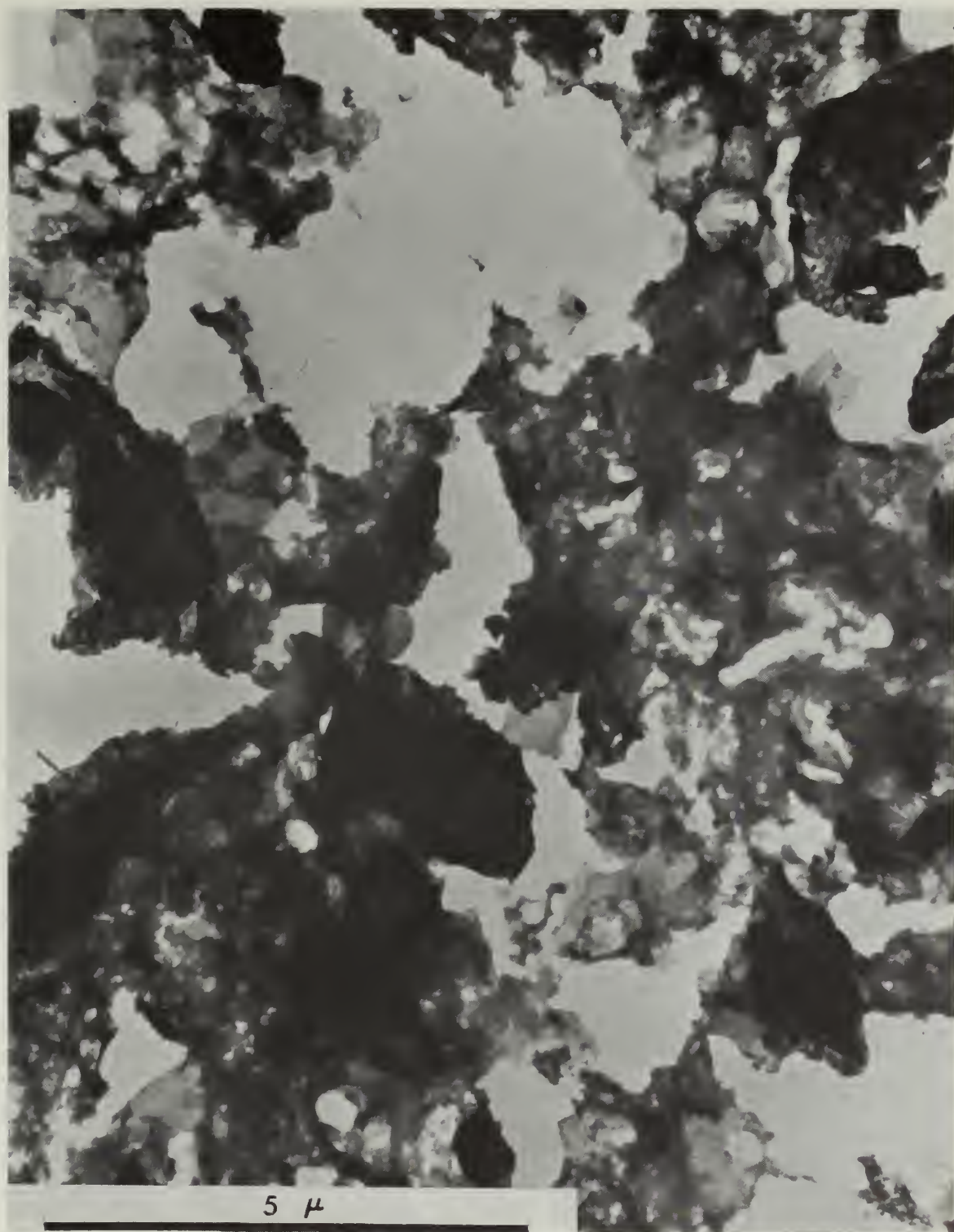


Figure 57. Sample C<sub>3</sub>A-HA(EX) - 3 Hours. This specimen consists entirely of torn and crumpled sheets and some pieces of plates (not shown in this micrograph). The plate phase is in the minority, although the sheets are probably related to the plate phase. Notable is the complete absence of the isometric hydrogarnet phase.



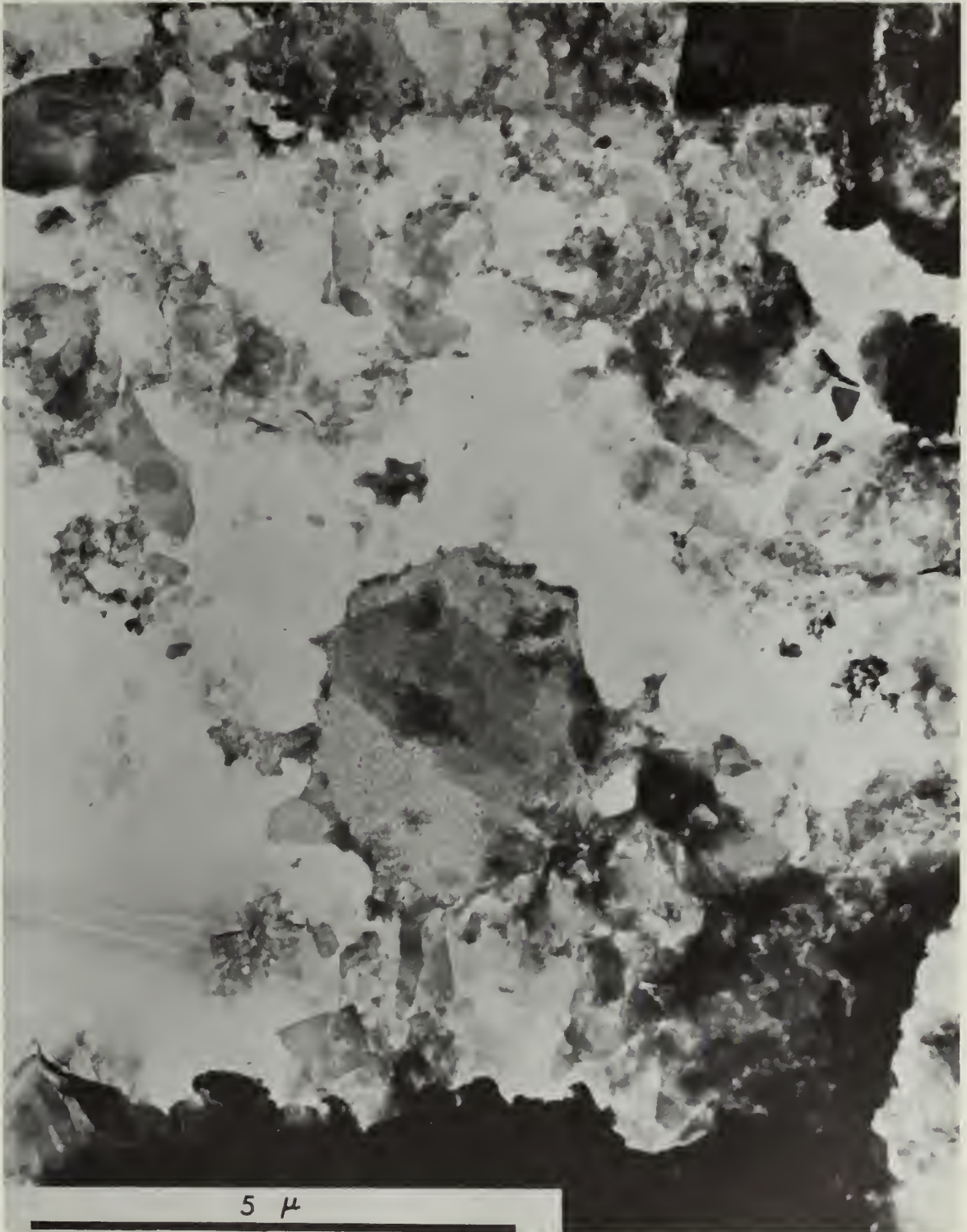


Figure 58(a). Sample C<sub>3</sub>A-HA(EX) - 6 Hours. Hexagonal plates and pieces of plates can be seen in this micrograph, as well as the crumpled sheets previously observed. Once again, the hydrogarnet phase is absent from the specimen.







Figure 58(b). Sample  $C_3A-HA(EX)$  - 6 Hours. An enlarged view shows the texture of the crumpled sheets, but fails to reveal any hydrogarnet crystals.



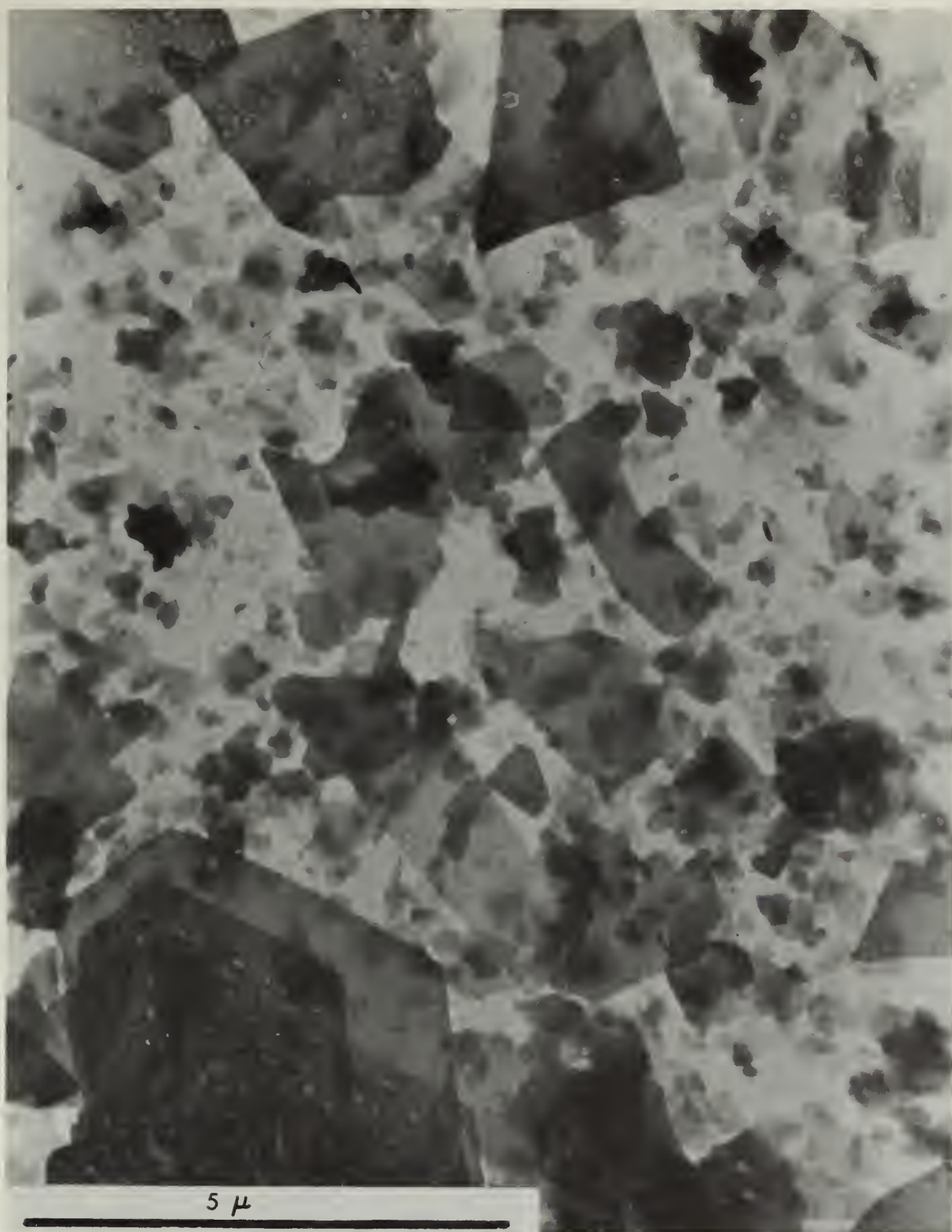


Figure 59. Sample  $C_3A$ -HA(EX) - 24 Hours. As hydration has progressed to twenty-four hours, as seen in this micrograph, the morphology of the specimen consists almost entirely of plates and pieces of plates. Apparently the excess acid has completely suppressed the formation of the hydrogarnet phase and, at least initially, suppressed the formation of the plate phase.





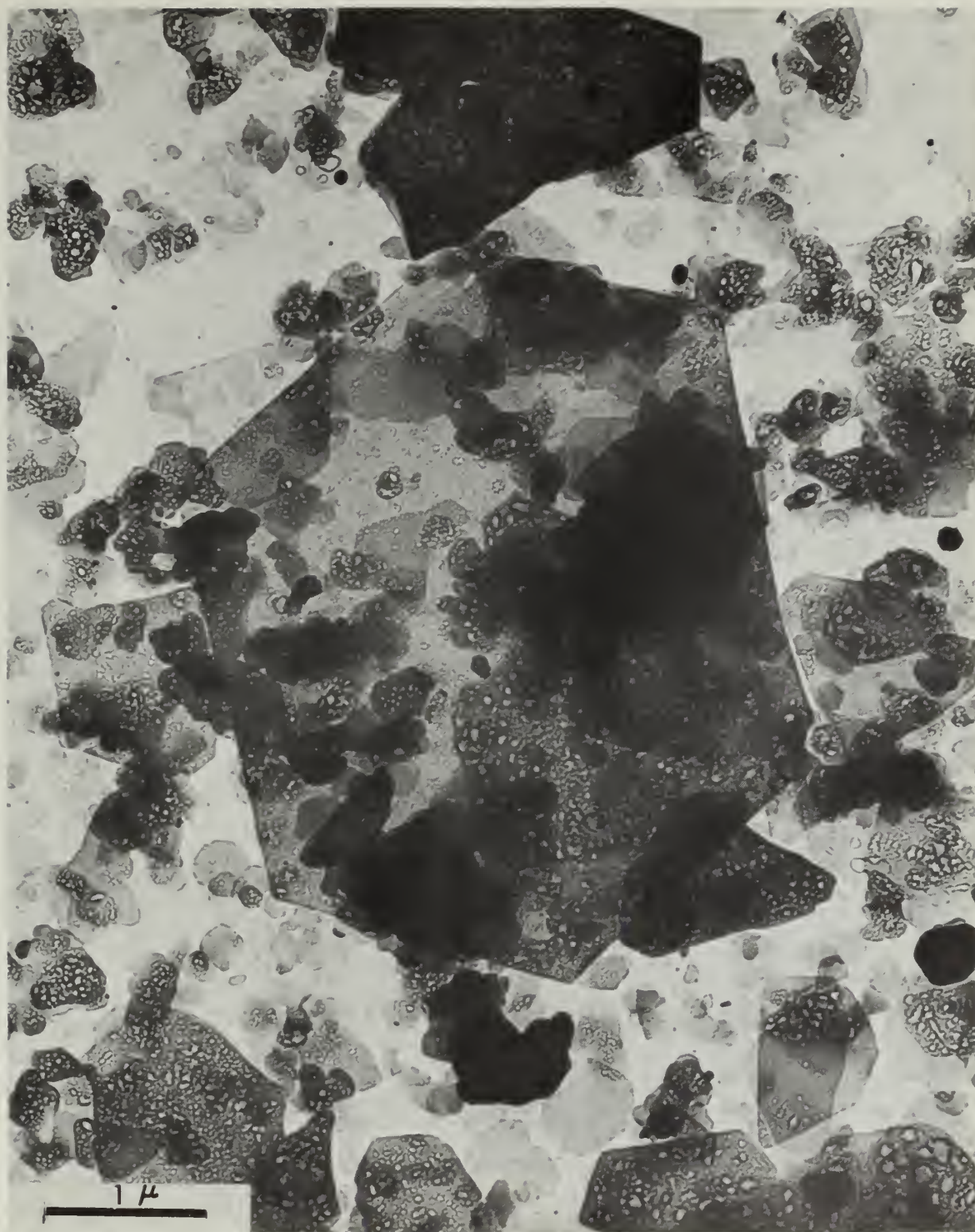


Figure 60. Sample  $C_3A$ -HA(EX) - 7 Days. In this view, the specimen consists of plates and pieces of plates. Hydration is apparently complete and virtually no change in morphology is observable over the previous specimen taken at twenty-four hours.





Figure 61. Sample  $C_3A-L$  - 3 Hours. In this specimen prepared without a carbon subtrait, two hydration products can be identified. The plates of the C-A-H gel phase are present as well as small rods also characteristic of the C-A-H gel phase. The hydrogarnet phase was not observed at three hours. These small rods were not observed in  $C_3A$  alone.







Figure 62. Sample C<sub>3</sub>A-L - 6 Hours. This is a poorly dispersed specimen prepared without a carbon subtrait with a considerable coating of latex. It consists primarily of dark masses with plates visible around the edges. Also visible are a few rods similar to those observed in the previous specimen.







Figure 63. Sample  $C_3A-L$  - 24 Hours. This specimen prepared without a carbon substrait strongly resembles the specimen seen in Figure 61. Once again, none of the hydrogarnet phase can be seen and most of the plates are covered with rods or fibers of the C-A-H phase. Much of the specimen appears to be coated with latex.





Figure 64(a). Sample C<sub>3</sub>A-L - 7 Days. Both hydrogarnet crystals and plates were observed in this specimen. The rods observed in earlier specimens have apparently decomposed at this stage of hydration. As seen in this micrograph, the plates and isometrics are well coated with latex which is generally representative of what was observed.





Figure 64(b). Sample C<sub>3</sub>A-L - 7 Days. Another area of the same specimen is seen here composed largely of plates. The latex is not so thick in this micrograph allowing a clear observation of the plate structure.







Figure 64(c). Sample C<sub>3</sub>A-L - 7 Days. An enlarged view of a few plates remarkably free of latex is shown here. Note the distinct hexagonal edges which are clearly visible.







Figure 65(a). Sample  $C_3A-G$  - 3 Hours. Nearly all of the products of hydration in the specimen are in the form of plates. As shown here, the plates are broken and irregularly shaped. Either they are not fully developed or have broken as a result of vibrating. A few rods were observed, but these were definitely in the minority. No isometric forms were observed.





Figure 65(b). Sample C<sub>3</sub>A-G - 3 Hours. In this micrograph, the hexagonal edges of broken plates are clearly visible. At the left of the micrograph appears what is believed to be a plate either on edge or partially rolled. In a similar specimen such a plate was seen to unroll or flatten out by increasing the intensity of the electron beam.





Figure 66(a). Sample C<sub>3</sub>A-G - 6 Hours. The predominant structure observed at six hours once again consists entirely of plates, some of which are extremely large. Some plates were observed exactly superimposed upon each other or nearly so, possibly accounting for the difference in transparency among the various plates.







Figure 66(b). Sample C<sub>3</sub>A-G - 6 Hours. This micrograph shows again the characteristic plate structure. However, it is interesting to note the dark band in the center of the figure which is probably a plate or sheet partially rolled up.



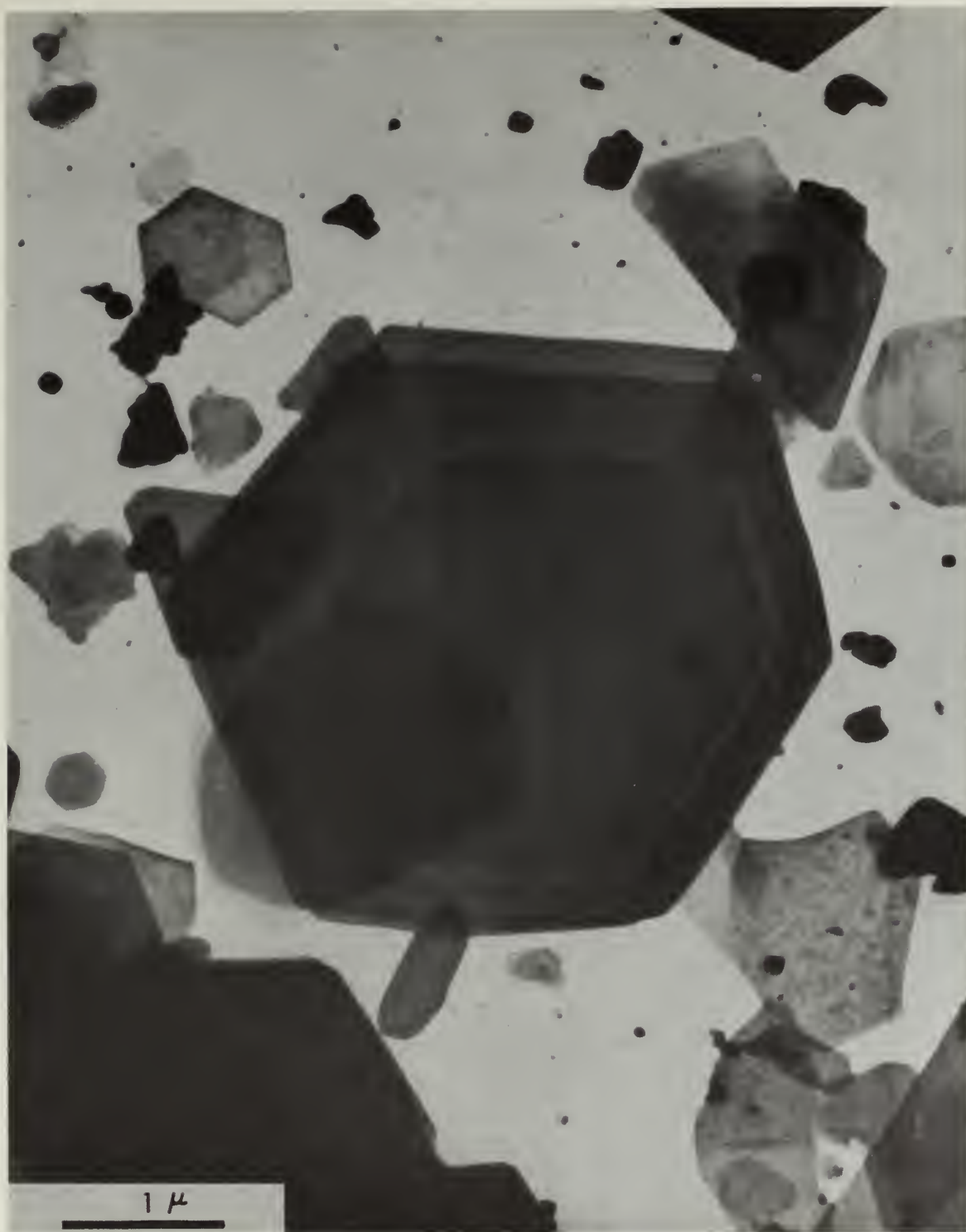


Figure 67(a). Sample C<sub>3</sub>A-G - 24 Hours. At twenty-four hours, little change can be observed in the morphology of the hydration products. Seen in this micrograph are plates and pieces of plates. Plates range in size from small to large. Note the smaller ill-defined plate in the center of the larger, more well defined hexagonal plate.





Figure 67(b). Sample C<sub>3</sub>A-G - 24 Hours. In this micrograph another area of the same specimen is observed. What appear to be irregularly shaped rods are probably plates on end or partially rolled plates.



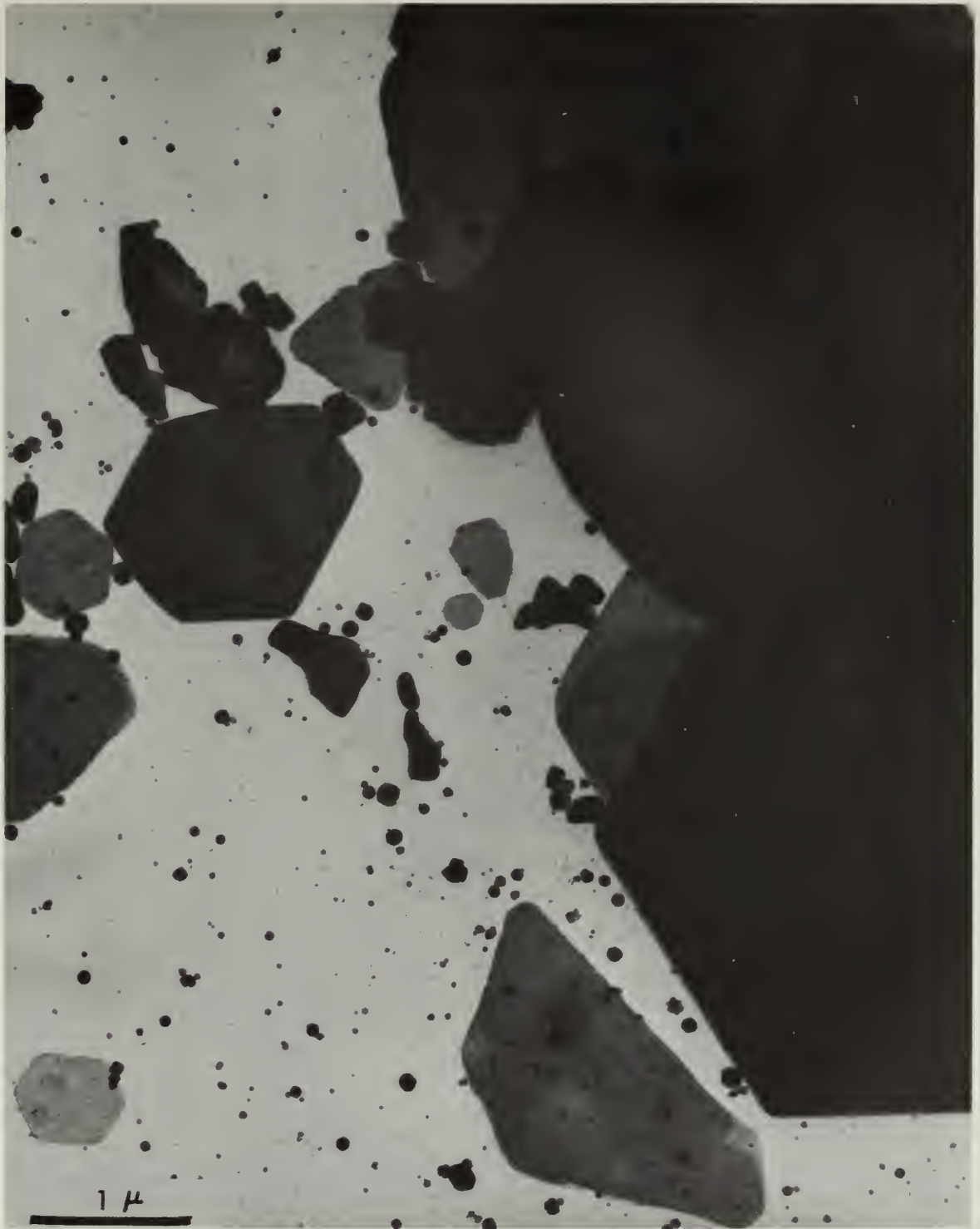


Figure 68. Sample C<sub>3</sub>A-G - 7 Days. At seven days, the plate structure again dominates the specimen. Note, however, the crumpled plate in the micrograph as well as the tiny black shapes. The morphology of the black shapes is not clear. They could be tiny plates or isometric forms.







Figure 69(a). Sample  $C_3A-G-HA$  - 3 Hours. In this specimen the hydration products have taken on two forms: plates and rods. The plate structure is similar to that observed in the comparable specimen without acid, but the addition of glycolic acid is apparently responsible for the presence of the rod-like structures seen in this micrograph at three hours.



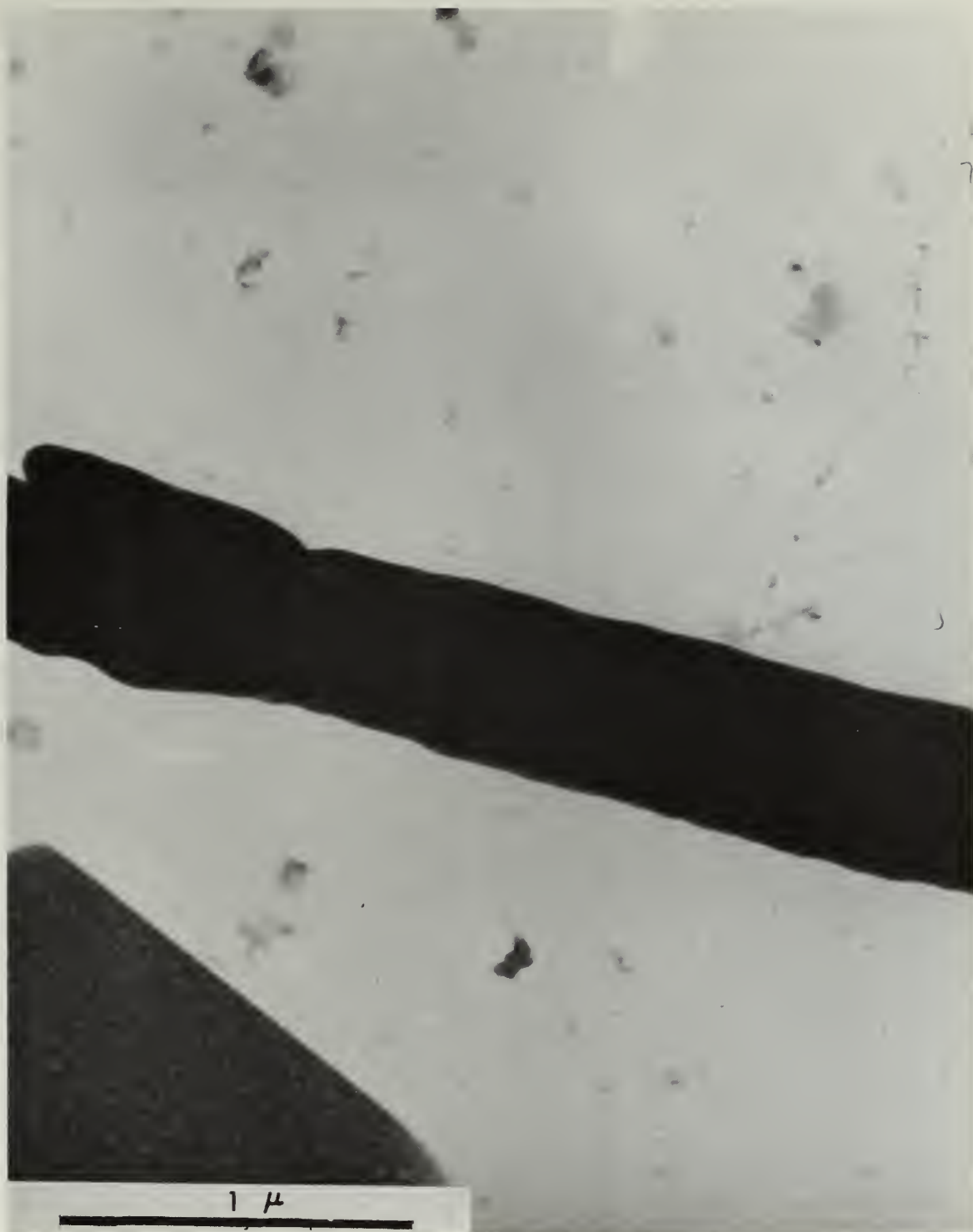


Figure 69(b). Sample  $C_3A$ -G-HA - 3 Hours. This micrograph provides an enlarged view of a typical rod observed in this specimen. A certain amount of texture may be observed in this rod characteristic of the C-A-H phase, not to be confused with similar rods observed in the tobermorite gel phase of  $C_2S$ ,  $C_3S$  and portland cement.





Figure 70(a). Sample  $C_3A$ -G-HA - 6 Hours. Once again, the characteristic plate structure of the C-A-H phase is observed in the micrograph. Plates and pieces of plates of various sizes are present, most with clearly defined hexagonal edges. Most of the rods present at three hours are gone. In fact, only a few were observed on the entire specimen.







Figure 70(b). Sample C<sub>3</sub>A-G-HA - 6 Hours. In this micrograph the textured structure of the plates can be observed. In addition, the micrograph reveals the presence of what appears to be two rods.



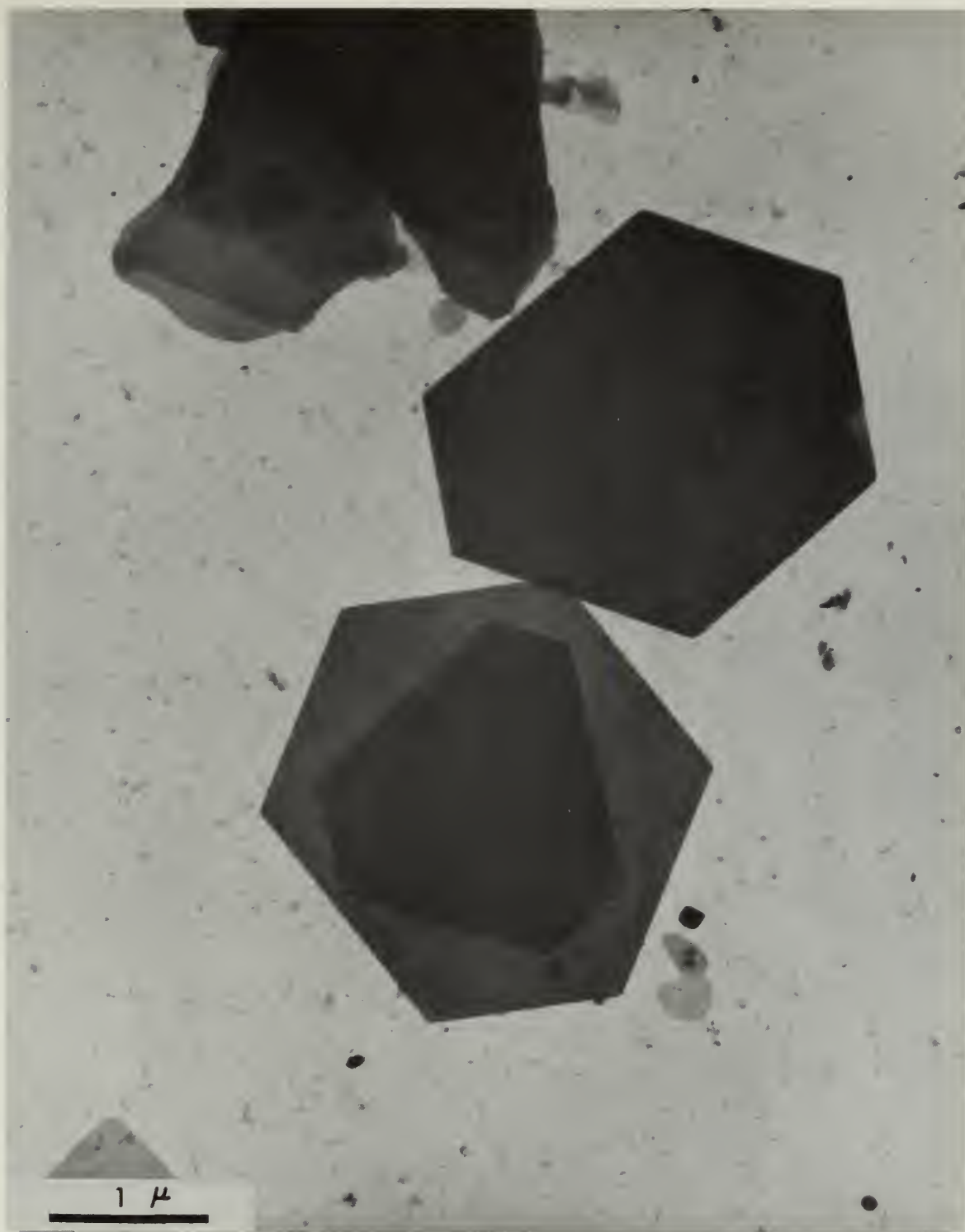


Figure 71(a). Sample  $C_3A-G-HA$  - 24 Hours. This micrograph reveals the hexagonal plate phase similar to that seen in Figure 70(a). This structure appeared throughout most of the specimen. Note the unusual shape of the small, darker plate superimposed on the large, thin hexagonal plate.





Figure 71(b). Sample C<sub>3</sub>A-G-HA - 24 Hours. In this area of the same specimen a different morphology is apparent. An area of crumpled plates or sheets is seen in this micrograph. Also present are large holes in many of the plates. This type of structure was not considered to be representative of the specimen in general.





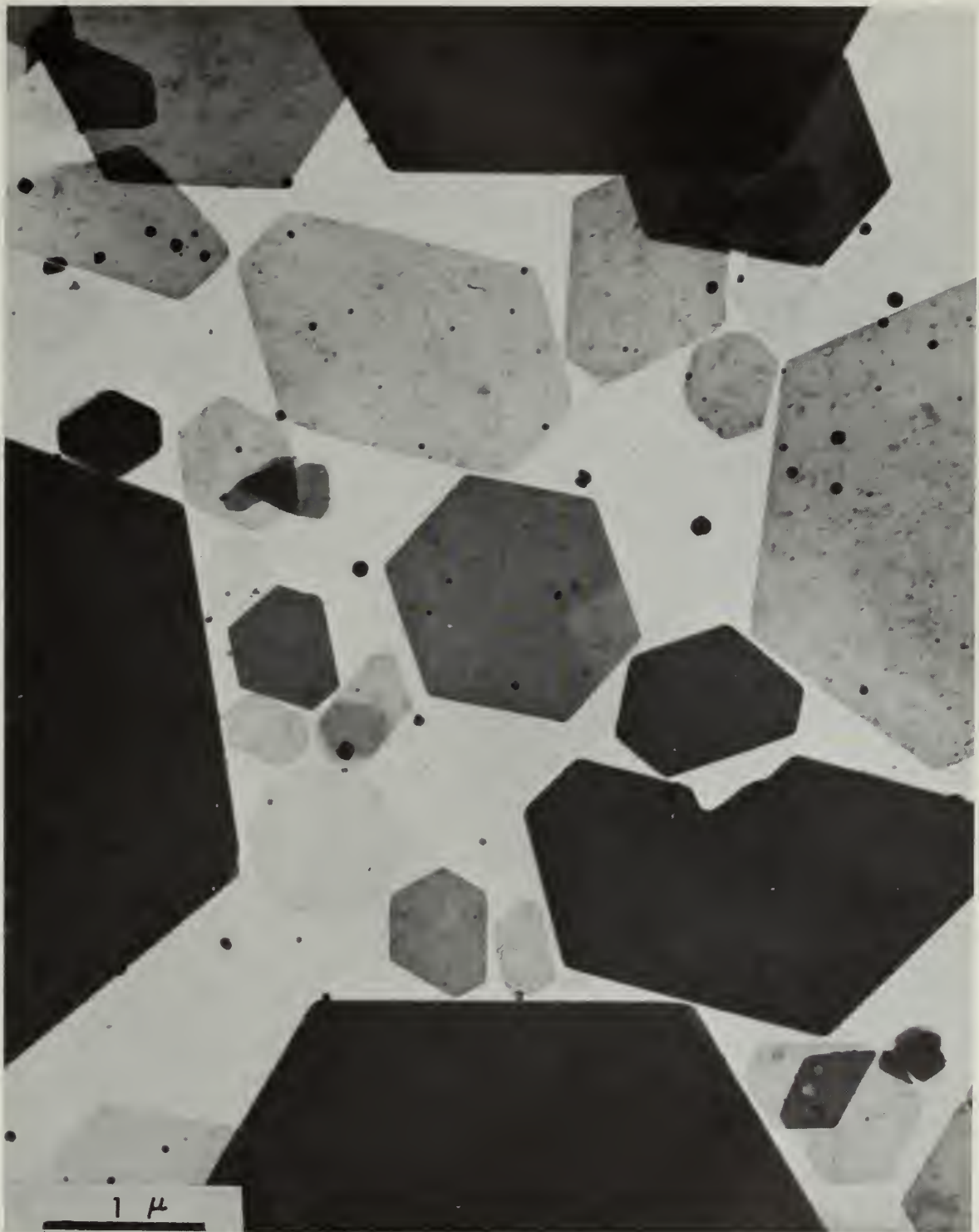


Figure 72. Sample  $C_3A$ -G-HA - 7 Days. In this micrograph, hydration has essentially completed. The specimen consists of plates varying in size from small to large. Some plates are whole, but many are broken. Tiny, black shapes can also be observed, which are either plates or isometric forms.







Figure 73(a). Sample C<sub>3</sub>A-G-HA(EX) - 3 Hours. This specimen consists of pieces of plates, shredded and crumpled plates or sheets, rods or fibers, and small, dark globules intermingled with the shredded plates. This micrograph is a representative example of the type of structure observed throughout the specimen.





Figure 73(b). Sample C<sub>3</sub>A-G-HA(EX) - 3 Hours. This area of the preceding specimen shows a lacy structure which exists in many of the rods and plates. Some of the holes in the rods and plates are rather large. Note the long, very thin rod and the short, thick rod shown in the micrograph.





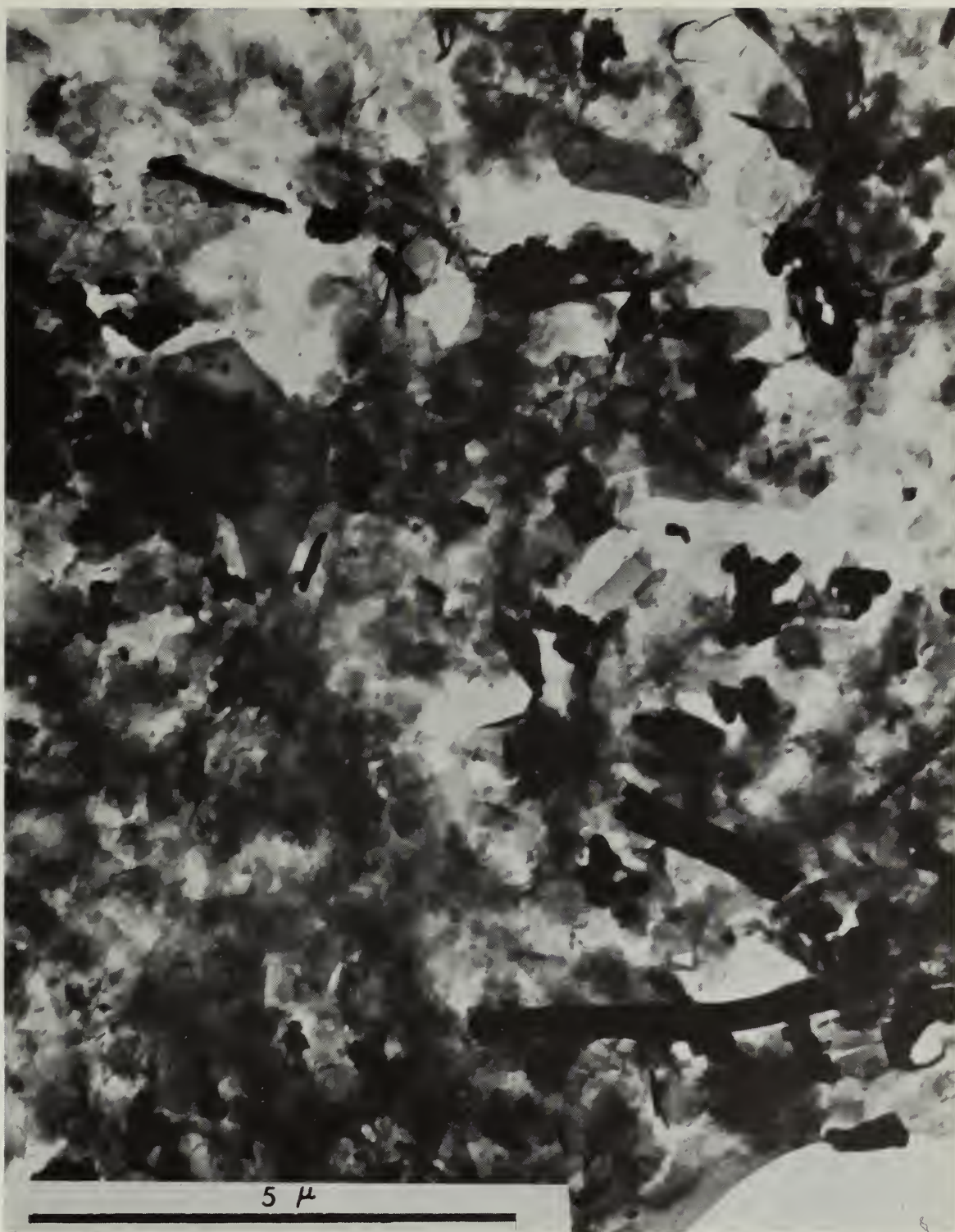


Figure 74(a). Sample  $C_3A$ -G-HA(EX) - 6 Hours. Like the previous specimen the morphology of this six hour specimen is a mixture of several phases. The identifiable hydration products consist of pieces of plates, shredded and crumpled plates, rods, and small, dark globules.







Figure 74(b). Sample C<sub>3</sub>A-G-HA(EX) - 6 Hours. In surveying the previous specimen a few large, rectangular forms similar to the one shown in the micrograph were observed. These are not believed to be significant, but are shown simply for their unusual morphology.



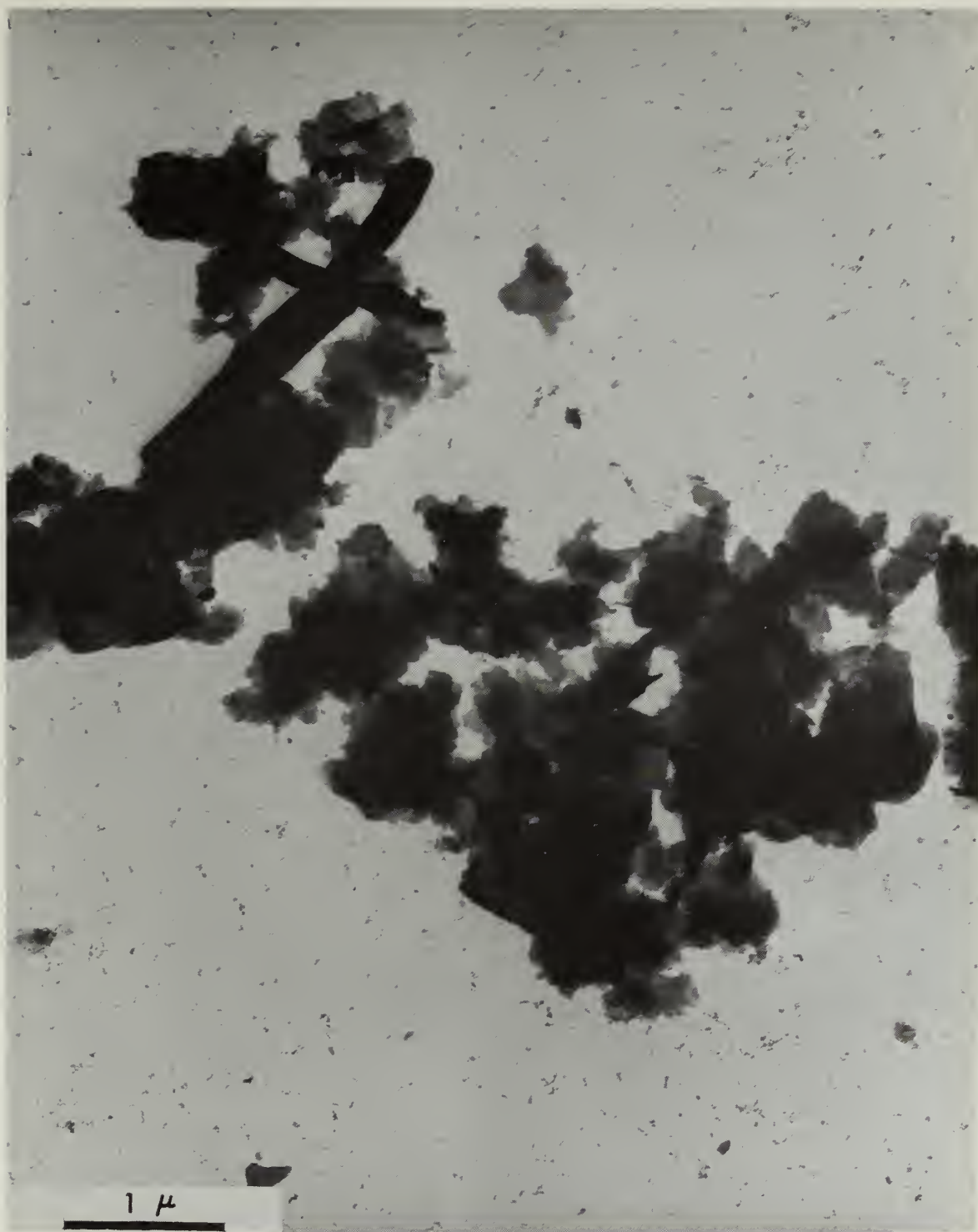


Figure 75(a). Sample C<sub>3</sub>A-G-HA(EX) - 24 Hours. The predominant hydration products observed at twenty-four hours are pieces of plates and crumpled and shredded plates. Also present in minor quantities are rods similar to those seen in previous specimens.





Figure 75(b). Sample  $C_3A-G-HA(EX)$  - 24 Hours. In this enlarged view taken from a different area of the previous specimen the lacy structure of the plates is once again apparent, with the size of the holes ranging from small to large.







Figure 76. Sample C<sub>3</sub>A-G-HA(EX) - 7 Days. This specimen is similar in morphology to the twenty-four hour specimen as can be seen by a comparison with Figure 75(a). Once again hydration products consisted of pieces of plates and crumpled and shredded plates. Also present are what appear to be partially rolled plates.







Figure 77. Sample PC - 3 Hours. In this representative micrograph are shown needles or fibers of thin to medium thickness, products of the C-S-H phase, and what appear to be parts of plates, products of the C-A-H phase. In the center of the micrograph note the end of the thick needle which gives it the appearance of a small bundle of fibers.





Figure 78(a). Sample PC - 6 Hours. The microstructure appears about the same as shown in the previous micrograph of portland cement at three hours, except that the needles or fibers are longer and somewhat thicker than at three hours and are more abundant. Note in the right center of the micrograph a particle which is possibly a foil or crumpled plate.







Figure 78(b). Sample PC - 6 Hours. This micrograph shows an enlarged view of the needles or fibers of the microstructure together with what appears to be crumpled foils. Note the texture of some of the needles.







Figure 79(a). Sample PC - 24 Hours. In this micrograph is seen the representative microstructure of the sample consisting of needles, most with irregular edges along their length, and foil-like particles. In other observations plates and a few dark particles were seen with curved edges which could have possibly been hydrogarnet crystals.





Figure 79(b). Sample PC - 24 Hours. Shown here is an enlarged view of one of the needles present in the microstructure. Note the tiny, dark spots in the surface texture of the lower needle.





Figure 80(a). Sample PC - 7 Days. In this micrograph are shown two of the particles seen in the microstructure at seven days, namely transparent plates and long needles. Note the texture of the needle surface and the angles of the plates. Foils and dark masses were the other two constituents in the microstructure.





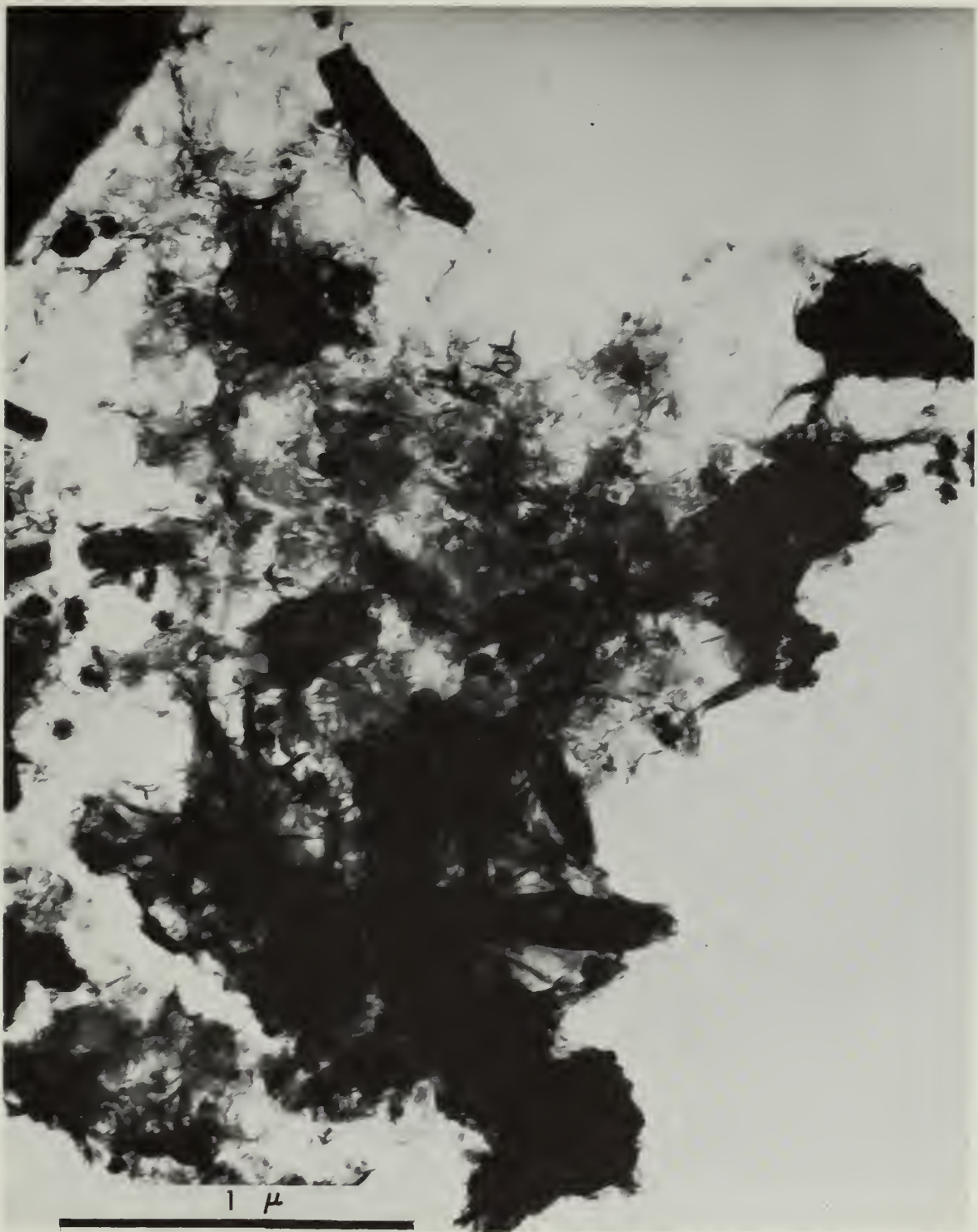


Figure 80(b). Sample PC - 7 Days. In this micrograph one sees crumpled foils, needles, and a possible plate in the upper left corner of the micrograph. The dark masses are possibly areas of many foils and/or needles grouped together or, as Grudemo (6) described such masses, large clumps of amorphous material.







Figure 80(c). Sample PC - 7 Days. This is an enlarged view of an area of the microstructure which shows the fibrous makeup of one of the dark masses. Note the plate at the lower right of the micrograph together with a long needle.





Figure 81. Sample PC-HA - 3 Hours. The predominant hydration products seen in this specimen are the hexagonal plates of the C-A-H phase and the characteristic needles of the C-S-H phase. Also present are some foil-like structures. Small quantities of the  $\text{CO}_2$  contaminated C-H phase are seen in this micrograph, but were generally present in greater quantities.







Figure 82. Sample PC-HA - 6 Hours. No apparent changes in morphology have occurred between three hours and six hours, although this micrograph is not as clear as the previous one. The structure of needles and plates is still present, but has unexplainably taken on a mottled appearance.







Figure 83. Sample PC-HA - 24 Hours. The foils and needles of the C-S-H phase dominate this specimen. The needles appeared slightly longer than in the comparable specimen without acid. Many plates were also observed in this specimen.





Figure 84. Sample PC-HA - 7 Days. The foils, needles and plates observed in earlier specimens of this series are again predominant. The needles observed were generally shorter and finer than in the previous specimen, although somewhat more numerous and longer than in portland cement alone.





Figure 85. Sample PC-HA(EX) - 3 Hours. The predominant structures observed in this specimen are plates and needles. Also present are small dark globules apparently oriented in chains and interwoven with the needles and plates. While their morphology is not clear, these are probably the result of the presence of the CO<sub>2</sub> contaminated C-H phase.







Figure 85. Sample PC-HA(EX) - 3 Hours. The predominant structures observed in this specimen are plates and needles. Also present are small dark globules apparently oriented in chains and interwoven with the needles and plates. While their morphology is not clear, these are probably the result of the presence of the  $\text{CO}_2$  contaminated C-H phase.







Figure 86(a). Sample PC-HA(EX) - 6 Hours. At six hours, the predominant structure observed was the interwoven needle structure shown in this micrograph. Several plates may be seen in the background as well as some of the CO<sub>2</sub> contaminated C-H phase seen in the previous specimen.





Figure 86(b). Sample PC-HA(EX) - 6 Hours. In this enlarged view the structure of the needles may be more clearly observed. Also some very thin needles are present, probably in the early stages of development. At the center of the micrograph appears to be a cube-shaped hydrogarnet crystal. In general the needles appear to be more numerous in this excess acid specimen.





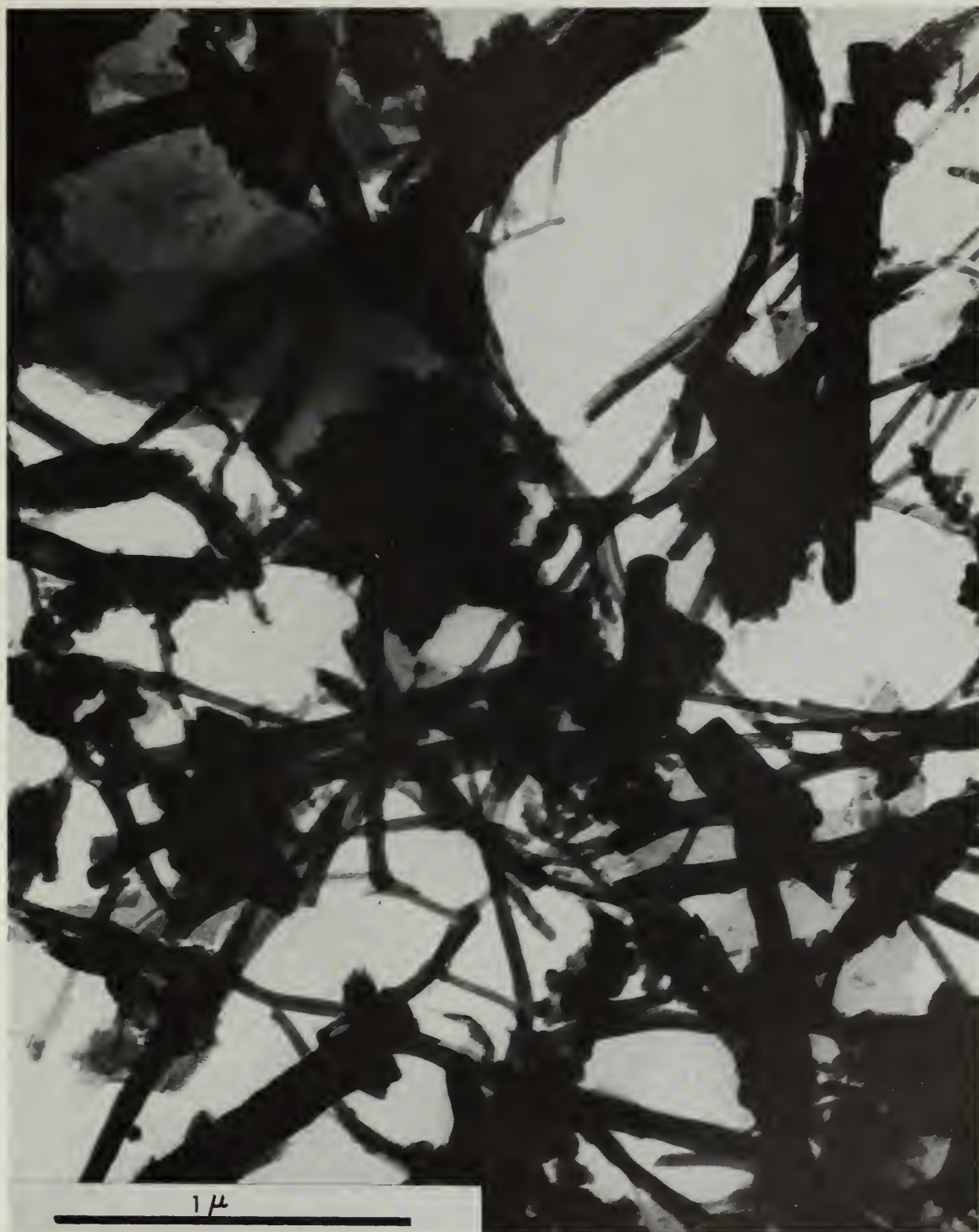


Figure 87. Sample PC-HA(EX) - 24 Hours. The hexagonal plates of the C-A-H phase and the needles of the tobermorite-like C-S-H phase are again the predominant hydration products. Many more needles are present than were observed in portland cement alone or in portland cement with a normal amount of glycolic acid.







Figure 88(a). Sample PC-HA(EX) - 7 Days. The interlocking needle structure is typical of this specimen. In the background can be seen many plates and foils. Also present are several very large needles similar to those observed in the hydration of  $C_3S$  with excess glycolic acid. Clearly many more needles are present than in comparable specimens without excess acid.





Figure 88(b). Sample PC-HA(EX) - 7 Days. This enlarged view shows the tips of some large needles. The needle tip observed in the center has the appearance of being rolled, thus appearing to be a single needle rather than a cluster of needles as observed in the  $C_3S$  specimens. A few smaller needles are also shown in this micrograph.





Figure 89. Sample PC-L - 3 Hours. In this micrograph is shown the latex structure which dominated the sample thereby making viewing of the products of the hydration of portland cement difficult. However, some of the needles are visible here. In other observations of the sample evidence of a few plates were seen.







Figure 90. Sample PC-L - 6 Hours. The microstructure of this sample has about the same appearance as did portland cement at six hours, except that a few isometric particles were observed, of cubic and hexagonal shapes. Latex structure appeared throughout the sample and seemed to coat everything.







Figure 91. Sample PC-L - 24 Hours. In this sample the latex was not quite as predominant, and in this micrograph foils, needles and a hexagonal shaped particle can be seen. This was representative of the sample.





Figure 92(a). Sample PC-L - 7 Days. Shown in this micrograph are foils and a particle which appears to be part of a larger C-A-H plate crystal. Stretched latex is visible in the left center of the micrograph. Outlines of needles can be seen also. The plates were not as numerous as in portland cement at seven days, but the foils and needles appeared the same as in portland cement at seven days.





Figure 92(b). Sample PC-L - 7 Days. This is an enlarged view of some of the needles present in the microstructure showing the holed texture of their surfaces.







Figure 92(c). Sample PC-L - 7 Days. This micrograph shows the foil-like areas and some needles and hexagonal plates, all held together by the latex structure.





Figure 93(a). Sample EM 1A. The best description of this micrograph is given in a statement by Grudemo as quoted by Copeland and Schulz (18). The specimen "consists of exceedingly ill-formed, colloidal products, in which it is... difficult to discern any definite morphology."





Figure 93(b). Sample EM 1A. In this micrograph can be seen clumps of amorphous material. Many areas are of a thin transparent nature, suggesting the presence of foils or plates.







Figure 93(c). Sample EM 1A. Clumps of amorphous material and a possible coarse bundle of fibers are seen in this micrograph. As in the previous micrograph many areas are of a thin transparent nature, suggesting the presence of foils or plates.







Figure 94. Sample EM 1C. Much of this specimen consists of amorphous colloidal hydration products; however, after only thirty minutes in water, many needles of various sizes have begun to form, presumably from previously unhydrated cement particles.





Figure 95(a). Sample EM 2A. This specimen strongly resembles that in Figure 93(a) and the same description is a fitting one for this micrograph. Here again no definite morphology is apparent when the paste has reached an age of three days. The only apparent difference between the specimens is in the better dispersion of sample EM 1A.





Figure 95(a). Sample EM 2A. This specimen strongly resembles that in Figure 93(a) and the same description is a fitting one for this micrograph. Here again no definite morphology is apparent when the paste has reached an age of three days. The only apparent difference between the specimens is in the better dispersion of sample EM 1A.







Figure 95(b). Sample EM 2A. The transparency of the edges of the specimen bears a resemblance to Figure 93(b). Once again, however, no definite morphology is apparent beyond the assumption that the transparent areas are plates or foils.





Figure 96. Sample EM 2C. As in Figure 94 the presence of amorphous material is readily apparent, however, many more needles have formed after thirty minutes in water than formed in sample EM 1C. The needles also appear smaller than those of sample EM 1C. The apparent change in morphology of the needles could be the result of the glycolic acid present in mix 2.





Figure 97. Sample EM 3A. This specimen appears to have the same amorphous structure as those in Figures 92(a) and 95(a). This specimen was not studied on the EM 200 nor was it rehydrated in water.







Figure 98. Sample EM 4A. The same amorphous structure of the paste is apparent at age three days as was observed in previous specimens. Even the presence of latex is not clearly apparent in this micrograph.







Figure 99. Sample EM 4C. In this rehydrated latex specimen the growth of needles is readily apparent. More needles have formed than in mix 1 after thirty minutes in water, however, fewer needles have formed than in mix 2. It is interesting to note the appearance of several small cigar-shaped particles. The dark area to the right of center appears to be coated with latex.





Figure 100(a). Sample EM 5A. In parts of this micrograph appear particles that resemble pieces of plate crystals which could be either plates of the C-H phase or of the C-A-H phase. Note especially the right center of the micrograph. The remainder of the specimen consists of the same amorphous-type structure observed in previous specimens.







Figure 100(b). Sample EM 5A. While no definite morphology can be detected in this specimen it is interesting to note the texture in the upper left of the micrograph. The texture is similar to that previously observed in needles and plates, but could possibly be latex as well.







Figure 101. Sample EM 5C. In this rehydrated latex specimen numerous small needles have formed. The needles are smaller and more plentiful than those observed in mix 1. No other products with a clear morphology can be seen in the micrograph.



## APPENDIX II

### LIST OF FIGURES

<u>FIGURE</u>	<u>TITLE</u>	<u>PAGE</u>
3.1	Schematic for Compressive Strength Calculations	31
3.2	Schematic for Flexural Strength Calculations	31
4.1	Compressive Strength vs. Curing Age for Glycolic Acid Mixes	36
4.2	Compressive Strength vs. Curing Age for Latex Mixes	37
4.3	Flexural Strength vs. Curing Age for Glycolic Acid Mixes	41
4.4	Flexural Strength vs. Curing Age for Latex Mixes	42
4.5	Stress-Strain Curves	45
5.1	The Effects of Admixtures on the Microstructure of $C_3S$ at 24 Hours	50
5.2	The Hydration of $C_3S$ with Excessive Glycolic Acid	52
5.3	The Effects of Admixtures on the Microstructure of $C_2S$ at 24 Hours	54
5.4	The Effects of Admixtures on the Microstructure of $C_4AF$ at 24 Hours	58
5.5	The Effects of Admixtures on the Microstructure of $C_3A$ at 24 Hours	61
5.6	The Hydration of $C_3A$ with Glycolic Acid	63
5.7	The Effects of Admixtures on the Microstructure of Portland Cement	68



### APPENDIX III

#### LIST OF TABLES

<u>TABLE</u>	<u>TITLE</u>	<u>PAGE</u>
3.1	Mix Proportions	20
3.2	Bottle Hydrated Specimen Pro- portions	23
4.1	Average Cylinder Compressive Strength	35
4.2	Average Beam Flexural Strength	40

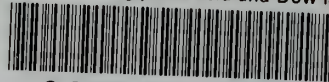






thesH497

The effects of glycolic acid and Dow lat



3 2768 001 91895 6

DUDLEY KNOX LIBRARY